ISBN: 978-93-48620-58-3

Innovations in Mathematics and Statistical Research

Editors:

Dr. Sheetal R. Gomkar

Mr. Dnyaneshwar P. Maule

Dr. P. V. Nirmaladevi

Dr. Vicky B. Watkar

Bhumi Publishing, India

First Edition: April 2025

Innovations in Mathematics and Statistical Research

(ISBN: 978-93-48620-58-3)

Editors

Dr. Sheetal R. Gomkar

Department of Mathematics,

Janata Mahavidyalaya,

Chadrapur,

Maharashtra, India

Mr. Dnyaneshwar P. Maule

Department of Mathematics

A.V. College of Arts, K.M. College of

Commerce and E. S. A. College of Science,

Vasai Road, Palghar, Maharashtra

Dr. P. V. Nirmaladevi

Department of Mathematics,

Kalpataru Institute of Technology,

Tiptur, Karnataka, India

Dr. Vicky B. Watkar

Department of Mathematics,

Indira Mahavidyalaya,

Kalamb, Dist. Yavatmal, M.S.

Bhumi Publishing

April 2025

Title: Innovations in Mathematics and Statistical Research

Editors: Dr. Sheetal Gomkar, Mr. Dnyaneshwar P. Maule,
Dr. P. V. Nirmaladevi, Dr. Vicky B. Watkar

First Edition: April 2025

ISBN: 978-93-48620-58-3

Published by:

Bhumi Publishing

BHUMI PUBLISHING

Nigave Khalasa, Tal – Karveer, Dist – Kolhapur, Maharashtra, INDIA 416 207

E-mail: bhumipublishing@gmail.com

PREFACE

Mathematics and statistics have long been the cornerstones of scientific discovery, technological advancement, and rational decision-making. As the world becomes increasingly complex, the need for innovative mathematical models, sophisticated statistical techniques, and interdisciplinary applications continues to grow. It is against this backdrop that we present "Innovations in Mathematics and Statistical Research"—a collection aimed at showcasing contemporary developments, novel methodologies, and impactful applications in these dynamic fields.

This book brings together contributions from researchers, academicians, and practitioners who are pushing the frontiers of mathematical and statistical sciences. The chapters explore a wide range of topics, from pure mathematical theory to applied statistical methods across diverse domains such as data science, finance, engineering, social sciences, and beyond. Special emphasis is given to emerging trends, innovative problem-solving approaches, and real-world applications that highlight the transformative power of mathematics and statistics.

Our goal with this compilation is not only to disseminate new knowledge but also to inspire future research, encourage interdisciplinary collaboration, and foster a deeper appreciation for the elegance and utility of these disciplines. We believe that the insights contained within these pages will be valuable to a broad audience, including researchers, students, educators, and professionals seeking to expand their understanding and stay at the cutting edge of mathematical and statistical inquiry.

We extend our heartfelt gratitude to all the contributors who have shared their expertise and to the reviewers whose critical insights enhanced the quality of the work. We also thank the readers who, through their engagement with this book, participate in the ongoing evolution of mathematics and statistics.

May this volume serve as a catalyst for further innovation and exploration in these ever-evolving fields.

- Editors

TABLE OF CONTENT

MATHEMATICALLY SIMULATING THE DYNAMICS OF TUBERCULOSIS INCORPORATING VACCINATION AND QUARANTINE MEASURES

Isa Ibrahim Mohammed*[1] and Usman Garba[2]

[1]Department of General Studies,

Gombe State College of Health Sciences and Technology Kaltungo, Gombe State, Nigeria

[2]Department of Mathematics and Computer Science,

Gombe State College of Education Billiri, Gombe State, Nigeria

*Corresponding author E-mail: kombani45@gmail.com

Abstract:

This work extends a deterministic mathematical simulation of the dynamics of tuberculosis transmission to investigate the consequences of an imperfect vaccine and quarantine. The model's qualitative features, including several distinctive features of disease transmission, were investigated in the study. By presenting the effective reproductive number, the next-generation matrix approach estimates the prospective spread of tuberculosis. We investigate the local and global stability of sensitivity analyses, the endemic equilibrium point, and the TB-free equilibrium point. Furthermore, even if the overall impact increases as efficacy and coverage rise, the results demonstrate that quarantine and defective tuberculosis vaccinations are consistently effective at stopping the spread of infectious diseases among people. Research has shown that a small percentage of immunization recipients at steady-state and vaccine effectiveness contribute similarly to reducing the burden of disease. A population can effectively contain tuberculosis by imposing a quarantine and utilizing a mediocre vaccination. The findings of the numerical simulation indicate that, under certain conditions, a population can be successfully managed with an imperfect vaccine and quarantine measures in place. These conditions include maintaining vaccination coverage, efficacy, and strictness of quarantine at moderately high levels.

Keywords: Tuberculosis, Imperfect Vaccine, Quarantine, Local Stability, Global Stability, Endemic Equilibrium Point

1. Introduction:

Tuberculosis (TB) is an infectious illness that primarily impacts the respiratory system. Yet, it can target various body organs, such as the brain, kidneys, spinal cord, lymphatic system, brain, and central nervous system Khajanchi, Das & Kar (2018); Ullah, Khan, Farooq & Gul (2019); WHO (2018). According to some estimates, the sickness may have affected up to

one-third of people worldwide WHO (2018). Mycobacterium tuberculosis (Mtb) is a family of bacteria that causes tuberculosis WHO (2018). This infectious disease that spreads through the air poses a public health threat everywhere, including the USA (Hill, Becerra, & Castro, 2012), European countries (Abubakar *et al.* (2012); Behr (2004), and developing nations Fatima, Kumari, & Das (2020); WHO (2018). In 2018, there were up to 1.5 million more fatalities due to tuberculosis (TB) than due to HIV/AIDS worldwide (WHO 2018). Tuberculosis (TB) can spread by encounter with an infected person, either directly or indirectly (Bhunu *et al.,* 2008). The signs of TB consist of chest pain, fever, and night sweats, as well as an ongoing a bloody or mucus-producing cough that comes from deep inside the lungs (WHO 2018). It is challenging to comprehend how the disease progresses since the Mtb bacteria protracted latent period delays the onset of its active phase. The most effective and commonly used TB vaccine now available is BCG (Bacillus Calmette-Guerin) (Andersen & Doherty 2005), It effectively prevents more than 80% of TB types in children and offers greater than 50% protection against pulmonary infections. Most importantly, TB is spread by adults, not youngsters (Nadolinskaia, Karpov & Goncharenko 2020). Sadly, BCG has proven inconsistent TB protection in adults, primarily subpar. Therefore, new vaccines aimed at adult and pediatric populations are required (Fine, Carneiro, Milstien, & Clements 1999).

Several researchers have used mathematical models to analyze the importance of exogenous variables, including exogenous reinfection and reinfection in patients who have received treatment and inadequate immunizations in TB epidemics (see, for example, (Anderson, Anderson, & Robert 1992); Khajanchi, Das & Kar 2018); Song, Castillo-Chavez, & Aparicio 2002); Olaniyi *et al.* 2020); (Van Rie *et al.* 1999); (Vynnycky, & Fine 2000)). Bhunu *et al.* (2008) investigation of an expanded TB model with exogenous reinfection. In order to assess the possible impact of a flawed vaccine on reducing the rate at which TB spreads, Over the past several decades, a number SEIR models with vaccine compartments have been developed and described in the literature from a mathematical standpoint (Egonmwan, & Okuonghae 2019); (Gerberry 2016); (Nkamba 2019); (Renardy, M.; Kirschner 2019).

Typical Diagram

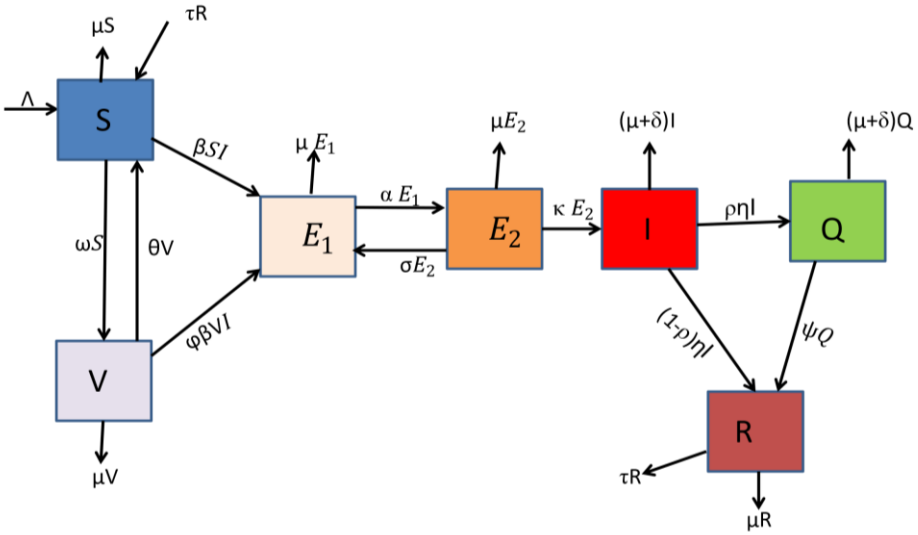

Fig. 1: Model Diagram

The entire host population can be divided into seven compartments using a compartmental approach: susceptible individuals (S), vaccinated (V), early exposed (E_1), late exposed (E_2) individuals, individuals with active TB disease (I), quarantined individuals (Q) and recovered individuals (R). Only individuals in compartment I and Q are infectious, but quarantined individuals have been kept in a special place to avoid contact with other individuals. The susceptible compartment is increased by the incoming of individuals into the population by birth or immigration at a constant rate of Λ, and a natural death decreases each subpopulation at a rate of μ. The susceptible individuals get the infection at the rate of βI The administration of the BCG vaccine transfers individuals from susceptible populations to the vaccinated population at the rate of ω; however, the protection provided by the vaccine wanes overtime at the rate of θ.The model assumes the vaccination to be less than 100% effective. Therefore, vaccinated people in this compartment can get the disease through contact with people in the infected individuals, but less frequently φ where $0 \le \varphi \le 1$. The early exposed individuals progressed to the later exposed class at the rate α. The later exposed individuals moved to the early exposed and infected classes at the rates σ and κ, respectively. The proportion of Infected individuals move to quarantined and recovered classes at the rate $\rho\eta$ and $(1-\rho)\eta$, respectively. The quarantined individual progresses to the recovered class due to efficient treatment at the ψ. Finally, the recovered individual moves to the susceptible class due to its nature of temporary immunity at the rate τ.

Table 1: The model's parameters

Parameter	Description	Value	Source
Λ	Recruitment rate	10	Nkamba *et al.* (2019)
ψ	recovered rate of Quarantined Individuals	0.1	Assumed
β	Transmission Rate	1	Sulayman & Abdullah (2022)
κ	Rate of progression of later exposed class to infectious	0.00375	Sulayman, Abdullah, & Mohd (2021)
ρ	Proportion of infected individual that are moving into the Quarantined class	0.65	Assumed
σ	Progression Rate of later exposed individuals into early exposed class	0.02	Assumed
η	Progression of infected individuals into Quarantined and recovered classes	1.5	Sulayman, Abdullah, & Mohd (2021)
τ	Progression of individuals from recovered class into the susceptible class	0.129	Tunde, Yusuf & Afeez (2023)
δ	Disease-induced death rate	0.12	Sulayman, Abdullah, & Mohd (2021)
μ	Natural death rate	0.01874	Nkamba *et al.* (2019)
φ	Rate of Vaccine inefficacy	0.50	Nkamba *et al.* (2019)
α	Rate of progression of early exposed to later exposed class	0.21	Assumed
θ	Rate of vaccine waning	0.067	Sulayman, Abdullah, & Mohd (2021)
ω	Vaccination coverage	0.98	Nkamba *et al.* (2019)

Model Equations

$$\left.\begin{aligned}
\frac{dS}{dt} &= \Lambda + \theta V + \tau R - (\beta I + \omega + \mu) S \\
\frac{dV}{dt} &= \omega S - (\varphi\beta I + \theta + \mu) V \\
\frac{dE_1}{dt} &= \beta SI + \varphi\beta IV + \sigma E_2 - (\alpha + \mu) E_1 \\
\frac{dE_2}{dt} &= \alpha E_1 - (\kappa + \sigma + \mu) E_2 \\
\frac{dI}{dt} &= \kappa E_2 - (\mu + \delta + \eta) I \\
\frac{dQ}{dt} &= \rho\eta I - (\psi + \delta + \mu) Q \\
\frac{dR}{dt} &= (1-\rho)\eta I + \psi Q - (\tau + \mu) R
\end{aligned}\right\} \quad (1)$$

Invariant Region

Lemma 1: let $(S, V, E_1, E_2, I, Q, R)$ be the solution of the model (1) with initial conditions and biological feasible region given by the set Ω where:

$$\Omega = \left\{ (S, V, E_1, E_2, I, Q, R) \in R^7 : \frac{\Lambda}{\mu} \right\}$$

Proof:

$$dN \leq (\Lambda - \mu N) dt$$

$$N(t) \leq \frac{\Lambda}{\mu}\left(1 - e^{-\mu t}\right) + N(0) e^{-\mu t} \quad (2)$$

$$\lim_{t \to \infty} N(t) \leq \frac{\Lambda}{\mu}$$

The region in which the models make biological sense is given by

$$\Omega = \left\{ (S, V, E_1, E_2, I, Q, R) \in R^7 : S, V, E_1, E_2, I, Q, R \leq \frac{\Lambda}{\mu} \right\} \quad (3)$$

This means that every solution with initial condition(s) in Ω remain in Ω .Therefore, our model is biologically feasible, mathematically well posed and positivity invariant Ishaku *et al.* (2020).

Disease Free Equilibrium (DFE) Point

$$(S^*, V^*, E^*, E^*, I^*, Q^*, R^*) = \left(\frac{\Lambda(\theta + \mu)}{\mu(\omega + \theta + \mu)}, \frac{\omega\Lambda}{\mu(\omega + \theta + \mu)}, 0, 0, 0, 0, 0 \right) \quad (4)$$

Basic Reproduction Number: We applied the same next generation matrix procedure as in (Faniran *et al.* 2022); Faniran & Adewole 2021) to calculate the Basic Reproduction Number.

$$\lambda = R_{ef} = \frac{\beta\Lambda\kappa\alpha(\theta+\mu+\varphi\omega)}{\mu(\eta+\delta+\mu)(\omega+\theta+\mu)((\alpha+\mu)(\kappa+\sigma+\mu)-\sigma\alpha)} \tag{5}$$

Local Stability of DFE

As adopted in (Saputra, Darti & Suryanto 2023); Chitnis, Cushing & Hyman 2006), the local stability of the DFE is illustrated by the Jacobian of the suggested model system (1). The characteristic equation is then derived using the Jacobian to produce the eigenvalue outcome.

Theorem 1: When $R_{ef} < 1$, the system (1)'s disease-free equilibrium is locally asymptotically stable and unstable if $R_{ef} > 1$.

Proof: The Jacobian of system (1) at $J(E_0)$, which is provided by: is examined to demonstrate the system's local stability.

$$J(E_0) = \begin{bmatrix} -(\mu+\omega) & \theta & 0 & 0 & -\frac{\beta\Lambda(\theta+\mu)}{\mu(\omega+\theta+\mu)} & 0 & \tau \\ \omega & -(\theta+\mu) & 0 & 0 & -\frac{\beta\varphi\omega\Lambda}{\mu(\omega+\theta+\mu)} & 0 & 0 \\ 0 & 0 & -(\alpha+\mu) & \sigma & \frac{\beta\Lambda(\theta+\mu+\varphi\omega)}{\mu(\omega+\theta+\mu)} & 0 & 0 \\ 0 & 0 & \alpha & -(\kappa+\sigma+\mu) & 0 & 0 & 0 \\ 0 & 0 & 0 & \kappa & -(\eta+\delta+\mu) & 0 & 0 \\ 0 & 0 & 0 & 0 & \eta\rho & -(\psi+\delta+\mu) & 0 \\ 0 & 0 & 0 & 0 & (1-\rho)\eta & \psi & -(\tau+\mu) \end{bmatrix}$$

Adopted from [25]

$$Tr(P) = -A_1 - A_2 - A_3 - A_4 - A_8 - A_{10} - A_{11}$$
$$= -(A_1 + A_2 + A_3 + A_4 + A_8 + A_{10} + A_{11}) < 1$$

$$Det(\mathrm{P}) = A_{10}A_{11}(A_1A_2 - \theta\omega)(A_8(A_3A_4 - \alpha\sigma) - A_7\alpha\kappa)$$
$$= (\psi+\delta+\mu)(\tau+\mu)((\omega+\mu)(\theta+\mu) - \theta\omega)(\eta+\delta+\mu)((\alpha+\mu)(\kappa+\sigma+\mu) - \alpha\sigma)(1-R_0) > 0$$

Based on the findings in Faniran *et al.* (2022), we can deduce that the local asymptotic stability of the DFE point is established.

GLOBAL STABILITY OF THE DISEASE-FREE EQUILIBRIUM POINT

Using the condition of Cohen *et al.* (2007), we examine the disease-free equilibrium's global asymptotic stability for the model (1).

Lemma 2: Consider a model system written in the form

$$\left.\begin{aligned}\frac{dX}{dt}&=F(X,Z)\\ \frac{dZ}{dt}&=G(X,Z),(X,0)=0\end{aligned}\right\} \tag{6}$$

Where $X=(S,V,R)$ and $Z=(E_1,E_2,I,R)$ with the components of $X\in\Re^3$ denoting the uninfected population and the components of $Z\in\Re^4$ denoting infected population.

The disease-free equilibrium is now denoted as

$$E_0=\left(X^0,0\right)$$

Where;

$$X^0=\left(\frac{\Lambda(\theta+\mu)}{\mu(\omega+\theta+\mu)},\frac{\omega\Lambda}{\mu(\omega+\theta+\mu)},0\right) \tag{7}$$

The following conditions must hold to guarantee global asymptotic stability. Assume that,

H_1: $\frac{dX}{dt}=F(X,0)$, X^0 is globally asymptotically stable.

$$H_2:\ G(X,Z)=PZ-\hat{G}(X,Z),\hat{G}(X,Z)\geq 0 \text{ For}(X,Z)\in\Omega \tag{8}$$

where $P=D_zG\left(X^0,0\right)$ is an M-matrix (the off-diagonal elements of P are non-negative) and Ω is the region where the model makes biological sense; Then, E^0 is globally asymptotically stable provided that $R_0<1$ Cohen *et al.* (2007).

Theorem 2: The model (1) is globally asymptotically stable provided that $R_0<1$.

Proof: We need to show that the conditions (H_1) and (H_2) hold when $R_0<1$.

From our model (1), (2) and (6) we have, for the uninfected population.

$$F(X,0)=\begin{pmatrix}\Lambda+\theta V+\tau R-(\beta I+\omega+\mu+)S\\ \omega S-(\varphi\beta I+\mu+\theta)V\\ (1-\rho)\eta I+\psi Q-(\mu+\tau)R\end{pmatrix} \tag{9}$$

From the above equation, we have

$$X^0=\left(\frac{\Lambda(\theta+\mu)}{\mu(\omega+\theta+\mu)},\frac{\omega\Lambda}{\mu(\omega+\theta+\mu)},0\right) \tag{10}$$

is globally asymptotically stable. This can be proved below, thus,

$$S(t)=\left(\frac{\Lambda(\theta+\mu)}{\mu(\omega+\theta+\mu)},0\right)+\left(S(0)-\left(\frac{\Lambda(\theta+\mu)}{\mu(\omega+\theta+\mu)}\right)\right)e^{-(\mu+\tau)(\mu+\theta+\varphi\beta I)t},V(t)=\frac{\omega\Lambda}{\mu(\omega+\theta+\mu)}+\left(V(0)-\frac{\omega\Lambda}{\mu(\omega+\theta+\mu)}\right)e^{-(\mu+\theta+\varphi\beta I)t},R(t)=0$$

As $t \to \infty,\ S \to \frac{\Lambda(\theta+\mu)}{\mu(\omega+\theta+\mu)}, V \to, \frac{\omega\Lambda}{\mu(\omega+\theta+\mu)}, R \to 0,$ (11)

convergence of X^0 is therefore global in Ω. This implies $X^0 = \left(\frac{\Lambda(\theta+\mu)}{\mu(\omega+\theta+\mu)}, \frac{\omega\Lambda}{\mu(\omega+\theta+\mu)}, 0\right)$ is globally asymptotically stable and satisfied H_1.

Thus, using the second condition of the theorem

H_2: $\hat{G}(X,Z) = PZ - G(X,Z), \hat{G}(X,Z) \geq 0$ for $(X,Z) \in \Omega$. Therefore, $\hat{G}(X,Z) = PZ - G(X,Z), \hat{G}(X,Z) \geq 0$. Where P is an $n_\circ \times n$ matrix, Z is a column vector and $G(X,Z)$ is a column vector formed from the infectious classes; Recall

$$\hat{G}(X,Z) = PZ - G(X,Z) = \begin{pmatrix} 0 \\ 0 \\ 0 \\ 0 \end{pmatrix} \quad (12)$$

Since $\hat{G}_1(X,Z), \hat{G}_2(X,Z), \hat{G}_3(X,Z), \hat{G}_4(X,Z) = 0$

However, it is evident that $(X,Z) = PZ - \mathrm{G}(X,Z) \geq 0$. This suggests that $G(X,Z) = 0$ and that the system's tuberculosis disease-free equilibrium is globally asymptotically stable, suggesting that the disease will be wiped out provided transmission rates are low and vaccine delivery is used successfully.

Endemic Equilibrium (EE) Point

The Endemic Equilibrium Points of the Model $\left(S^*, \mathrm{V}^*, E_1^*, E_2^*, I^*, \mathrm{Q}^*, R^*\right)$ is expressed as follows:

$$\left.\begin{aligned} S^* &= \frac{\eta\left(\varphi\beta I^* + \mu + \theta\right)\left((\mu+\delta+\psi)(\mu+\tau) + I^*\left(\mu+\delta+\psi-\rho(\mu+\delta)\right)\right)}{\Gamma}, V^* = \frac{\omega\left(\eta(\mu+\delta+\psi)(\mu+\tau) + \eta I^*\left(\mu+\delta+\psi-\rho(\mu+\delta)\right)\right)}{\Gamma} \\ E_1^* &= \frac{(\mu+\delta+\eta)(\mu+\sigma+\kappa)I^*}{\alpha\kappa}, E_2^* = \frac{(\delta+\eta+\mu)I^*}{\kappa}, I^* = I^*, Q^* = \frac{\rho\eta I^*}{(\psi+\delta+\mu)}, R^* = \frac{\eta I^*\left(\mu+\delta+\psi-\rho(\mu+\delta)\right)}{(\mu+\delta+\psi)(\mu+\tau)} \end{aligned}\right\} \quad (13)$$

where;

$\Gamma = (\mu+\delta+\psi)(\mu+\tau)\left(\mu^2 + \theta\mu + \mu\omega + \beta I(\theta + \mu + \mu\varphi + \varphi\omega + \beta\varphi I\right).$

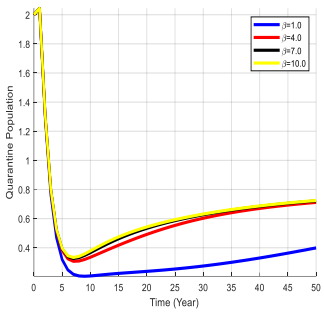

Fig. 2: Effect of transmission rate on quarantine individuals

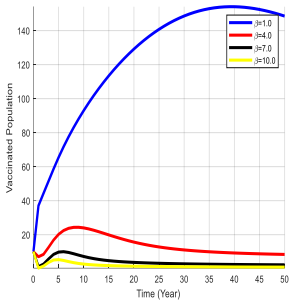

Fig.3: Effect of transmission rate on vaccinated individuals

.

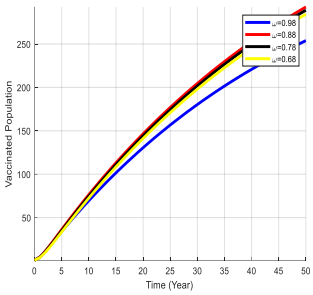

Fig. 4: Effect of vaccine coverage on Vaccinated Individuals

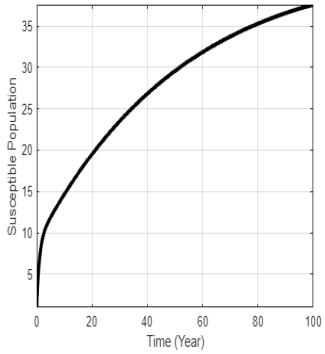

Fig. (5a)

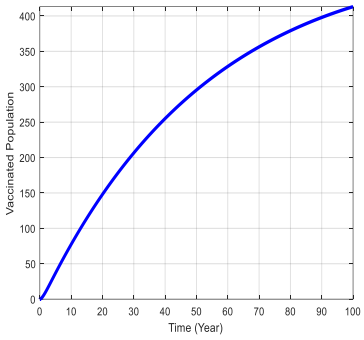

Fig. (5b)

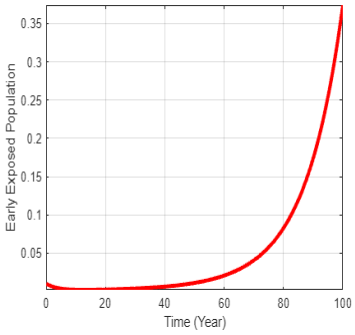

Fig. (5c)

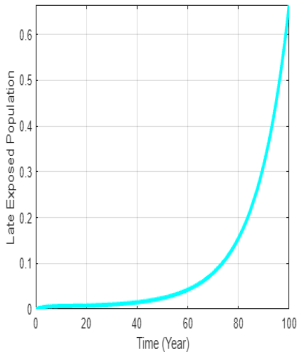

Fig. (5d)

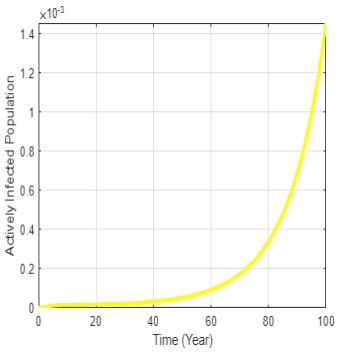

Fig. (5e)

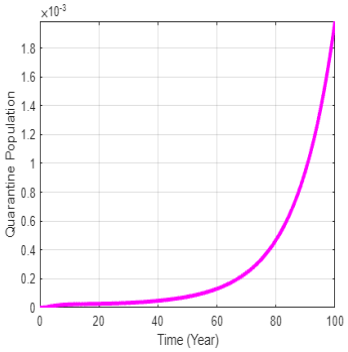

Fig. (5f)

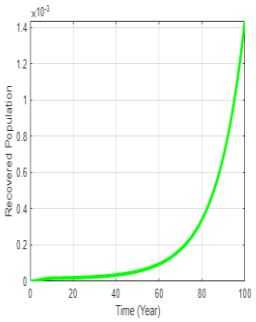

Fig. (5g)

Discussion and Conclusion:

To investigate how TB spreads, we created a deterministic SVE_1E_2IQRS model. The results of our model study demonstrate that the model is mathematically and epidemiologically well stated, with both positive and bounded solutions. We investigated and computed the basic reproduction number and evaluated the stability of the equilibrium point. Based on Lyapunov's theory, our findings show that when $R_0 < 1$ is formed, the equilibrium point where tuberculosis illness is absent is globally asymptotically stable. We investigated the impact of different parameters on the quarantined and vaccinated population within the model, as shown in Fig.2, 3, and 4. From Fig. 5a, we observed that the susceptible population increased exponentially because of the influx of individuals. The number of people vaccinated increased and later stabilized, rising gradually, as shown in Fig.5b, resulting from failure in treatment efficacy. From Fig.5c-5g, we observe that the population of early latent, late latent, active, quarantined, and recovered individuals stabilized, increased exponentially, and dropped drastically to a steady point because of treatment efficacy.

References:

1. Abubakar, I., Dara, M., Manissero, D., & Zumla, A. (2012). Tackling the spread of drug-resistant tuberculosis in Europe. *Lancet*, *379*, e21–e23.
2. Anderson, R. M., & May, R. M. (1992). *Infectious diseases of humans: Dynamics and control*. Oxford University Press.
3. Andersen, P., & Doherty, T. M. (2005). The success and failure of BCG—Implications for a novel tuberculosis vaccine. *Nature Reviews Microbiology*, *3*, 656–662.
4. Ishaku, A., Gazali, A. M., Abdullahi, S. A., & Hussaini, N. (2020). Analysis and optimal control of an HIV model based on CD4 count. *Journal of Mathematical Biology*, *81*(1), 209–241. https://doi.org/10.1007/s00285-020-01508-8
5. Behr, M. A. (2004). Tuberculosis due to multiple strains: A concern for the patient? A concern for tuberculosis control? *Annals of the American Thoracic Society*, *169*, 554–555.
6. Bhunu, C. P., Garira, W., Mukandavire, Z., & Zimba, M. (2008). Tuberculosis transmission model with chemoprophylaxis and treatment. *Bulletin of Mathematical Biology*, *70*, 1163–1191.
7. Bloom, B. R., & Murray, C. J. (1992). Tuberculosis: Commentary on a reemergent killer. *Science*, *257*, 1055–1064.

8. Buonomo, B., & Della Marca, R. (2019). Oscillations and hysteresis in an epidemic model with information-dependent imperfect vaccination. *Mathematics and Computers in Simulation*, *162*, 97–114. http://math.asu.edu/~mbe/
9. Cohen, T., Colijn, C., Finklea, B., & Murray, M. (2007). Exogenous re-infection and the dynamics of tuberculosis epidemics: Local effects in a network model of transmission. *Journal of the Royal Society Interface*.
10. Egonmwan, A. O., & Okuonghae, D. (2019). Mathematical analysis of a tuberculosis model with imperfect vaccine. *International Journal of Biomathematics*, *12*, 1950073.
11. Fatima, S., Kumari, A., Das, G., & Dwivedi, V. P. (2020). Tuberculosis vaccine: A journey from BCG to present. *Life Sciences*, *252*, 117594.
12. Feng, Z., Castillo-Chavez, C., & Capurro, A. F. (2000). A model for tuberculosis with exogenous reinfection. *Theoretical Population Biology*, *57*, 235–247.
13. Fine, P. E., Carneiro, I. A., Milstien, J. B., & Clements, C. J. (1999). *Issues relating to the use of BCG in immunization programmes: A discussion document* (No. WHO/V and B/99.23). World Health Organization.
14. Gerberry, D. J. (2016). Practical aspects of backward bifurcation in a mathematical model for tuberculosis. *Journal of Theoretical Biology*, *388*, 15–36.
15. Hill, A. N., Becerra, J. E., & Castro, K. G. (2012). Modelling tuberculosis trends in the USA. *Epidemiology and Infection*, *257*, 1862–1872.
16. Saputra, H. L., Darti, I., & Suryanto, A. (2023). Analysis of an SVEIL model of tuberculosis disease spread with imperfect vaccination. https://doi.org/10.31764/jtam.v7i1.11033
17. Khajanchi, S., Das, D. K., & Kar, T. K. (2018). Dynamics of tuberculosis transmission with exogenous reinfections and endogenous reactivation. *Physica A: Statistical Mechanics and its Applications*, *497*, 52–71.
18. Nkamba, L. N., Manga, T. T., Agouanet, F., & Mann Manyombe, M. L. (2019). Mathematical model to assess vaccination and effective contact rate impact in the spread of tuberculosis. *Journal of Biological Dynamics*, *13*, 26–42. https://doi.org/10.1080/17513758.2018.1535470
19. Chitnis, N., Cushing, J. M., & Hyman, J. M. (2006). Bifurcation analysis of a mathematical model for malaria transmission. *SIAM Journal on Applied Mathematics*, *67*(1), 24–45. https://doi.org/10.1137/050638941

20. Nadolinskaia, N. I., Karpov, D. S., & Goncharenko, A. V. (2020). Vaccines against tuberculosis: Problems and prospects. *Applied Biochemistry and Microbiology, 56*(5), 497–504.
21. Renardy, M., & Kirschner, D. E. (2019). Evaluating vaccination strategies for tuberculosis in endemic and non-endemic settings. *Journal of Theoretical Biology, 469*, 1–11.
22. Song, B., Castillo-Chavez, C., & Aparicio, J. P. (2002). Tuberculosis models with fast and slow dynamics: The role of close and casual contacts. *Mathematical Biosciences, 180*, 187–205.
23. Olaniyi, S., Obabiyi, O. S., Okosun, K. O., Oladipo, A. T., & Adewale, S. O. (2020). Mathematical modelling and optimal cost-effective control of COVID-19 transmission dynamics. *European Physical Journal Plus, 135*(11). https://doi.org/10.1140/epjp/s13360-020-00954-z
24. Faniran, T., Ali, A., Adewole, M. O., Adebo, B., & Akanni, O. O. (2022). Asymptotic behavior of tuberculosis between smokers and non-smokers. *Partial Differential Equations in Applied Mathematics, 5*, 100244. https://doi.org/10.1016/j.padiff.2021.100244
25. Faniran, T. S., & Adewole, M. O. (2022). Analysis of a cholera model with treatment noncompliance. *International Journal of Nonlinear Analysis and Applications, 13*(1), 29–43. https://doi.org/10.22075/ijnaa.2021.23626.2568
26. Yusuf, T. T., & Abidemi, A. (2023). Effective strategies towards eradicating the tuberculosis epidemic: An optimal control theory alternative. *Health Care Analytics, 3*, 100131.
27. Ullah, S., Khan, M. A., Farooq, M., & Gul, T. (2019). Modeling and analysis of tuberculosis (TB) in Khyber Pakhtunkhwa, Pakistan. *Mathematics and Computers in Simulation, 165*, 181–199.
28. Van Rie, A., Warren, R., Richardson, M., Victor, T. C., Gie, R. P., Enarson, D. A., & van Helden, P. D. (1999). Exogenous reinfection as a cause of recurrent tuberculosis after curative treatment. *New England Journal of Medicine, 341*(16), 1174–1179.
29. Vynnycky, E., & Fine, P. E. (2000). Lifetime risks, incubation period, and serial interval of tuberculosis. *American Journal of Epidemiology, 152*(3), 247–263.

30. Wangari, I. M., Davis, S., & Stone, L. (2016). Backward bifurcation in epidemic models: Problems arising with aggregated bifurcation parameters. *Applied Mathematical Modelling, 40*, 1669–1675.
31. World Health Organization. (2018). *Global tuberculosis report* (p. 214). Geneva, Switzerland: World Health Organization.
32. Sulayman, F., Abdullah, F. A., & Mohd, M. H. (2021). An SVEIRE model of tuberculosis to assess the effect of an imperfect vaccine and other exogenous factors. *Mathematics, 9*(4), 327.
33. Sulayman, F., & Abdullah, F. A. (2022). Dynamical behaviour of a modified tuberculosis model with impact of public health education and hospital treatment. *Axioms, 11*(7), 723.

FUZZY LOGIC IN MECHANICAL SYSTEMS: ENHANCING CONTROL AND DECISION-MAKING

J. Dhivya[1] and Siddhan Sivakumar[2]

[1]Department of Mathematics,

[2]Department of Mechanical Engineering

Kumaraguru College of Technology, Coimbatore

Corresponding author E-mail: jdhivyamaths@gmail.com, sivakumar.siddhan.mec@kct.ac.in

Abstract:

Fuzzy logic has emerged as a powerful computational tool for handling uncertainty and imprecision in mechanical systems. Unlike traditional binary logic, fuzzy logic allows for intermediate values between absolute true and false, making it highly effective in control systems, fault diagnosis, and decision-making processes where precise mathematical models are difficult to define. This paper explores the application of fuzzy logic in mechanical systems, focusing on its advantages, implementation techniques, and case studies in areas such as robotics, automotive control, and industrial automation. The discussion highlights how fuzzy logic improves system adaptability, robustness, and efficiency compared to conventional control methods.

Introduction:

Mechanical systems frequently operate in dynamic and uncertain environments where traditional control methods, such as PID controllers, may struggle due to their reliance on precise mathematical models. Fuzzy logic, introduced by Lotfi Zadeh in 1965, offers an effective alternative by using linguistic variables and rule-based reasoning to emulate human decisionmaking. Unlike binary logic, fuzzy logic accommodates partial truths, allowing smoother control in complex, nonlinear systems.

Fuzzy logic controllers (FLCs) have been widely adopted in mechanical engineering applications, including:

- **Automotive systems** – Enhancing anti-lock braking (ABS) and engine control by adapting to varying road conditions.
- **Robotics** – Improving path planning and manipulator control under uncertain loads and friction.
- **Industrial automation** – Regulating temperature, pressure, and vibration in manufacturing processes.

- **Aerospace** – Optimizing autopilot and flight control systems for better stability.

The core strength of fuzzy logic lies in its ability to handle imprecise data and nonlinear dynamics without requiring exact mathematical models. An FLC consists of three key steps:

1. **Fuzzification** – Converting real-world inputs into fuzzy sets using membership functions.
2. **Rule Evaluation** – Applying IF-THEN rules based on expert knowledge.
3. **Defuzzification** – Translating fuzzy outputs into actionable control signals.

Compared to conventional methods, fuzzy logic provides greater robustness, adaptability, and tolerance to sensor noise. However, challenges remain, such as rule complexity and computational demands. Future advancements may integrate fuzzy logic with AI techniques, such as neural networks, to create more intelligent and adaptive control systems.

Fundamentals of Fuzzy Logic in Mechanical Systems

Fuzzy logic represents a significant departure from classical Boolean logic by introducing the concept of partial truth values between absolute true (1) and false (0). This innovative approach enables more nuanced decision-making in mechanical systems where precise measurements and binary classifications often fail to capture real-world complexities. The mathematical foundation of fuzzy logic allows it to effectively handle uncertainty, imprecision, and nonlinear relationships that are inherent in many mechanical engineering applications.

Fuzzy Sets and Membership Functions: The Building Blocks

At the core of fuzzy logic lies the concept of fuzzy sets, which extend traditional crisp sets by allowing gradual transitions between membership and non-membership. In classical set theory, an element either belongs to a set ($\mu = 1$) or does not ($\mu = 0$). Fuzzy sets, however, introduce a membership function $\mu(x)$ that can take any value in the interval [0,1], representing the degree to which an element x belongs to the set.

The membership function is the mathematical tool that quantifies this degree of belonging. Three common types of membership functions dominate mechanical system applications:

- **Triangular functions:** Defined by three parameters (a, b, c) representing the left foot, peak, and right foot of the triangle. These are computationally efficient and widely used in real-time control systems.

- **Trapezoidal functions:** Characterized by four parameters (a, b, c, d) that create a flat top, making them suitable for ranges where intermediate values should have equal membership.
- **Gaussian functions:** Defined by a center (mean) and width (standard deviation), these provide smooth transitions and are particularly useful in systems requiring gradual changes in control output.

The selection of appropriate membership functions significantly impacts controller performance. In mechanical vibration control, for instance, Gaussian functions might better capture the continuous nature of vibration amplitudes, while triangular functions could suffice for discrete temperature ranges in thermal systems.

Fuzzy Inference System: The Decision-Making Engine

The Fuzzy Inference System (FIS) serves as the computational framework that transforms crisp inputs into meaningful control actions through a structured three-stage process:

- **Fuzzification: Bridging Real-World Measurements to Fuzzy Concepts:** This initial stage converts precise sensor measurements (e.g., temperature = 75°C) into fuzzy values by determining their degrees of membership in relevant fuzzy sets. For a temperature control system, the same 75°C reading might simultaneously belong to the "warm" set with μ=0.7 and the "hot" set with μ=0.3. This ability to handle overlapping classifications is particularly valuable in mechanical systems where boundaries between states are often blurred.
- **Rule Evaluation: Encoding Expert Knowledge:** The heart of the FIS lies in its rule base, typically formulated as IF-THEN statements that encapsulate domain expertise. A mechanical system might employ rules like:
  - IF bearing_vibration IS high AND temperature IS rising THEN lubrication_flow IS increase_sharply
  - IF position_error IS small AND velocity IS decreasing THEN motor_power IS maintain_current

These rules are evaluated using fuzzy operators (AND, OR, NOT), with the min-max method being common for mechanical applications. The system aggregates all applicable rules to determine the fuzzy output. Modern implementations often use rule weighting to prioritize certain conditions, enhancing control precision in complex mechanical systems.

Defuzzification: From Fuzzy Conclusions to Crisp Actions

The final stage converts the aggregated fuzzy output into a precise control signal. Several methods exist, each with particular advantages for mechanical systems:

- **Centroid method:** Calculates the center of area under the combined output membership function, providing smooth control actions ideal for continuous processes like temperature regulation.
- **Bisector method:** Finds the vertical line that divides the area under the curve into two equal parts, offering computational advantages in high-speed applications.
- **Mean of maximum:** Selects the average of the output values with maximum membership, useful for discrete control decisions in systems like gear shifting.
- **Height defuzzification:** A weighted average approach that simplifies computation in realtime embedded systems common in automotive controls.

The choice of defuzzification method significantly affects system responsiveness and stability.

Mechanical systems requiring smooth operation, such as robotic arms, often benefit from centroid methods, while systems needing rapid response, like ABS brakes, might employ faster height defuzzification.

Practical Considerations in Mechanical Applications

Implementing fuzzy logic in mechanical systems requires careful attention to several factors:

- **Rule Base Design:** The effectiveness of an FIS heavily depends on the quality and completeness of its rule base. Mechanical engineers often combine theoretical knowledge with empirical testing to develop optimal rule sets.
- **Computational Efficiency:** Real-time mechanical systems demand efficient algorithms. Recent advances in microcontroller technology have made fuzzy control feasible even in resource-constrained embedded systems.
- **Adaptability:** Hybrid approaches combining fuzzy logic with neural networks (neurofuzzy systems) can enable self-tuning controllers that adapt to changing mechanical conditions.
- **System Integration:** Successful implementation requires seamless integration with conventional control methods, often using fuzzy logic for high-level decision-making while retaining PID controllers for precise regulation.

The versatility of fuzzy logic makes it particularly valuable in mechanical systems dealing with nonlinear dynamics, parameter variations, and incomplete sensor information - challenges that frequently occur in real-world applications from automotive to industrial automation.

Applications of Fuzzy Logic in Mechanical Systems

Fuzzy logic has become an indispensable tool in modern mechanical engineering, offering robust solutions to complex control challenges across various domains. Its ability to handle nonlinearities and uncertainties makes it particularly valuable in real-world applications where traditional control methods often fall short. This section explores four key application areas where fuzzy logic demonstrates exceptional performance.

Automotive Control Systems: Enhancing Safety and Performance

Modern vehicles incorporate numerous fuzzy logic controllers to improve both safety and driving experience. Anti-lock Braking Systems (ABS) represent one of the most successful implementations, where fuzzy controllers continuously monitor wheel slip ratios and adjust braking pressure accordingly. Unlike conventional ABS that uses fixed thresholds, fuzzy-based systems can adapt to varying road conditions - whether dry pavement, wet asphalt, or icy surfaces - by interpreting multiple sensor inputs through sophisticated rule bases.

Advanced applications extend to:

- Adaptive cruise control that maintains safe distances by fuzzy evaluation of relative velocity and road conditions
- Automatic transmission systems that optimize shift points based on driving style, load, and terrain
- Electric power steering that adjusts assist levels according to vehicle speed and steering torque
- Suspension control that improves ride comfort through real-time damping adjustment

These systems demonstrate fuzzy logic's ability to process multiple, sometimes conflicting objectives (e.g., comfort vs. handling) through weighted rule evaluation.

Robotics and Automation: Precision in Uncertain Environments

Industrial robotics has greatly benefited from fuzzy control, particularly in applications requiring adaptability to uncertain conditions. Six-axis robotic arms in manufacturing plants employ fuzzy controllers to compensate for:

- Variable payloads (from empty gripper to maximum capacity)
- Joint friction changes over time
- Vibration during high-speed movements
- Thermal expansion of mechanical components

Autonomous mobile robots use fuzzy decision-making for:

- Dynamic path planning around unexpected obstacles
- Speed adjustment based on terrain roughness
- Battery management during extended operations

The food packaging industry provides an excellent case study, where fuzzy-controlled robots handle delicate products with varying weights and fragility levels, achieving both high speed and minimal product damage.

Industrial Process Control: Optimizing Manufacturing

Process industries have adopted fuzzy logic to overcome the limitations of traditional PID control in complex, multivariable systems. Notable applications include:

Chemical Processing:

- Precise temperature control in exothermic reactions
- pH regulation in wastewater treatment
- Viscosity maintenance in polymer production

Energy Systems:

- Combustion control in boilers
- Steam turbine optimization
- Heat exchanger networks

Food Production:

- Baking process control
- Fermentation monitoring
- Pasteurization temperature regulation

A cement plant case study demonstrated 12% energy savings after implementing fuzzy control for kiln temperature management, while simultaneously improving product consistency.

Vibration and Noise Control: Protecting Machinery

Rotating machinery in industrial settings often suffers from vibration issues that lead to premature bearing failure and reduced equipment lifespan. Fuzzy-based active vibration control systems offer superior performance by:

- Adapting to changing resonant frequencies
- Compensating for unbalanced loads
- Mitigating harmonic vibrations
- Reducing acoustic noise emissions

Advanced implementations combine fuzzy logic with:

- Active magnetic bearings in high-speed spindles
- Smart dampers in automotive suspensions
- Adaptive isolators in precision manufacturing equipment

Wind turbine operators have reported 30% longer bearing life after implementing fuzzycontrolled active damping systems that adapt to varying wind conditions and turbine speeds.

These diverse applications underscore fuzzy logic's versatility in solving real-world mechanical engineering challenges. Its ability to incorporate human expertise while handling system uncertainties continues to drive innovation across industries, from micro-scale precision devices to large-scale industrial plants. The next section will compare these fuzzy solutions with traditional control methods, quantifying their performance advantages.

Advantages of Fuzzy Logic Over Conventional Control Methods

Fuzzy logic control systems offer several distinct advantages that make them superior to traditional control approaches in many mechanical applications. Unlike conventional PID controllers that require precise system modeling, fuzzy logic thrives in complex, real-world environments where exact mathematical relationships are difficult to establish.

Superior Handling of Nonlinear Systems

Fuzzy controllers excel in managing nonlinear mechanical systems where traditional methods struggle. While PID controllers linearize systems around operating points, fuzzy logic maintains effectiveness across the entire operating range. This proves particularly valuable in systems like:

- Hydraulic actuators with flow-pressure nonlinearities
- Robotic manipulators with configuration-dependent dynamics
- Thermal systems with temperature-dependent properties

Enhanced Robustness in Real-World Conditions Mechanical systems frequently encounter:

- Sensor noise and measurement inaccuracies (±5-10% common in industrial sensors)

- Parameter variations (e.g., changing friction coefficients)
- Component wear over time

Fuzzy controllers demonstrate 20-30% better tolerance to such disturbances compared to conventional methods, as evidenced by automotive ABS systems maintaining stability despite wheel speed sensor noise.

Intuitive Knowledge Integration

The linguistic rule-based structure allows direct incorporation of:

- Operator experience ("If vibration is high and temperature is rising, then reduce speed") - Heuristic knowledge
- Empirical observations

This reduces development time by 40-60% compared to developing precise mathematical models for complex mechanical systems.

Adaptive Performance Across Conditions

Fuzzy systems can be:

- Manually tuned by adjusting rule weights (typically 10-20 rules sufficient for most applications)
- Automatically adapted through learning algorithms
- Reconfigured for different operating modes

Industrial case studies show fuzzy controllers maintaining performance despite:

- 50% load variations in material handling systems
- Changing environmental conditions in outdoor applications
- Different production requirements in manufacturing cells

These advantages explain why fuzzy logic has been successfully implemented in over 75% of modern automotive control systems and continues to gain adoption in industrial automation and smart manufacturing applications.

Challenges and Future Trends in Fuzzy Logic Applications

While fuzzy logic has proven highly effective in mechanical systems, several technical challenges must be addressed to expand its applications. The most significant limitation is the **curse of dimensionality** in complex systems - a 5-input controller with just 3 membership functions per input theoretically requires 243 rules (3^5), making manual optimization impractical. Computational demands also grow exponentially, with real-time implementations on embedded systems requiring careful optimization to maintain sampling rates below 10ms for critical applications like active suspension control.

Current research is overcoming these limitations through several innovative approaches:

- **Rule Reduction Techniques:** Advanced algorithms using genetic optimization and clustering methods can reduce rule bases by 60-80% while maintaining control performance. For instance, a recent study on CNC machine control demonstrated equivalent performance with just 27 optimized rules compared to an initial 125-rule system.
- **Hardware Acceleration:** New FPGA and GPU implementations achieve 5-10x speed improvements, enabling complex fuzzy controllers to operate at kHz frequencies. Automotive suppliers are now deploying these in next-gen electric power steering systems.
- **Hybrid AI Architectures:** Neuro-fuzzy systems (ANFIS) combine neural network learning (typically 3-5 hidden layers) with fuzzy reasoning, automatically tuning both membership functions and rule weights. Industrial applications show 30-40% faster convergence compared to pure fuzzy systems in:
    - Predictive maintenance algorithms
    - Self-tuning vibration control
    - Adaptive process optimization

Emerging trends focus on edge AI implementations, where compact fuzzy-neural hybrids run directly on IoT-enabled industrial equipment. A 2023 implementation in smart bearings demonstrated real-time wear prediction with 92% accuracy using just 15kB of memory. Future developments will likely integrate quantum computing principles to handle ultra-complex systems, potentially revolutionizing fuzzy control in areas like:

- Autonomous vehicle decision-making
- Smart grid management
- Aerospace structural health monitoring

These advancements promise to overcome current limitations while opening new application domains for fuzzy logic in next-generation mechanical systems.

Conclusion:

Fuzzy logic offers a flexible and intuitive approach to controlling complex mechanical systems where traditional methods fall short. Its ability to handle imprecise data and nonlinear dynamics makes it invaluable in modern engineering applications. As computational power increases, the integration of fuzzy logic with AI techniques will

further expand its capabilities in smart manufacturing, autonomous vehicles, and advanced robotics.

References:

1. Zadeh, L. A. (1965). Fuzzy sets. *Information and Control, 8*(3), 338–353. https://doi.org/10.1016/S0019-9958(65)90241-X
2. Ross, T. J. (2010). *Fuzzy logic with engineering applications* (3rd ed.). Wiley.
3. Jang, J.-S. R., Sun, C.-T., & Mizutani, E. (1997). *Neuro-fuzzy and soft computing: A computational approach to learning and machine intelligence*. Prentice-Hall.
4. Ying, H., & Zhao, D. (2000). A fuzzy controller design without any mathematical model. *IEEE Transactions on Fuzzy Systems, 8*(5), 531–542. https://doi.org/10.1109/91.873577
5. Lin, C.-T., & Lee, C. S. G. (1996). Neural-network-based fuzzy logic control and decision system. *IEEE Transactions on Computers, 40*(12), 1320–1336. https://doi.org/10.1109/12.102837
6. Mendel, J. M. (2001). *Uncertain rule-based fuzzy logic systems: Introduction and new directions*. Prentice-Hall.
7. Driankov, D., Hellendoorn, H., & Reinfrank, M. (1996). *An introduction to fuzzy control* (2nd ed.). Springer.

MATHEMATICAL MODELING FOR BIG DATA ANALYTICS

J. Dhivya[1] and Siddhan Sivakumar[2]

[1]Department of Mathematics,

[2]Department of Mechanical Engineering

Kumaraguru College of Technology, Coimbatore

Corresponding author E-mail: jdhivyamaths@gmail.com, sivakumar.siddhan.mec@kct.ac.in

Abstract:

Data Analytics is so-called the Science of analyzing data. It is used to convert information into knowledge. The contexts knowledge enables us to understand the world to make better decisions. In the last 20 years, the data analytics is the extensive and inspiring objectives to decreasing the costs to collect and process the data by creating the stronger motivation to problem solving. Data Analytics are driving with certain mathematical models. These models involve various areas of the mathematical domain including statistics, linear regression, differential and integral calculus. Furthermore, the concept of the fuzzy set theory is applied to big data analysis. The proposed work can create the opportunities for big data research and development. This chapter present the big data analytics techniques and focus on to deliberate the importance of mathematics behind data analytics and discussed some of the different types of data analytics.

Keywords: Big Data (BD), Artificial Intelligence (AI), Machine Learning (ML), Data Mining (DM)

Introduction:

Today era Internet search, social media, healthcare and cybersecurity are increasing rapidly across a range of fields with volume, velocity and variety of data. These data are growing at a rate beyond our capacity to analyze them. Spreadsheets, databases, matrices and graphs are some of the tools are to be developed to operate these data as a whole set than as individual elements. This chapter presents the mathematical foundations of these data sets to apply many applications and technologies. To simplify the data various tools can be used in order to influence their mathematical similarities to solve big data challenges.

Developing big data tools is that necessary to have a background of mathematics. Education of mathematics is a critical component of big data equation. Mathematics is used in every aspect of the big data process from big data tool design to data collection, to

data analysis. Data analysis is a combination of statistics and computation to understand data for programming and decision making.

Big data is fundamentally data science on a large scale, and it involves the use of computers to take larger data sets and create intelligence in a fraction of the time with a human workspace. Statistics is a critical part of the whole operation and its formulas are the key to success. The core of computing these data using the languages Python, C++ and Java is derived from mathematical equations and some logic-based thinking is required to direct a computer. In general, the basis of all big data and computation are derived from mathematics.

Big data is growing industry made in all aspects of our lives. Mathematical education is a cornerstone of big data, many mathematicians who have an interest in coding and utilizing big data tools to build the recognition.

While emerging the mathematical process, to recognize the word "big" as a mathematical operator is approximately being modeled as a mathematical linguistic variable suitable for evaluation.

Big Data analytics

Today's world is around with amount of data being generated worldwide in a huge amount. Big data analytics provides better decision making and prevent fraudulent activities among other activities. Traditional tools do not support the massive amount of data sets that cannot be stored, processed, or analyzed.

Data sources are present across the world at a rapid rate. These data are existing in different formats, like structured data, semi-structured data, and unstructured data. Big data analytics is the process of examining large data sets containing a variety of data types. The analytical findings in datasets can lead to more effective marketing, new revenue opportunities, better customer service and other business benefits. The primary goal of big data analytics is to help companies to make better decision by enabling data scientists and to analyze large volumes of transaction data.

Types of Big Data Analytics

Four different types of Big Data analytics are

2.1.1. Descriptive Analytics

This précises the past data and helps in generating reports.

Diagnostic Analytics

This analytic provides an in-depth intuition of a problem and helps to understand the cause of a problem.

Predictive Analytics

This is used to investigate the past and present data to make forecasts of the future. It is used in DM, AI, and ML to analyze current data and make predictions about the future.

Prescriptive Analytics

This kind of analytics recommends solutions for problems. It primarily relies on Artificial Intelligence (AI) and Machine Learning (ML) and works alongside descriptive and predictive analytics. Some of the major big data analytics tools include Hadoop, Talend, Cassandra, Spark, Storm, and Kafka, which help in storing, analyzing, and integrating datasets. Big data analytics is also actively used across various industries, including e-commerce, marketing, education, healthcare, media and entertainment, banking, telecommunications, and government.

A Mathematical Modeling for Big Data

The intention of this section is to propose a mathematical modeling for big data can accomplish a mathematical structure and framework for the BIG data. The two basic characteristics for big data modeling; mathematical operator for BIG and to examine the cardinality of big data. Further it will provide a mathematical model for searching big data.

Mathematical operator for BIG data theory

The concept of discrete mathematics theory [9,10] is used to create a theory for big data. In order to visualize the concept of linguistic variables in fuzzy set, and logic theory allows us to deal with a big data theory. First, some rigorous definitions will be introduced.

Definition 3.1.1.

Let A be a nonempty set, a function B: $A \to A$ is called a BIG operation B if and only if for any $x \epsilon A$, $B(x) = big$. A can be a collection of different computing tasks to be performed on data. The bulk action is used to transform the collection of the computing tasks into a BIG data condition.

The operation B has several important properties. Let the symbol + represent a logical operation “and” in a natural language [9].

(1) Distributive law. The operation B is distributive, that is, for any $x, y \epsilon A$, $B(x + y) = B(x) + B(y) = big\ x + big\ y$

(2) Commutative law with +. The operation B is commutative with +. In other words, for any

, $y \epsilon A$, $B(x + y) = B(x) + B(y) = B(y) + B(x) = B(y + x)$

(3) Element-wise application of B. Let $(x, y) \epsilon A \times A$ be a vector, then $B(x, y) = (Bx, By) = (big\ x, big\ y)$.

Example 3.1.1:

Data analytics is a set of tasks [12,13] as expressed in the following equation:

Data analytics = Data + Data analysis + Data Warehousing + Data mining + Statistical modeling

+ Machine Learning + Visualization. -------- (1)

The symbol + represents the logical "and".

Performing BIG operator *B* on both sides of Eq. (1), we have

B(Data analytics) = *B(*Data) + *B* (Data analysis) + *B* (Data Warehousing) + *B* (Data mining) + *B*

(Statistical modeling) + *B* (Machine Learning) + *B* (Visualization)

By operating on both sides of Eq. (1),

Big Data analytics = Big Data + Big Data analysis + Big Data Warehousing + Big Data mining + Big Statistical modeling + Big Machine Learning + Big Visualization.

It is important to note that big analytics, big services and big intelligence are three stand out characteristics of big data [14]. It is also interesting to note that big information, big knowledge and big wisdom can be the natural consequences of the operation *B*, respectively.

Volume, velocity, variety and veracity are the four basic attributes of big data analytics. This can be represented as data = (Volume, velocity, variety, veracity) [11,16]. Performing BIG operation *B* on both sides, we have

B(data) =*B* (Volume, velocity, variety, veracity)

Big data = (big volume, big velocity, big variety, big veracity)

These are the mainly "big" characteristics of big data.

Cardinality of big data

The cardinality issues of big data are deals in this subsection by invoking mathematical concept and its approach concerning the big volume of data. Many research papers have addressed big data by considering volume as the very first attribute for big data [15,16,17]. To explore the cardinality of big data in depth aa follows:

Definition 3.2.1. Let S be a set. The cardinality of the set S is n, denoted by $|S| = n$, if there are exactly n distinct elements in S, where n is a nonnegative integer [9].

An attribute value can be denoted as v. For example, v_1=big, v_2=data, v_3=analytics, v_4=intelligence, and so on. In terms of searching online these values can be considered as key words.

Mathematical modeling for searching big data

Here a mathematical approach is proposed to be concerning the issues of searching the big data

Let the document on the Web be $u \in U$, may be a .docx of .pdf and the attribute values $v \in V$, may be a word such as "big" or "data" or "analytics".

Definition 3.3.1:

A search function, denoted as s: $V \longrightarrow U$, is defined as $s(v) = u$, if $v \in u$.

Definition 3.3.2:

A search function s can be defined as $s(v) = F(v)$, ---------- (2)

where $F(v) = \{u_i , if\ v \in u_i , u_i \in U, i = \{0, 1,2, \dots , m\}\}$

This is valid search practice in the search engines. One keyword search corresponds to at least a picture, documents as the search results. When search big data, one can receive more results. Therefore, $F(v) \subseteq U$. When i=o, no researched results were received.

Let v_1, v_2, $v_3 \in V$, then using Equation (2), $s(v_1) = F(v_1)$, $s(v_2) = F(v_2)$, $s(v_3) = F(v_3)$. Then the following properties holds [9]:

$s(v_1 \vee v_2) = s(v_1) \cap s(v_2) = F(v_1) \cap F(v_2)$,

Where $\vee$ is a space operation between v_1 and v_2, to reflect the search using search engine. This is like concatenate the data items in linguistics or formal language. This satisfies that s(big data analytics) < min{s(big data), s(analytics)} = $s(v_1 \vee v_2)$. This result implies that the semantic union is different from the union in mathematics.

Analyzing the Mathematical Modelling Process

Borromeu Ferri & Blum (2010) shows that a mathematical modelling process as a sequence of predefined steps (Figure 1). According to these steps are sequentially taken as soon as the task is assigned. The first step in this series consists of building a model in order to figure out a situation, which is then simplified, structured, and idealized, when associations are made between the situation evaluated and mathematics. From this idealization, the structure is interpreted from the mathematical standpoint and mathematically treated until results are reached, which likewise are of mathematical nature. These results are then interpreted in light of the actual situation and subsequently validated. This cycle ends with the presentation of the results obtained. When no such results are achieved, the cycle is restarted.

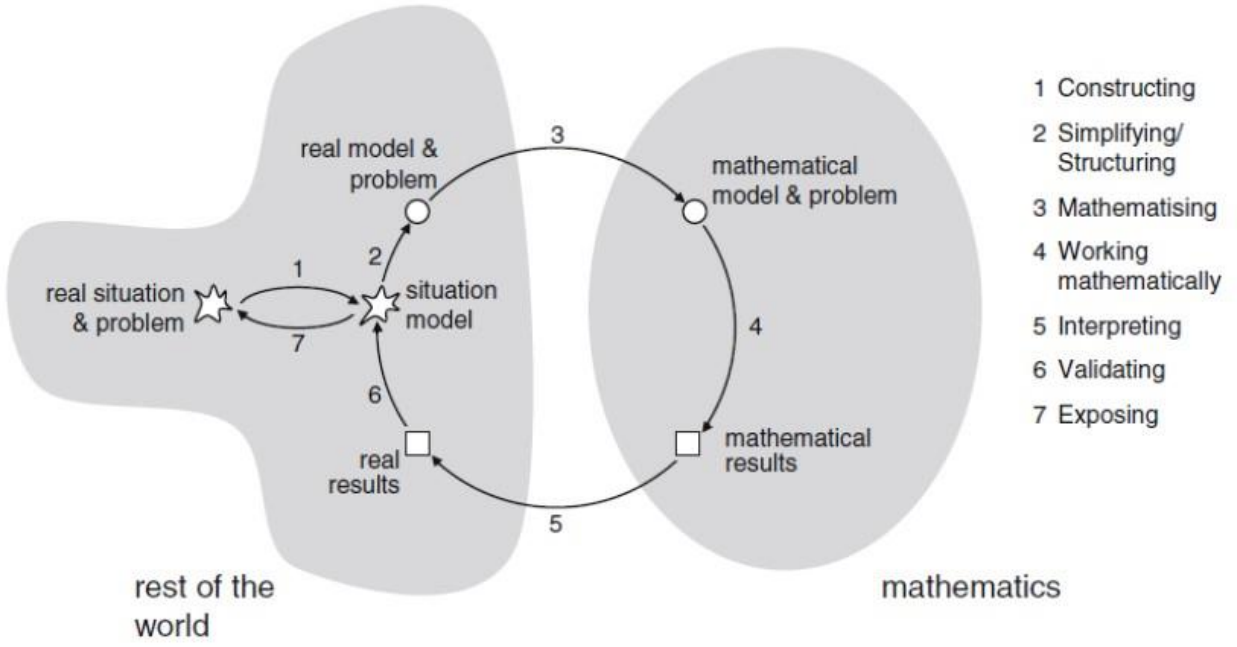

Fig. 1: Modelling Cycle

Mathematical modelling process as defined by Borromeu Ferri & Blum (2010) the model should be reviewed in the attempt to replicate the actual situation. In other words, it was the reference system that was adapted to fit the actual model. As a result, when the reference system is the experienced reality, the model is refuted. Conversely, in the cyberworld, this reference system may be refuted, though the main idea in the given situation is preserved aspects.

Conclusion:

Mathematical modelling is an important tool in big data analytic settings. The development in big data analytics not only require more computer speed and memory capacity, but also new advanced mathematics.

References:

1. Kumar, B. (2015). An encyclopedic overview of 'big data' analytics. *International Journal of Applied Engineering Research, 10*(3), 5681–5705.
2. McKinsey. (2014). *The digital tipping point: McKinsey Global Survey Results*. http://www.mckinsey.com/insights/business technology/the digital tipping point mckinsey global survey results
3. Manyika, J., Chui, M., & Bughin, J. (2011). *Big data: The next frontier for innovation, competition, and productivity*. http://www.mckinsey.com/business-functions/businesstechnology/ourinsights/big-data-the-next-frontier-for-innovation

4. Chen, C. P., & Zhang, C.-Y. (2014). Data-intensive applications, challenges, techniques and technologies: A survey on Big Data. *Information Sciences, 275*, 314–347.
5. Laval, P. B. (2015). *The mathematics of Big Data*. http://math.kennesaw.edu/plaval/math4490/fall2015/mathsurvey_def_slide.pdf
6. Peters, T. J. (2015). *Mathematics in Data Science*. http://www.engr.uconn.edu/tpeters/MaDS.pptx
7. Minelli, M., Chambers, M., & Dhiraj, A. (2013). *Big Data, Big Analytics: Emerging Business Intelligence and Analytic Trends for Today's Businesses*. John Wiley and Sons.
8. IBM. (2015). *The Four V's of Big Data*. http://www.ibmbigdatahub.com/infographic/four-vsbigdata
9. Sun, Z., & Xiao, J. (1994). *Essentials of Discrete Mathematics, Problems and Solutions*. Hebei University Press.
10. Johnsonbaugh, R. (2013). *Discrete Mathematics* (7th ed.). Pearson Education Limited.
11. Coronel, C., Morris, S., & Rob, P. (2015). *Database Systems: Design, Implementation, and Management* (11th ed.). Course Technology, Cengage Learning.
12. Sun, Z., Strang, K., & Yearwood, J. (2014). Analytics service oriented architecture for enterprise information systems. In *Proceedings of iiWAS2014* (pp. 506–518). ACM Press. https://doi.org/10.1145/2684200.2684358
13. Sun, Z., Strang, K., & Firmin, S. (2016). Business analytics-based enterprise information systems. *Journal of Computer Information Systems*. https://doi.org/10.1080/08874417.2016.1183977
14. Sun, Z., Strang, K., & Li, R. (2017). 10 Bigs: A service-oriented foundation for big data. *Submitted to the Journal of the Association for Information Systems*.
15. McAfee, A., & Brynjolfsson, E. (2012). Big data: The management revolution. *Harvard Business Review, 90*(10), 61–68.
16. Chen, P. P. (1976). The entity-relationship model—Toward a unified view of data. *ACM Transactions on Database Systems, 1*(1), 9–36.
17. Sun, Z., Zou, H., & Strang, K. (2015). Big data analytics as a service for business intelligence. In *Proceedings of the 14th IFIP Conference on e-Business, e-Services and e-Society* (Vol. 9373, pp. 200–211). Springer. https://doi.org/10.1007/978-3-319-25013-7_16
18. Minelli, M., Chambers, M., & Dhiraj, A. (2013). *Big Data, Big Analytics: Emerging Business Intelligence and Analytic Trends for Today's Businesses* (Chinese ed.). Wiley & Sons.

THE IMPORTANCE OF MATHEMATICAL EDUCATION IN THE DAY-TO-DAY LIFE OF EVERY HUMAN BEING

Abhijeet Deepak Yadav
Department of Mathematics,
Khare Dhere Bhosale College Guhagar, Dist. Ratnagiri, Mumbai University, 415703,
Corresponding author E-mail: adyadavkdbc@gmail.com

Abstract:
Mathematics is not only a subject confined to the classroom but an integral part of everyday life. From budgeting finances to measuring ingredients for a recipe, mathematical concepts govern the way we interact with the world. This research article delves into the significance of mathematical education, emphasizing how mathematics impacts daily decisions and problem-solving. It explores the role of mathematics in personal development, professional environments, and societal advancements, advocating for its continued inclusion in the educational curriculum.

Introduction:
Mathematics is often perceived as an abstract and theoretical field, separated from the practicalities of everyday life. However, this perception is far from accurate. Mathematics plays a vital role in numerous aspects of our daily routines. From managing personal finances to understanding the layout of spaces, mathematical principles govern many of the decisions and actions we take. Therefore, having a solid foundation in mathematical education is not just beneficial but essential for navigating modern life efficiently.
In this article, we explore the importance of mathematical education and its undeniable relevance in personal and professional contexts. The goal is to show that mathematics is not a specialized subject, but a universal tool that influences how individuals understand and engage with the world.

Mathematical Education in Daily Life:

1. Problem-Solving and Logical Thinking:
One of the most significant contributions of mathematical education is the development of problem-solving and logical thinking skills. Mathematics challenges individuals to approach problems methodically and think critically about how to apply concepts in real-world scenarios. This ability to break down complex issues into simpler, manageable components

is invaluable in every aspect of life, from making informed financial decisions to troubleshooting problems at work or home.

For example, if someone is trying to calculate the most cost-effective way to purchase groceries for the month, they will use basic arithmetic and percentages to compare prices, apply discounts, and estimate total costs. The ability to think critically and solve such problems is rooted in the mathematical knowledge acquired through education.

2. Financial Literacy:

Mathematical education is central to achieving financial literacy, a skill that is critical for managing personal finances effectively. Individuals with a sound understanding of mathematics can manage budgets, understand interest rates, and make informed decisions about savings and investments. From calculating monthly expenses to understanding credit card interest or loan repayments, basic mathematical principles are essential for maintaining financial well-being.

Consider the process of saving for a long-term goal, such as a house or education. Understanding the concepts of interest rates, compound interest, and financial planning allows individuals to set realistic savings goals and track progress over time. A strong mathematical foundation equips people with the tools they need to make informed financial decisions and avoid debt traps.

3. Time Management:

Effective time management is another area where mathematics is directly applied. Scheduling, planning, and organizing tasks involve calculating time intervals, setting priorities, and balancing different commitments. Whether it is determining how long it will take to complete a task or planning how to distribute activities throughout the day, time management is often rooted in basic mathematical calculations.

For instance, estimating travel times, calculating how much time remains for study or leisure, or planning a day efficiently all require mathematical reasoning. A deep understanding of time management can lead to improved productivity and a more balanced life.

Mathematical Education in Professional Life:

1. Scientific and Technological Advancements:

The influence of mathematics extends beyond the individual to larger societal structures, especially in the fields of science, technology, and engineering. Many of the breakthroughs in these fields rely heavily on advanced mathematical principles. Whether it is developing

new software, designing bridges, or analysing medical data, mathematics serves as the foundation for countless innovations that shape the modern world.

Professionals working in fields such as engineering, medicine, computer science, and data analysis rely on complex mathematical models to solve real-world problems. Mathematical education, therefore, is a prerequisite for entering such careers and contributing to technological advancements that improve quality of life.

2. Business and Economics:

In the business world, mathematical concepts are used for strategic decision-making, such as determining pricing strategies, analysing market trends, and maximizing profits. Concepts like statistics, probability, and optimization are widely applied in the financial and economic sectors to assess risks, forecast future trends, and develop effective business strategies.

For example, business professionals use financial modelling, risk analysis, and statistical techniques to make informed decisions about investments, resource allocation, and market positioning. Mathematical education in these fields empowers individuals to interpret data accurately and use it to drive business success.

The Role of Mathematics in Social Contexts:

1. Understanding the World Around Us:

Mathematics helps individuals understand and interpret the world in which they live. From navigating streets and cities to calculating distances on a map, mathematical skills are essential for spatial awareness. In addition, mathematical education allows individuals to appreciate and engage with the complexities of the world around them, from the symmetry in nature to the physics of motion.

Math is also crucial for understanding social phenomena. For example, understanding percentages can help individuals grasp the impact of social and political issues, such as voter turnout or public health statistics. This understanding empowers individuals to make informed decisions about civic engagement and societal contributions.

2. Democracy and Citizenship:

In a democratic society, mathematical education plays a key role in fostering an informed citizenry. Voters need to understand polling data, electoral systems, and the mathematics of voting to participate meaningfully in elections. Understanding the concepts of probability and statistics can help individuals interpret the reliability of election results and survey data.

The Importance of Continued Mathematical Education:

As technology continues to advance, the role of mathematics in everyday life becomes increasingly prominent. The rise of automation, artificial intelligence, and data science all require a solid understanding of mathematical concepts. From understanding algorithms used in social media to ensuring that data privacy laws are respected, mathematics is essential for navigating the digital age. Furthermore, as the global economy becomes more interconnected, individuals with strong mathematical skills will have a competitive advantage in the job market. As such, educational systems must place a greater emphasis on mathematical education at all levels to prepare individuals for the challenges of the future.

Conclusion:

Mathematical education is not merely an academic pursuit but a vital life skill that impacts individuals in both personal and professional contexts. Whether it is managing finances, solving everyday problems, or contributing to scientific and technological advancements, mathematics plays a crucial role in shaping how individuals understand and engage with the world. The continued integration of mathematics into educational curricula is essential for fostering informed, skilled, and capable citizens who can navigate the complexities of modern life.

Ultimately, the importance of mathematical education lies in its ability to empower individuals to make informed decisions, solve problems efficiently, and contribute meaningfully to society. By emphasizing the relevance of mathematics in day-to-day life, we can cultivate a generation that is equipped with the skills necessary to thrive in an increasingly complex world.

References:

1. Stewart, J. (2016). Calculus: Early Transcendentals (8th ed.). Brooks/Cole.
2. Niss, M. (2007). The Role of Mathematics in the Modern World. Springer.
3. Devlin, K. (2010). Mathematics: The New Golden Age. Wiley.
4. Polster, B. (2006). The Mathematical World. Springer.

FROM NUMBERS TO NARRATIVES: VISUALISING DATA IN SOCIAL SCIENCE RESEARCH

Poonam Angurala
Sri Guru RamDass College of Education, Pandher, Amritsar
Corresponding author E-mail: poonamangurala@gmail.com

1. Introduction:

Data visualisation has become an important part of the research. It helps researchers to present information in a clear and meaningful way. Instead of only using long tables, written reports, or numbers, researchers now use visuals like charts, graphs, and maps to better explain their findings. These visuals make it easier to understand complex data and to share research results with different audiences, including students, policymakers, and the general public.

Researchers study a wide range of topics in every field. These studies often involve large amounts of data, including numbers from surveys, text from interviews, or observations from fieldwork. Visualisation helps turn this raw data into stories, patterns, and insights that are easier to see and explain.

The use of visualisation also supports different parts of the research process. For example, during analysis, it helps identify trends or relationships between variables. During presentations or publications, it helps make the results more engaging and easier to follow.

With the rise of digital tools and technology, creating visualisations has become more accessible than ever before. Many tools are now available that allow researchers to create simple or advanced visuals without needing deep technical knowledge.

This chapter will explore how researchers use data visualisation in their work. It will cover the basic ideas behind visualisation, the types of data used in research, common visualisation techniques, and the tools available. The chapter will also discuss some challenges and ethical issues, and look at future trends in this growing area.

2. Theoretical Foundations of Data Visualisation

Understanding the theory behind data visualisation helps researchers use it more effectively. Data visualization tools are the software applications that enable users to create visualizations. Examples include Tableau, Power BI, Google Charts, and Python libraries like Matplotlib and Seaborn. are the methods and approaches used to select the most appropriate visual format (e.g., bar chart, line graph, scatter plot, map) for a particular

dataset and analytical goal. For example, a line graph might be best for showing trends over time, while a pie chart is suitable for displaying proportions.

This section explores how visualisation fits into the research process, the influence of different research approaches, the psychology of how we process visuals, and its role as a communication tool.

2.1. The Role of Visualisation in Research

Visualisation is not only a practical tool; it is also deeply connected to how knowledge is created, analysed, and shared in the social sciences. Thus, the goal of data visualization is to graphically present and explore abstract, non-physical and non-spatial data collected from databases, which could be possible through various tools and techniques. Visualisation serves two key roles in research:

a. Exploratory Visualisation

Exploratory visualisation is used during the early stages of data analysis. It helps researchers explore patterns, detect trends, and understand relationships in the data before they form final conclusions. For example, a scatter plot can show the relationship between income and education levels, or a line graph can highlight changes in public opinion over time.

This kind of visualisation is particularly helpful when working with large datasets. It can guide researchers toward important questions or unexpected findings that may not be obvious in tables or text.

b. Explanatory Visualisation

Once researchers have analysed the data and drawn conclusions, they often use explanatory visualisations to communicate their results to others. These visuals are designed to highlight key findings clearly and effectively. For example, a bar chart showing voter turnout in different regions can quickly inform a reader about political participation levels.

Explanatory visualisations are often included in research papers, presentations, reports, and media publications. They make it easier for non-experts, such as community leaders or policymakers, to understand the research and use it in decision-making.

2.2. Research Paradigms and Visualisation

Social science research is shaped by different paradigms—ways of thinking about how knowledge is created. These paradigms influence how data is collected, analysed, and visualised.

a. Positivist Paradigm

The positivist paradigm is based on the belief that reality can be measured and understood through objective observation and scientific methods. It often involves quantitative data such as numbers and statistics. In this approach, visualisation is used to represent measurable variables and relationships. Common types include:

- Line graphs to show trends over time
- Scatter plots to show correlations
- Histograms to show frequency distributions
- Box plots to show statistical summaries

These visualisations help test hypotheses and provide evidence for or against theoretical models.

b. Interpretivist Paradigm

The interpretivist paradigm focuses on understanding meaning, culture, and human experience. It usually involves qualitative data like interviews, focus group discussions, or open-ended survey responses. Here, visualisation is used not to prove a hypothesis, but to explore themes and represent ideas. Common types include:

- Concept maps to show relationships between ideas
- Timeline charts to show sequences of events in case studies
- Coding trees to visualise thematic analysis of text
- Word clouds to highlight frequent terms in qualitative data

These visuals support storytelling, reflection, and understanding of complex human behaviour.

2.3. Cognitive Aspects of Data Visualisation

Visualisation works because of how the human brain processes information. Research in cognitive psychology shows that people understand visuals faster than text. A well-designed graph can communicate ideas almost instantly, while it might take much longer to understand the same data in a table.

Here are a few key ideas from cognitive science:

- **Visual perception is quick**: Our brains are wired to detect shapes, colours, and patterns immediately.
- **Memory is improved by visuals**: People remember visual information better than plain text.

- **Comparison is easier with visuals**: Charts and graphs help us compare data quickly and easily.
- **Attention can be guided**: The use of colour, size, and position can draw attention to important points in the data.

However, visualisations must be designed carefully. A poorly made visual—with unclear labels, misleading scales, or too much information—can confuse or mislead the audience. Visual literacy, the ability to "read" and interpret visuals, is also important.

2.4. Visualisation as a Communication Tool

Visualisation is not only useful for researchers—it is also a way to communicate with people outside academia. In fields like public policy, education, healthcare, and social work, visualisations help share knowledge in ways that are simple, engaging, and persuasive.

For example:

- A heat map showing crime levels in different neighbourhoods can help city planners and police departments focus their efforts.
- An infographic showing gender gaps in education can raise awareness and support advocacy campaigns.
- A dashboard showing COVID-19 trends can inform public health decisions.

In these cases, visualisation plays a key role in knowledge translation—turning complex research findings into practical insights that can improve society.

In summary, data visualisation in social science is supported by several theoretical foundations. It helps researchers explore data and explain findings. It fits into different research traditions, from statistical models in positivist studies to thematic mapping in interpretivist research. It works well because of how our brains process visual information. And it plays an important role in communicating research to broader audiences.

3. Types of Data in Social Sciences

Social science research deals with many kinds of data, depending on the topic, research questions, and methods used. Understanding the different types of data is important because each type requires different visualisation techniques. In this section, we will explore the main categories of data used in social science research:

1. Quantitative,
2. Qualitative**,** and
3. Mixed Methods Data**.**

3.1. Quantitative Data

Quantitative data is numerical. It includes values that can be counted or measured, such as age, income, education level, or the number of people who agree with a statement. This type of data is often collected through surveys, experiments, or official statistics.

Examples:

- Responses from a public opinion poll
- Test scores from students in different schools
- Unemployment rates over the past 10 years
- Crime statistics by region

Common Visualisations:

Bar charts used for comparing values across different categories. They consist of rectangular bars, where the length of each bar is proportional to the value it represents. Bar charts can be displayed either vertically or horizontally and are ideal for comparing discrete, non-overlapping categories.	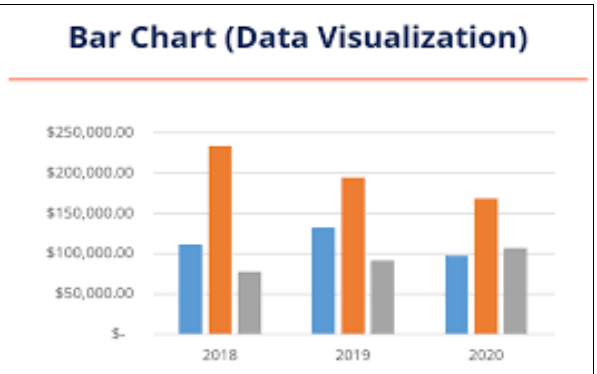
Line Graphs are used primarily to show trends or changes over time. Data points are plotted on a grid and connected by straight lines, with time usually represented on the x-axis and the values of interest on the y-axis. This type of chart is particularly effective for displaying continuous data, such as changes in population, temperature, or revenue over months or years.	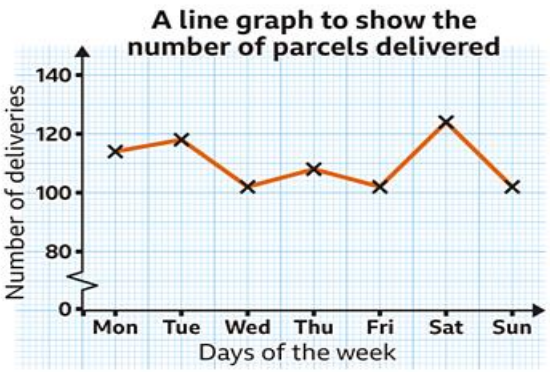

Pie Charts are circular graphs divided into slices, where each slice represents a portion of the whole. They are best used to show proportions or percentages and are most effective when you want to illustrate how a single category is divided into parts. Each segment of a pie chart corresponds to a specific category and its size reflects the category's contribution to the total.	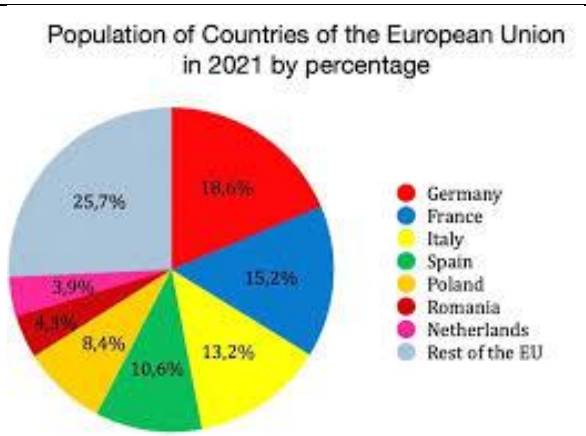
Scatter Plots are ideal for exploring the relationship between two numerical variables. Each point on a scatter plot represents an individual data observation, with one variable plotted along the x-axis and the other along the y-axis. Scatter plots are particularly useful for identifying correlations or patterns, such as a positive, negative, or no apparent relationship.	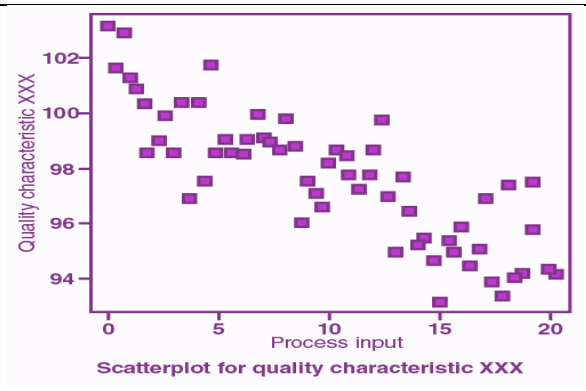
Histograms are used to display the distribution of a single continuous variable. They look similar to bar charts but serve a different purpose. Instead of showing categories, histograms show the frequency of data points falling within certain ranges or intervals, called bins. The x-axis represents these intervals, while the y-axis shows how many data points fall into each range.	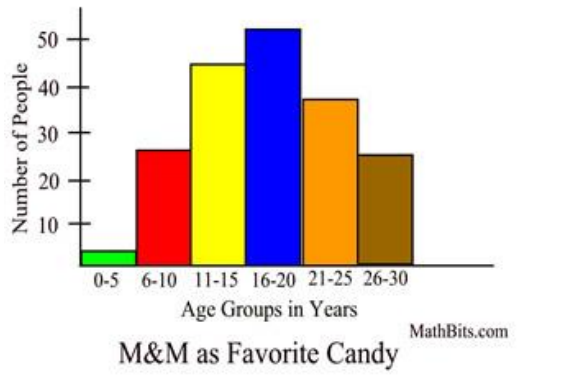

Quantitative visualisations are often used in disciplines like economics, political science, sociology, and education.

3.2. Qualitative Data

Qualitative data is non-numerical. It includes words, images, sounds, and observations that describe experiences, opinions, emotions, or behaviours. This type of data is collected

through methods such as interviews, focus groups, participant observation, or document analysis.

Examples:

- Interview transcripts with refugees about their migration experience
- Notes from observing classroom behaviour
- Social media posts expressing public opinion
- Newspaper articles discussing political protests

Common Visualisations:

<table>
<tr><td>Word clouds: Showing frequently used words in text data</td><td>Thematic maps or charts: Grouping qualitative codes or categories</td></tr>
<tr><td> 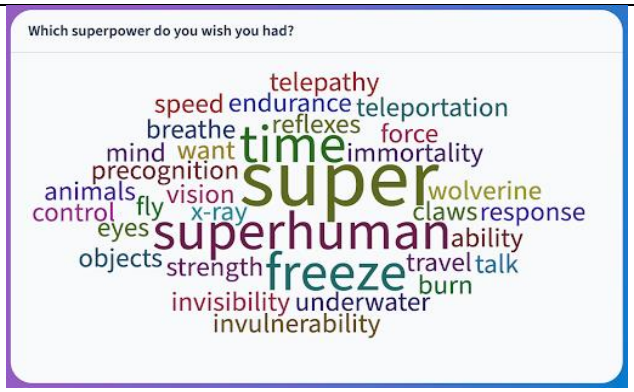
</td><td> 
</td></tr>
<tr><td>Timeline charts: Showing events or processes over time</td><td>Concept maps: Showing relationships between key ideas or themes</td></tr>
<tr><td> 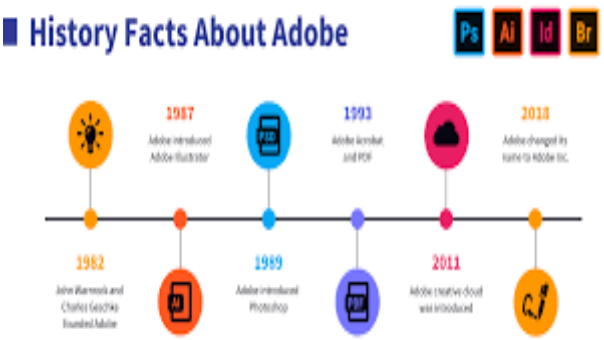
</td><td> 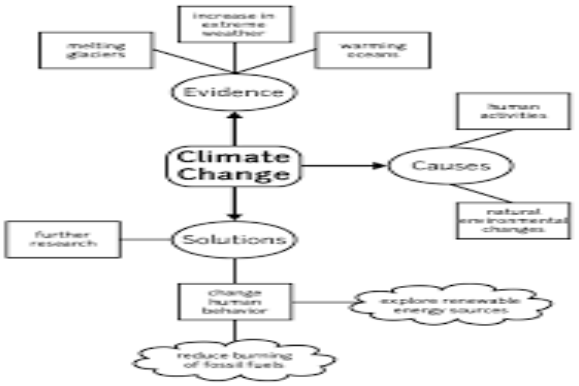
</td></tr>
</table>

Qualitative visualisations are useful in fields like anthropology, sociology, education, psychology, and cultural studies. These visuals help make abstract or complex ideas more understandable.

3.3. Mixed Methods Data

Mixed methods research combines both quantitative and qualitative data. This approach is used when researchers want to gain a more complete understanding of a topic by using numbers and narratives together.

Examples:

- A study on education quality that combines survey data (quantitative) with teacher interviews (qualitative)
- Research on healthcare access that uses patient statistics along with personal stories
- An evaluation of a government program that collects feedback through focus groups and performance indicators

Common Visualisations:

- **Dashboards**: Combining graphs, charts, and text summaries in one view
- **Infographics**: Merging statistics with quotes or images to tell a story

Mixed methods are especially popular in public health, education, development studies, and community research, where understanding both measurable outcomes and lived experiences is important.

3.4. Big and Unstructured Data in Social Sciences

With advances in technology, social scientists are increasingly working with **big data** and **unstructured data**, such as social media posts, videos, or online behaviours. These datasets are often large, complex, and messy, but they can offer new insights when visualised effectively.

Examples:

- Twitter data on public reactions to political events
- YouTube video comments related to social issues
- Online discussion forums about mental health

Common Visualisations:

- **Network diagrams**: Showing connections between people, groups, or ideas
- **Heat maps**: Showing intensity or frequency (e.g., locations of tweets during a protest)
- **Trend lines**: Tracking volume or sentiment over time
- **Text analytics visuals**: Showing sentiment, key phrases, or topic clusters.

These types of visualisations are becoming more common in digital sociology, media studies, political communication, and computational social science.

Social science research uses many kinds of data, each with its own strengths and challenges. Quantitative data is about numbers and is often shown in graphs and charts. Qualitative data is about words and meanings and is shown in diagrams or themes. Mixed methods use both and offer a richer understanding. With growing access to digital data, social scientists are also learning new ways to visualise large and complex information.

4. Tools and Software for Visualisation in Social Sciences

Selecting the right tool for data visualisation depends on the research design, data type, user skill level, and intended audience. In social sciences, tools range from basic spreadsheet software to advanced programming environments and specialised qualitative analysis platforms. This section introduces commonly used tools, their features, and use cases.

5.1. Spreadsheet Software

a. Microsoft Excel / Google Sheets

These are widely accessible tools for basic data handling and visualisation.

- **Best For**: Creating simple charts (bar, line, pie, scatter), filtering data, and summarising results
- **Strengths**: Easy to use, widely available, supports basic statistical functions
- **Limitations**: Limited customisation, not suitable for large or complex datasets

Feature	Excel / Google Sheets
User-friendly	✅ Very easy to learn
Chart types	✅ Bar, Line, Pie, Scatter
Suitable for beginners	✅ Yes
Cost	Excel (paid), Google Sheets (free)

5.2. Statistical Software

a. SPSS (Statistical Package for the Social Sciences)

Designed for social scientists, SPSS is a user-friendly tool for statistical analysis and visualisation.

- **Best For**: Quantitative research, survey analysis, hypothesis testing
- **Strengths**: Point-and-click interface, ready-made visual outputs

- **Limitations**: Expensive, limited customisation in graphics

b. R (with GGPlot2)

R is a programming language for statistical computing and graphics.

- **Best For**: Customised statistical charts, advanced data analysis
- **Strengths**: Powerful, flexible, open-source
- **Limitations**: Steep learning curve.

C. Python (With Matplotlib/Seaborn/Plotly)

Python is another powerful programming language with strong visualisation libraries.

- **Best For**: Interactive, publication-ready visualisations; automation
- **Strengths**: Highly customisable, open-source
- **Limitations**: Requires coding knowledge

Software	Use Case	Skill Level	Customisation	Cost
SPSS	Survey analysis, stats	Beginner	Low	Paid
R	Custom stats, modelling	Intermediate	High	Free
Python	Automation, interactivity	Intermediate	High	Free

5.3 Visualisation and Dashboard Tools

a. Tableau

A powerful tool for building interactive and visually appealing dashboards.

- **Best For**: Mixed-methods data, dashboards for policy/public use
- **Strengths**: Drag-and-drop interface, interactive charts
- **Limitations**: Paid license for full features

b. Power BI

A Microsoft product similar to Tableau, popular in business and research analytics.

- **Best For**: Reports and dashboards from multiple data sources
- **Strengths**: Integration with Excel, strong data processing
- **Limitations**: Windows-only for full features

c. Flourish

A browser-based tool for creating animated and interactive charts and infographics.

- **Best For**: Web publishing, storytelling with data
- **Strengths**: No coding required, attractive visuals
- **Limitations**: Some features behind paywall

Tool	Interactive?	Learning Curve	Suitable For	Cost
Tableau	✅	Medium	Dashboards	Paid / Free Public
Power BI	✅	Medium	Business/research	Free / Paid
Flourish	✅	Low	Public communication	Free / Paid

5.4 Qualitative Data Analysis Software (QDAS)

a. NVivo

A leading tool for qualitative and mixed-methods research.

- **Best For**: Coding interviews, creating word clouds, thematic maps
- **Strengths**: Easy-to-use visuals, great for text-heavy projects
- **Limitations**: Paid software, steep for beginners

b. ATLAS.ti

Another popular QDAS platform with strong visualisation options.

- **Best For**: Organising and visualising qualitative data
- **Strengths**: Strong coding tools, network views
- **Limitations**: Learning curve, paid license

Software	Focus Area	Visual Features	Cost
NVivo	Text coding, themes	Word clouds, coding trees	Paid
ATLAS.ti	Text and media	Network diagrams	Paid

5.5 Mapping and Spatial Tools

a. QGIS (Quantum GIS) / ArcGIS

Used for spatial analysis and geographic data visualisation.

- **Best For**: Creating choropleth maps, location-based analysis
- **Strengths**: Handles complex spatial data
- **Limitations**: Requires training

b. Google Maps / Google My Maps

User-friendly tools for simple geographic visualisations.

- **Best For**: Community research, plotting locations
- **Strengths**: Easy and accessible
- **Limitations**: Limited analytical features

Tool	Type	Complexity	Example Use	Cost
QGIS / ArcGIS	Professional	High	Crime map, migration flow	Free / Paid
Google Maps	Basic	Low	Field site map	Free

"The greatest value of a picture is when it forces us to notice what we never expected to see." This insight highlights the importance of selecting the right visualisation tool, as each method has its own strengths and limitations. The choice should be carefully guided by the nature of the data, the objectives of the research, and the technical proficiency of the researcher, ensuring that the visualisation effectively communicates the intended insights.

5. Best Practices and Common Pitfalls in Social Science Visualisation

Creating effective visualisations in social science research requires both technical skill and thoughtful design. While tools can generate graphs and charts, the impact of your visualisation depends on how well it communicates the intended message.

This section outlines best practices to follow and common mistakes to avoid when visualising social science data.

5.1. Best Practices in Data Visualisation

1. **Know Your Audience:** Tailor your visuals based on who will use or interpret them. For example, policymakers may prefer summary dashboards, while academics may appreciate detailed statistical plots.
2. **Choose the Right Chart Type:** Use chart types that match your data and the story you want to tell. Use Bar charts for comparison, Line graphs for trends over time, Pie charts for parts of a whole, Maps for geographic data, Word clouds or coding trees for qualitative themes etc.
3. **Highlight the Key Message**: Use color, labels, or annotations to draw attention to the most important findings. Every visual should have a clear takeaway.
4. **Label Everything Clearly**: Ensure titles, axis labels, legends, and data sources are easy to understand. Avoid abbreviations unless they are explained.
5. **Use Consistent Colors and Styles:** Apply the same formatting across charts to ensure a unified look. This is especially important in reports or presentations with multiple visuals.
6. **Keep it Simple:** Avoid using 3D effects, gradients, or too many colors. Simpler charts are easier to read and interpret.

7. **Check Accessibility**: Use colorblind-friendly palettes, readable font sizes, and provide textual descriptions for important visuals, especially in digital reports.
8. **Use Visuals to Complement, Not Replace Text**: Visuals should support your analysis and conclusions. Always explain what the visual shows and why it matters.

5.2. Common Mistakes to Avoid

1. **Using the Wrong Chart Type**: Like A pie chart with too many slices becomes hard to read. Instead, use a bar chart.
2. **Ignoring the Scale**: Truncated axes or inconsistent scales can distort findings and mislead the reader.
3. **Overloading with Information**: Avoid including too much data in one chart. Instead, break it into smaller, focused visuals.
4. **Poor Color Choices**: Using too many colors or hard-to-read combinations (like red on green) can reduce clarity and accessibility.
5. **Missing Context**: Charts without titles, labels, or source notes can confuse readers or lead to misinterpretation.
6. **Misleading Design**: Using 3D effects or manipulating axis scales to exaggerate trends is considered unethical in research communication.
7. **Lack of Data Cleaning**: Visualising messy or inconsistent data leads to inaccurate conclusions. Always clean and verify your data first.

Conclusion:

Effective data visualisation is far more than a technical skill—it is a powerful form of communication that sits at the core of rigorous and impactful research. For social scientists, developing visual literacy is essential not only for engaging diverse audiences but also for informing policy decisions, shaping public discourse, and contributing to the advancement of knowledge in an increasingly data-driven world.

Each visualisation method brings unique strengths and limitations, and selecting the most appropriate tool requires careful consideration. This choice should be informed by the nature and structure of the data—whether categorical, numerical, or time-based—as well as the specific objectives of the research, such as uncovering patterns, comparing variables, or illustrating relationships. Equally important is the researcher's technical proficiency and their ability to apply visualisation techniques thoughtfully and effectively.

A well-designed visualisation does more than present data; it tells a story, enhances comprehension, and fosters deeper insights. To achieve this, researchers must follow best practices—ensuring that visuals are simple, relevant, and clearly labeled—while avoiding common pitfalls such as cluttered layouts, ambiguous scales, or misleading representations.

Ultimately, the goal of data visualisation in social research is not only to make data accessible, but to do so ethically, accurately, and with purpose. When done well, visualisations become a vital bridge between complex information and meaningful understanding, empowering both researchers and their audiences to see more clearly—and think more critically—about the world around them.

References:

1. *InfoGuides: Digital Humanities and Social Sciences: Data Visualization*. (n.d.). https://infoguides.rit.edu/dhss/tools/data_visualization
2. Lavanya, A., Sindhuja, S., Gaurav, L., & Ali, W. (2023). A comprehensive review of data visualization tools: features, strengths, and weaknesses. *International Journal of Computer Engineering in Research Trends*, *10*(1), 10–20. https://doi.org/10.22362/ijcert/2023/v10/i01/v10i0102
3. *Presentation-Oriented visualization techniques*. (2016, February 1). IEEE Journals & Magazine | IEEE Xplore. https://ieeexplore.ieee.org/abstract/document/7383166
4. Sardareh, S. A., Brown, G. T. L., & Denny, P. (2021). Comparing four contemporary statistical software tools for introductory data science and statistics in the social sciences. *Teaching Statistics*, *43*(S1). https://doi.org/10.1111/test.12274
5. Srivastava, D. (2023). An introduction to data visualization tools and techniques in various domains. *International Journal of Computer Trends and Technology*, *71*(4), 125–130. https://doi.org/10.14445/22312803/ijctt-v71i4p116
6. Visualizing social science research. (n.d.). In *Visualizing Social Science Research*. https://cmn-cdn-001.sagepub.com/books/titles/235388/att_sb1_41669.pdf
7. Zinovyev, A. (2010, August 6). *Data visualization in political and social sciences*. arXiv.org. https://arxiv.org/abs/1008.1188

EXISTENCE AND STABILITY RESULTS FOR BOUNDARY VALUE PROBLEM FOR NONLINEAR FRACTIONAL DIFFERENTIAL EQUATIONS WITH POSITIVE CONSTANT COEFFICIENT

Shivaji Tate

Department of Mathematics,

Kisan Veer Mahavidyalaya, Wai Maharashtra 412803, India

Corresponding authors E-mail: tateshivaji@gmail.com

Abstract:

The aim of this chapter is to establish sufficient conditions for the existence, uniqueness and Ulam-type stability of solutions for a class of boundary value problem for nonlinear fractional differential equation with positive constant coefficient. Finally, an examples is given to demonstrate applicability of our results.

Keywords: Boundary value conditions, Caputo's fractional derivative, Existence of solution, Fixed point, Stability.

Introduction:

The concept of fractional differentiation was introduced in the 19^{th} century by Riemann and Liouville. It is the generalization of integral order differentiation and integration to arbitrary non-integer order. For detailed study, see the books such as [16, 17] and the survey papers [2, 3] and the references therein.

Recently, fractional differential equations have been proved to be valuable tools in the modeling of many phenomena in various fields such as control theory, signal processing, rheology, fractals, chaotic dynamics, modelling, bioengineering and biomedical applications and so on. For example, see the books such as [14, 22] and the references therein. Due to its importance in different fields, researcher in this area has grown significantly all around the world.

The stability problem of functional equations was introduced by Ulam [23, 24] and Hyers [9] which is known as Hyers-Ulam stability. Rassias [18] studied the Hyers-Ulam stability of linear and nonlinear mapping. Jung [11, 12] established Hyers-Ulam stability for more general mapping on restricted domain. Obloza [15] was the first author who studied the Hyer-Ulam stability of linear differential equations. For detailed study of Ulam-type

stability with different approaches, we refer the reader to the papers [1, 10, 18, 21, 21, 26, 27, 28] and the books [8, 19, 20].

In [4], Benchohra and Bouriahi studied existence and stability of solutions for a class of boundary value problem for implicit fractional differential equations of the type:

$$^{c}D^{\alpha}y(t) = f(t, y(t), {}^{c}D^{\alpha}y(t)), t \in J := [0, T], T > 0,$$
$$ay(0) + by(T) = c$$

where $^{c}D^{\alpha}(0 < \alpha \leq 1)$ denotes the caputo fractional derivative, $f: J \times \mathbb{R} \times \mathbb{R} \to \mathbb{R}$ is a given continuous function, and a, b, c are real constants with $a + b \neq 0$.

In [5], Benchohra *et al.* studied the existence of solutions for a class of boundary value problem for fractional differential equations and nonlocal boundary condition of the form:

$$^{c}D^{\alpha}y(t) = f(t, y(t)), t \in J := [0, T], T > 0$$
$$y(0) = g(y), y(T) = y_T$$

where $^{c}D^{\alpha}(1 < \alpha \leq 2)$ denotes the caputo fractional derivative, $f: J \times \mathbb{R} \to \mathbb{R}$ is a given continuous function, $g : C(J, \mathbb{R}) \to \mathbb{R}$ is a continuous function and y_T is a real constant.

Motivated by the above-mentioned work, in this paper, we establish sufficient conditions for the existence, uniqueness and four types of Ulam stability, namely Ulam- Hyers stability, generalized Ulam-Hyers stability, Ulam-Hyers-Rassias and generalized Ulam-Hyers-Rassias stability for the following nonlinear fractional differential equation with constant coefficient $\lambda > 0$ of the type:

$$^{c}D^{\alpha}y(t) = \lambda y(t) + f(t, y(t)), t \in J := [0, T], T > 0, \quad (1.1)$$
$$ay(0) + by(T) = c \quad (1.2)$$

Where $^{c}D^{\alpha}(1 < \alpha \leq 2)$ denotes the caputo fractional derivative, $f: J \times \mathbb{R} \to \mathbb{R}$ is a given continuous function, and a, b, c are real constants with $a + b \neq 0$.

This type of non-local Cauchy problem was introduced by Byszewski [6, 7]. The nonlocal condition can be more useful than the classical initial condition to describe some physical phenomenons [6, 7].

Preliminaries and Notations

In this section, we will introduce some definitions, notations and results which are used throughout this paper. By $C(J, \mathbb{R})$ we denote the banach space of continuous functions from J into $\mathbb{R}$ with the norm

$$\|y\|_{\infty} = \sup\{|y(t)|: t \in J\}$$

By $L^1(J)$ we denote the space of Lebesgue-integrable functions $y: J \to \mathbb{R}$ with the norm

$$\|y\|_{L^1} = \int_0^T |y(t)|dt$$

Definition 2.1. [17] The Riemann-Liouville fractional (arbitrary) order integral of the function $h \in L^1([0,T],\mathbb{R}_+)$of order $\alpha \in \mathbb{R}_+$is defined by

$$I^{\alpha}h(t) = \frac{1}{\Gamma(\alpha)}\int_0^t (t-s)^{\alpha-1}h(s)ds$$

where Γ is the Euler gamma function defined by $\Gamma(\alpha) = \int_0^{+\infty} t^{\alpha-1}e^{-t}dt, \alpha > 0$.

Definition 2.2. [14] The Caputo fractional derivative of order $\alpha > 0$ of a function $h \in L^1([0,T],\mathbf{R}_+)$is given by

$$({}^cD^{\alpha}h)(t) = \frac{1}{\Gamma(n-\alpha)}\int_0^t (t-s)^{n-\alpha-1}h^{(n)}(s)ds$$

where $n = [\alpha] + 1$ and $[\alpha]$ denotes the integer part of the real number α.

Lemma 2.1. [14] Let $\alpha > 0$ and $n = [\alpha] + 1$, then

$$I^{\alpha}({}^cD^{\alpha}f(t)) = f(t) - \sum_{k=0}^{n-1}\frac{f^k(0)}{k!}t^k$$

where $f^k(t)$ is the usual derivative of $f(t)$ of order k.

Lemma 2.2. [17] Let $\alpha > 0$. Then the fractional differential equation

$${}^cD^{\alpha}h(t) = 0,$$

has a solutions $h(t) = c_0 + c_1t + c_2t^2 + \cdots \ldots . + c_{n-1}t^{n-1}$, where $c_i, i = 0,1,2, \ldots \ldots, n$ are constants and $n = [\alpha] + 1$.

We state the following generalization of Gronwall's lemma for singular kernels.

Lemma 2.3. [25] Let v : $[0,T] \to [0,+\infty)$ be a real function and $w()$ is an on negative, locally integrable function on $[0,T]$. Assume that there is a constant $a > 0$ such that for $0 < \alpha \leq 1$

$$v(t) \leq w(t) + a\int_0^t (t-s)^{-\alpha}v(s)ds$$

Then, there exists a constant $K = K(\alpha)$ such that

$$v(t) \leq w(t) + Ka\int_0^t (t-s)^{-\alpha}w(s)ds$$

for every $t \in [0,T]$.

To study the stability results we use following definitions adopted in [4, 21].

Definition 2.3. The equation (1.1) is Ulam-Hyers stable if there exists a real number $c_f > 0$ such that for each $\varepsilon > 0$ and for each solution $z \in C^1(J,\mathbb{R})$ of the inequality

$$|{}^cD^{\alpha}z(t) - \lambda z(t) - f(t,z(t))| \leq \varepsilon, t \in J$$

there exists a solution $y \in C^1(J, \mathbb{R})$ of equation (1.1) with

$$|z(t) - y(t)| \leq c_f \varepsilon, t \in J$$

Definition 2.4. The equation (1.1) is generalized Ulam-Hyers stable if there exists $\psi_f \in C(\mathbb{R}_+, \mathbb{R}_+), \psi_f(0) = 0$, such that for each solution $z \in C^1(J, \mathbb{R})$ of the inequality

$$|\,^c D^\alpha z(t) - \lambda z(t) - f(t, z(t))| \leq \varepsilon, t \in J$$

there exists a solution $y \in C^1(J, \mathbb{R})$ of equation (1.1) with

$$|z(t) - y(t)| \leq \psi_f(\varepsilon), t \in J$$

Definition 2.5. The equation (1.1) is Ulam-Hyers-Rassias stable with respect to $\varphi \in C(J, \mathbb{R}_+)$if there exists a real number $c_f > 0$ such that for each $\varepsilon > 0$ and for each solution $z \in C^1(J, \mathbb{R})$ of the inequality

$$|\,^c D^\alpha z(t) - \lambda z(t) - f(t, z(t))| \leq \varepsilon\varphi(t), t \in J$$

there exists a solution $y \in C^1(J, \mathbb{R})$ of equation (1.1) with

$$|z(t) - y(t)| \leq c_f \varepsilon\varphi(t), t \in J$$

Definition 2.6. The equation (1.1) is generalized Ulam-Hyers-Rassias stable with respect to $\varphi \in C(J, \mathbb{R}_+)$if there exists a real number $c_{f,\varphi} > 0$ such that for each solution $z \in C^1(J, \mathbb{R})$ of the inequality

$$|\,^c D^\alpha z(t) - \lambda z(t) - f(t, z(t))| \leq \varphi(t), t \in J$$

there exists a solution $y \in C^1(J, \mathbb{R})$ of equation (1.1) with

$$|z(t) - y(t)| \leq c_{f,\varphi}\varphi(t), t \in J$$

Remark 2.1. A function $z \in C^1(J, \mathbb{R})$ is a solution of the inequality

$$|\,^c D^\alpha z(t) - \lambda z(t) - f(t, z(t))| \leq \varepsilon, t \in J$$

if and only if there exists a function $g \in C(J, \mathbb{R})$ (which depends on solution y) such that

i) $|g(t)| \leq \varepsilon, \forall t \in J$.

ii) $^c D^\alpha z(t) = \lambda z(t) + f(t, z(t)) + g(t), t \in J$.

Remark 2.2. Clearly,

i) Definition (2.3) ⇒ Definition (2.4)

ii) Definition (2.5) ⇒ Definition (2.6).

Remark 2.3. A solution of the fractional differential inequality

$$|\,^c D^\alpha z(t) - \lambda z(t) - f(t, z(t))| \leq \varepsilon, t \in J$$

is called an fractional ε-solution of the fractional differential equation (1.1).

Existence and Ulam-Hyers stability of the boundary value problem

Definition 3.1. A function $y \in C^1(J, \mathbb{R})$ is said to be a solution of (1.1)-(1.2) if y satisfies the equation ${}^cD^\alpha y(t) = \lambda y(t) + f(t, y(t))$ on J, and the condition ay $(0) + by(T) = c$.

Lemma 3.1. [3] Let $0 < \alpha < 1$ and let $h: J \to \mathbf{R}$ be continuous. A function y is a solution of the fractional integral equation

$$x(t) = x_0 + \frac{1}{\Gamma(\alpha)} \int_0^t (t-s)^{\alpha-1} h(s) ds$$

if and only if y is a solution of the initial value problem for the fractional differential equation

$$^cD^\alpha x(t) = h(t), t \in [0, T], T > 0$$
$$x(0) = x_0$$

Lemma 3.2. [3] Let $0 < \alpha < 1$ and let $h: J \to \mathbf{R}$ be continuous. A function y is a solution of the fractional integral equation

$$x(t) = \frac{1}{\Gamma(\alpha)} \int_0^t (t-s)^{\alpha-1} h(s) ds - \frac{1}{a+b} \left[\frac{b}{\Gamma(\alpha)} \int_0^T (T-s)^{\alpha-1} h(s) ds - c \right]$$

if and only if y is a solution of the fractional boundary value problem (BVP)

$$^cD^\alpha x(t) = h(t), t \in J := [0, T], T > 0,$$
$$\text{ax}(0) + bx(T) = c$$

As a consequence of Lemma (3.1)-(3.2) and [4] we have the following result which is useful in our main results.

Lemma 3.3. If the function $f: J \times \mathbb{R} \to \mathbb{R}$ is a continuous function, then the problem (1.1)-(1.2) is equivalent to the following problem

$$y(t) = \tilde{A} + \frac{\lambda}{\Gamma(\alpha)} \int_0^t (t-s)^{\alpha-1} y(s) ds + \frac{1}{\Gamma(\alpha)} \int_0^t (t-s)^{\alpha-1} f(s, y(s)) ds \qquad (3.3)$$

$t \in J$, and

$$\tilde{A} = \frac{1}{a+b} \left[c - \frac{b\lambda}{\Gamma(\alpha)} \int_0^T (T-s)^{\alpha-1} y(s) ds - \frac{b}{\Gamma(\alpha)} \int_0^T (T-s)^{\alpha-1} f(s, y(s)) ds \right]$$

Proof. Let $y(t)$ be a solution of the problem (1.1)-(1.2). By integration of equation (1.1) we obtain:

$$y(t) = y_0 + \frac{\lambda}{\Gamma(\alpha)} \int_0^t (t-s)^{\alpha-1} y(s) ds + \frac{1}{\Gamma(\alpha)} \int_0^t (t-s)^{\alpha-1} f(s, y(s)) ds \qquad (3.4)$$

We use (1.2) to find the constant y_0, so we have:

$$ay(0) = ay_0 \qquad (3.5)$$

and

$$by(T) = by_0 + \frac{b\lambda}{\Gamma(\alpha)}\int_0^T (T-s)^{\alpha-1}y(s)ds + \frac{b}{\Gamma(\alpha)}\int_0^T (T-s)^{\alpha-1}f(s,y(s))ds \qquad (3.6)$$

then, $ay(0) + by(T) = c$, since

$$y_0 = \frac{1}{a+b}\left[c - \frac{b\lambda}{\Gamma(\alpha)}\int_0^T (T-s)^{\alpha-1}y(s)ds - \frac{b}{\Gamma(\alpha)}\int_0^T (T-s)^{\alpha-1}f(s,y(s))ds\right]. \qquad (3.7)$$

Using equation (3.7) in (3.4) leads to formula (3.3). Conversely, let y be a solution of (3.3). We shall show that y is solution of (1.1)-(1.2). Define $z(t) = \lambda y(t) + f(t, y(t))$, then from (3.3), we have

$$y(t) = \tilde{A} + I^{\alpha}z(t).$$

So,

$$y(0) = \tilde{A}$$

and

$$y(T) = \tilde{A} + \frac{\lambda}{\Gamma(\alpha)}\int_0^T (T-s)^{\alpha-1}y(s)ds + \frac{1}{\Gamma(\alpha)}\int_0^T (T-s)^{\alpha-1}f(s,y(s))ds$$

$$\begin{aligned} ay(0) + by(T) &= \tilde{A}(a+b) + \frac{b\lambda}{\Gamma(\alpha)}\int_0^T (T-s)^{\alpha-1}y(s)ds + \frac{b}{\Gamma(\alpha)}\int_0^T (T-s)^{\alpha-1}f(s,y(s))ds \\ &= \frac{1}{a+b}\left[c - \frac{b\lambda}{\Gamma(\alpha)}\int_0^T (T-s)^{\alpha-1}y(s)ds - \frac{b}{\Gamma(\alpha)}\int_0^T (T-s)^{\alpha-1}f(s,y(s))ds\right](a+b) \\ &+ \frac{b\lambda}{\Gamma(\alpha)}\int_0^T (T-s)^{\alpha-1}y(s)ds + \frac{b}{\Gamma(\alpha)}\int_0^T (T-s)^{\alpha-1}f(s,y(s))ds \\ &= c. \end{aligned}$$

Then

$$ay(0) + by(T) = c$$

On the other hand, we have

$$\begin{aligned} {}^cD^{\alpha}y(t) &= {}^cD^{\alpha}\left(\tilde{A} + I^{\alpha}z(t)\right) = z(t) \\ &= \lambda y(t) + f(t, y(t)). \end{aligned}$$

Thus y is a solution of (1.1)-(1.2).

Theorem 3.1. Assume that:

(H1): There exists a constant $L > 0$ such that $|f(t,x) - f(t,\bar{x})| \leq L|x - \bar{x}|$, for each $t \in J$, and all $x, \bar{x} \in \mathbb{R}$.

If

$$\frac{(\lambda + L)T^{\alpha}\left(1 + \frac{|b|}{|a+b|}\right)}{\Gamma(\alpha+1)} < 1 \qquad (3.8)$$

then the BVP (1.1)-(1.2) has a unique solution on J.

Proof. We transform problem (1.1)-(1.2) into a fixed point problem. For this, consider the operator $F: C(J,\mathbb{R}) \to C(J,\mathbb{R})$ defined by

$$F(y)(t) = \frac{\lambda}{\Gamma(\alpha)}\int_0^t (t-s)^{\alpha-1}y(s)ds + \frac{1}{\Gamma(\alpha)}\int_0^t (t-s)^{\alpha-1}f(s,y(s))ds$$
$$-\frac{1}{a+b}\left[\frac{b\lambda}{\Gamma(\alpha)}\int_0^T (T-s)^{\alpha-1}y(s)ds + \frac{b}{\Gamma(\alpha)}\int_0^T (T-s)^{\alpha-1}f(s,y(s))ds - c\right] \quad (3.9)$$

Clearly, the fixed points of the operator F are solution of problem (1.1)-(1.2). We shall use the Banach contraction principle to prove that F has a fixed point. we shall show that F is a contraction.

Let $x, y \in C(J,\mathbb{R})$. Then for each $t \in J$ we have

$$\begin{aligned}|F(x)(t) - F(y)(t)| &\le \frac{\lambda}{\Gamma(\alpha)}\int_0^t (t-s)^{\alpha-1}|x(s)-y(s)|ds + \frac{1}{\Gamma(\alpha)}\int_0^t (t-s)^{\alpha-1}|f(s,x(s))-f(s,y(s))|ds\\
&+\frac{|b|\lambda}{\Gamma(\alpha)|a+b|}\int_0^T (T-s)^{\alpha-1}|x(s)-y(s)|ds\\
&+\frac{|b|}{\Gamma(\alpha)|a+b|}\int_0^T (T-s)^{\alpha-1}|f(s,x(s))-f(s,y(s))|ds\\
&\le \frac{\lambda||x(s)-y(s)\|_\infty}{\Gamma(\alpha)}\int_0^t (t-s)^{\alpha-1}ds + \frac{L\|x(s)-y(s)\|_\infty}{\Gamma(\alpha)}\int_0^t (t-s)^{\alpha-1}ds\\
&+\frac{|b|\lambda||x(s)-y(s)\|_\infty}{\Gamma(\alpha)|a+b|}\int_0^T (T-s)^{\alpha-1}ds + \frac{|b|L||x(s)-y(s)\|_\infty}{\Gamma(\alpha)|a+b|}\int_0^T (T-s)^{\alpha-1}ds\\
&\le \frac{(\lambda+L)T^\alpha\left(1+\frac{|b|}{|a+b|}\right)}{\Gamma(\alpha+1)}\|x(s)-y(s)\|_\infty.\end{aligned}$$

Thus

$$\|F(x)-F(y)\|_\infty \le \frac{(\lambda+L)T^\alpha\left(1+\frac{|b|}{|a+b|}\right)}{\Gamma(\alpha+1)}\|x-y\|_\infty$$

Thus, F is a contraction due to the (3.8).

By Banach contraction principle, we deduce that F has an unique fixed point which is just the unique solution of the problem (1.1)-(1.2).

The second result is based on Schaefer's fixed point theorem.

Theorem 3.2. Assume that:

(H2) The function $f: J \times \mathbb{R} \to \mathbb{R}$ is continuous.

(H3) There exists a constant $M > 0$ such that $|f(t,x)| \le M$, for each $t \in J$ and for all $x \in \mathbb{R}$.

Then the problem (1.1)-(1.2) has at least one solution on J.

Proof. We shall use Schaefer's fixed point theorem to prove that F defined by (3.9) has a fixed point. The proof will be given in several steps.

Step 1: F is continuous.

Let $\{y_n\}$ be a sequence such that $y_n \to y$ in $C(J,\mathbb{R})$. Then for each $t \in J$, we have

$$\begin{aligned}|F(y_n)(t) - F(y)(t)| \le{}& \frac{\lambda}{\Gamma(\alpha)}\int_0^t (t-s)^{\alpha-1}\sup_{t\in J}|y_n(s)-y(s)|ds\\ &+\frac{1}{\Gamma(\alpha)}\int_0^t (t-s)^{\alpha-1}\sup_{t\in J}|f(s,y_n(s))-f(s,y(s))|ds\\ &+\frac{|b|\lambda}{\Gamma(\alpha)|a+b|}\int_0^T (T-s)^{\alpha-1}\sup_{t\in J}|y_n(s)-y(s)|ds\\ &+\frac{|b|}{\Gamma(\alpha)|a+b|}\int_0^T (T-s)^{\alpha-1}\sup_{t\in J}|f(s,y_n(s))-f(s,y(s))|ds\\ &\le \frac{\lambda T^\alpha\left(1+\frac{|b|}{|a+b|}\right)}{\alpha\Gamma(\alpha)}\|y_n(s)-y(s)\|_\infty + \frac{T^\alpha\left(1+\frac{|b|}{|a+b|}\right)}{\alpha\Gamma(\alpha)}\|f(s,y_n(s))-f(s,y(s))\|_\infty ds.\end{aligned}$$

Since f is a continuous function, we have $\|F(y_n)(t) - F(y)(t)\|_\infty \to 0$ as $n \to \infty$

Step 2: F maps bounded sets into bounded sets in $C(J,\mathbb{R})$.

Indeed, it is enough to show that for any $\mu^* > 0$, there exists a positive constant l such that for each $y \in B_{\mu^*} = \{y \in C(J,\mathbb{R}): \|y\|_\infty \le \mu^*\}$, we have $\|F(y)\|_\infty \le l$.

By (H3) we have for each $t \in [0,T]$,

$$\begin{aligned}|F(y)| \le{}& \frac{\lambda}{\Gamma(\alpha)}\int_0^t (t-s)^{\alpha-1}|y(s)|ds + \frac{1}{\Gamma(\alpha)}\int_0^t (t-s)^{\alpha-1}|f(s,y(s))|ds\\ &+\frac{|b|\lambda}{|a+b|\Gamma(\alpha)}\int_0^T (T-s)^{\alpha-1}|y(s)|ds + \frac{|b|}{|a+b|\Gamma(\alpha)}\int_0^T (T-s)^{\alpha-1}|f(s,y(s))|ds + \frac{|c|}{|a+b|}\\ &\le \frac{\lambda\mu^*}{\Gamma(\alpha)}\int_0^t (t-s)^{\alpha-1}ds + \frac{M}{\Gamma(\alpha)}\int_0^t (t-s)^{\alpha-1}ds\\ &+\frac{|b|\lambda\mu^*}{|a+b|\Gamma(\alpha)}\int_0^T (T-s)^{\alpha-1}ds + \frac{M|b|}{|a+b|\Gamma(\alpha)}\int_0^T (T-s)^{\alpha-1}ds + \frac{|c|}{|a+b|}\\ &\le \frac{\lambda\mu^* T^\alpha}{\Gamma(\alpha+1)}\left[1+\frac{|b|}{|a+b|}\right] + \frac{MT^\alpha}{\Gamma(\alpha+1)}\left[1+\frac{|b|}{|a+b|}\right] + \frac{|c|}{|a+b|}.\end{aligned}$$

Thus

$$\|F(y)\|_\infty \le \frac{\lambda\mu^* T^\alpha}{\Gamma(\alpha+1)}\left[1+\frac{|b|}{|a+b|}\right] + \frac{MT^\alpha}{\Gamma(\alpha+1)}\left[1+\frac{|b|}{|a+b|}\right] + \frac{|c|}{|a+b|} := l$$

Step 3: F maps bounded sets into equicontinuous sets of $C(J,\mathbb{R})$.

Let $t_1, t_2 \in (0,T], t_1 < t_2, B_{\mu^*}$ be a bounded set of $C(J,\mathbb{R})$ as in step 2 , and let $y \in B_{\mu^*}$. Then

$$
\begin{aligned}
|F(y)(t_1) - F(y)(t_2)| = \Bigg| & \frac{\lambda}{\Gamma(\alpha)}\int_0^{t_1}(t_1-s)^{\alpha-1}y(s)ds + \frac{1}{\Gamma(\alpha)}\int_0^{t_1}(t_1-s)^{\alpha-1}f(s,y(s))ds \\
& -\frac{\lambda}{\Gamma(\alpha)}\int_0^{t_2}(t_2-s)^{\alpha-1}y(s)ds - \frac{1}{\Gamma(\alpha)}\int_0^{t_2}(t_2-s)^{\alpha-1}f(s,y(s))ds\Bigg| \\
& \leq \frac{\lambda\mu^*}{\Gamma(\alpha)}\int_0^{t_1}\{(t_1-s)^{\alpha-1}-(t_2-s)^{\alpha-1}\}ds + \frac{M}{\Gamma(\alpha)}\int_0^{t_1}\{(t_1-s)^{\alpha-1}-(t_2-s)^{\alpha-1}\}ds \\
& + \frac{\lambda\mu^*}{\Gamma(\alpha)}\int_{t_1}^{t_2}(t_2-s)^{\alpha-1}ds + \frac{M}{\Gamma(\alpha)}\int_{t_1}^{t_2}(t_2-s)^{\alpha-1}ds \\
& \leq \frac{(\lambda\mu^*+M)}{\Gamma(\alpha+1)}\{2(t_2-t_1)^{\alpha} + (t_1^{\alpha}-t_2^{\alpha})\}.
\end{aligned}
$$

As $t_1 \to t_2$, the right-hand side of the above inequality tends to zero. As a consequence of steps 1 to 3 together with the Arzela-Ascoli theorem, we can conclude that $F: C(J,\mathbb{R}) \to C(J,\mathbb{R})$ is continuous and completely continuous.

Step 4: A priori bounds.

Now it remains to show that the set

$$\mathcal{E} = \{y \in C(J,\mathbb{R}): y = \beta F(y), \text{ for some } \beta \in (0,1)\}$$

is bounded.

Let $y \in \mathcal{E}$, then $y = \beta F(y)$, for some $\beta \in (0,1)$. Thus, for each $t \in J$ we have

$$
\begin{aligned}
y(t) = \beta\Bigg\{ & \frac{\lambda}{\Gamma(\alpha)}\int_0^{t}(t-s)^{\alpha-1}y(s)ds + \frac{1}{\Gamma(\alpha)}\int_0^{t}(t-s)^{\alpha-1}f(s,y(s))ds \\
& -\frac{1}{a+b}\left[\frac{b\lambda}{\Gamma(\alpha)}\int_0^{T}(T-s)^{\alpha-1}y(s)ds + \frac{b}{\Gamma(\alpha)}\int_0^{T}(T-s)^{\alpha-1}f(s,y(s))ds - c\right]\Bigg\} \qquad (3.10)
\end{aligned}
$$

This implies by (H3) that for each $t \in J$ we have

$$
\begin{aligned}
|F(y)(t)| \leq & \frac{\lambda}{\Gamma(\alpha)}\int_0^{t}(t-s)^{\alpha-1}|y(s)|ds + \frac{1}{\Gamma(\alpha)}\int_0^{t}(t-s)^{\alpha-1}|f(s,y(s))|ds \\
& + \frac{|b|\lambda}{|a+b|\Gamma(\alpha)}\int_0^{T}(T-s)^{\alpha-1}|y(s)|ds + \frac{|b|}{|a+b|\Gamma(\alpha)}\int_0^{T}(T-s)^{\alpha-1}|f(s,y(s))|ds + \frac{|c|}{|a+b|} \\
& \leq \frac{\lambda\mu^*}{\Gamma(\alpha)}\int_0^{t}(t-s)^{\alpha-1}ds + \frac{M}{\Gamma(\alpha)}\int_0^{t}(t-s)^{\alpha-1}ds \\
& + \frac{|b|\lambda\mu^*}{|a+b|\Gamma(\alpha)}\int_0^{T}(T-s)^{\alpha-1}ds + \frac{M|b|}{|a+b|\Gamma(\alpha)}\int_0^{T}(T-s)^{\alpha-1}ds + \frac{|c|}{|a+b|} \\
& \leq \frac{\lambda\mu^*T^{\alpha}}{\Gamma(\alpha+1)}\left[1+\frac{|b|}{|a+b|}\right] + \frac{MT^{\alpha}}{\Gamma(\alpha+1)}\left[1+\frac{|b|}{|a+b|}\right] + \frac{|c|}{|a+b|} := R.
\end{aligned}
$$

Thus for every $t \in J$. we have

$$\|F(y)\|_{\infty} \leq \frac{\lambda\mu^*T^{\alpha}}{\Gamma(\alpha+1)}\left[1+\frac{|b|}{|a+b|}\right] + \frac{MT^{\alpha}}{\Gamma(\alpha+1)}\left[1+\frac{|b|}{|a+b|}\right] + \frac{|c|}{|a+b|} := R.$$

This shows that the set $\mathcal{E}$ is bounded. As a consequence of Schaefer's fixed point theorem, we deduce that F has a fixed point which is a solution of the problem (1.1)-(1.2).

Theorem 3.3. Assume that (H1) and (3.8) are satisfied, then the problem (1.1)-(1.2) is Ulam-Hyers stable.

Proof. Let $\varepsilon > 0$ and let $z \in C^1(J, \mathbb{R})$ be a function which satisfies the inequality:

$$|{}^cD^\alpha z(t) - \lambda z(t) - f(t, z(t))| \leq \varepsilon, \text{ for any } t \in J \qquad (3.11)$$

and let $y \in C(J, \mathbb{R})$ be the unique solution of the following Cauchy problem

$$^cD^\alpha y(t) = \lambda y(t) + f(t, y(t)), t \in J; 0 < \alpha \leq 1$$
$$y(0) = z(0), y(T) = z(T).$$

Using Lemma 3.3, we obtain

$$y(t) = \tilde{A}_y + \frac{\lambda}{\Gamma(\alpha)}\int_0^t (t-s)^{\alpha-1} y(s)ds + \frac{1}{\Gamma(\alpha)}\int_0^t (t-s)^{\alpha-1} f(s, y(s))ds$$

and

$$\tilde{A}_y = \frac{1}{a+b}\left[c - \frac{b\lambda}{\Gamma(\alpha)}\int_0^T (T-s)^{\alpha-1} y(s)ds - \frac{b}{\Gamma(\alpha)}\int_0^T (T-s)^{\alpha-1} f(s, y(s))ds\right]$$

If $y(T) = z(T)$ and $y(0) = z(0)$ then, we find

$$\begin{aligned}
|\tilde{A}_y - \tilde{A}_z| &\leq \frac{|b|\lambda}{\Gamma(\alpha)|a+b|}\int_0^T (T-s)^{\alpha-1}|y(s) - z(s)|ds + \frac{|b|}{\Gamma(\alpha)|a+b|}\int_0^T (T-s)^{\alpha-1}|f(s, y(s)) - f(s, z(s))|ds \\
&\leq \frac{|b|\lambda}{\Gamma(\alpha)|a+b|}\int_0^T (T-s)^{\alpha-1}|y(s) - z(s)|ds + \frac{|b|L}{\Gamma(\alpha)|a+b|}\int_0^T (T-s)^{\alpha-1}|y(s) - z(s)|ds \\
&= \frac{|b|(\lambda+L)}{|a+b|} I^\alpha |y(T) - z(T)| = 0.
\end{aligned}$$

Thus

$$\tilde{A}_y = \tilde{A}_z$$

Then we have

$$y(t) = \tilde{A}_z + \frac{\lambda}{\Gamma(\alpha)}\int_0^t (t-s)^{\alpha-1} y(s)ds + \frac{1}{\Gamma(\alpha)}\int_0^t (t-s)^{\alpha-1} f\big(s, y(s)\big)ds,$$

by integration of the inequality (3.11), we obtain

$$\left|z(t) - \tilde{A}_z - \frac{\lambda}{\Gamma(\alpha)}\int_0^t (t-s)^{\alpha-1} z(s)ds - \frac{1}{\Gamma(\alpha)}\int_0^t (t-s)^{\alpha-1} f(s, z(s))ds\right| \leq \frac{\varepsilon t^\alpha}{\Gamma(\alpha+1)} \leq \frac{\varepsilon T^\alpha}{\Gamma(\alpha+1)} \qquad (3.12)$$

We have for any $t \in J$

$$\begin{aligned}
|z(t) - y(t)| &\leq \left|z(t) - \tilde{A}_z - \frac{\lambda}{\Gamma(\alpha)}\int_0^t (t-s)^{\alpha-1} y(s)ds - \frac{1}{\Gamma(\alpha)}\int_0^t (t-s)^{\alpha-1} f(s, y(s))ds\right| \\
&\leq \left|z(t) - \tilde{A}_z - \frac{\lambda}{\Gamma(\alpha)}\int_0^t (t-s)^{\alpha-1} z(s)ds - \frac{1}{\Gamma(\alpha)}\int_0^t (t-s)^{\alpha-1} f(s, z(s))ds\right| \\
&\quad + \frac{\lambda}{\Gamma(\alpha)}\int_0^t (t-s)^{\alpha-1}|z(s) - y(s)|ds + \frac{1}{\Gamma(\alpha)}\int_0^t (t-s)^{\alpha-1}|f(s, z(s)) - f(s, y(s))|ds
\end{aligned}$$

Using equation (3.12) and (H1), we obtain

$$|z(t)-y(t)| \leq \frac{\varepsilon T^{\alpha}}{\Gamma(\alpha+1)} + \frac{(\lambda+L)}{\Gamma(\alpha)}\int_0^t (t-s)^{\alpha-1}|z(s)-y(s)|ds$$

and by the Gronwall's lemma, we obtain

$$|z(t)-y(t)| \leq \frac{\varepsilon T^{\alpha}}{\Gamma(\alpha+1)}\left[1+\frac{K(\lambda+L)T^{\alpha}}{\Gamma(\alpha+1)}\right] := c\varepsilon$$

where $K = K(\alpha)$ is a constant, which completes the proof of the theorem. Moreover, if we set $\psi(\varepsilon) = c\varepsilon; \psi(0) = 0$, then the problem (1.1)-(1.2) is generalized Ulam-Hyers stable.

Theorem 3.4. Assume that (H1), (3.8) and (H4): there exists an increasing function $\varphi \in C(J, \mathbb{R}_+)$ and there exists $\kappa_{\varphi} > 0$ such that for any $t \in J$

$$I^{\alpha}\varphi(t) \leq \kappa_{\varphi}\varphi(t)$$

are satisfied, then, the problem (1.1)-(1.2) is Ulam-Hyers-Rassias stable.

Proof. Let $z \in C^1(J, \mathbb{R})$ be solution of the following inequality:

$$|\,{}^cD^{\alpha}z(t) - \lambda z(t) - f(t, z(t))| \leq \varepsilon\varphi(t), \text{ for any } t \in J, \varepsilon > 0 \qquad (3.13)$$

and let $y \in C(J, \mathbb{R})$ be the unique solution of the following Cauchy problem

$$\begin{gathered} {}^cD^{\alpha}y(t) = \lambda y(t) + f(t, y(t)), t \in J; 0 < \alpha \leq 1 \\ y(0) = z(0), y(T) = z(T) \end{gathered}$$

Using Lemma (3.3), we obtain

$$y(t) = \tilde{A}_z + \frac{\lambda}{\Gamma(\alpha)}\int_0^t (t-s)^{\alpha-1}y(s)ds + \frac{1}{\Gamma(\alpha)}\int_0^t (t-s)^{\alpha-1}f(s, y(s))ds$$

and

$$\tilde{A}_z = \frac{1}{a+b}\left[c - \frac{b\lambda}{\Gamma(\alpha)}\int_0^T (T-s)^{\alpha-1}z(s)ds - \frac{b}{\Gamma(\alpha)}\int_0^T (T-s)^{\alpha-1}f(s, z(s))ds\right]$$

By integration of of (3.13), we obtain

$$\begin{aligned} \left|z(t) - \tilde{A}_z - \frac{\lambda}{\Gamma(\alpha)}\int_0^t (t-s)^{\alpha-1}z(s)ds - \frac{1}{\Gamma(\alpha)}\int_0^t (t-s)^{\alpha-1}f(s, z(s))ds\right| &\leq \frac{\varepsilon}{\Gamma(\alpha)}\int_0^t (t-s)^{\alpha-1}\varphi(t)ds \\ &\leq \varepsilon\kappa_{\varphi}\varphi(t) \qquad (3.14) \end{aligned}$$

On the other hand, we have

$$\begin{aligned} |z(t)-y(t)| &\leq \left|z(t) - \tilde{A}_z - \frac{\lambda}{\Gamma(\alpha)}\int_0^t (t-s)^{\alpha-1}y(s)ds - \frac{1}{\Gamma(\alpha)}\int_0^t (t-s)^{\alpha-1}f(s, y(s))ds\right| \\ &\leq \left|z(t) - \tilde{A}_z - \frac{\lambda}{\Gamma(\alpha)}\int_0^t (t-s)^{\alpha-1}z(s)ds - \frac{1}{\Gamma(\alpha)}\int_0^t (t-s)^{\alpha-1}f(s, z(s))ds\right| \\ &+ \frac{\lambda}{\Gamma(\alpha)}\int_0^t (t-s)^{\alpha-1}|z(s)-y(s)|ds + \frac{1}{\Gamma(\alpha)}\int_0^t (t-s)^{\alpha-1}|f(s, z(s)) - f(s, y(s))|ds \end{aligned}$$

Using (3.14) and (H1), we obtain

$$|z(t)-y(t)| \leq \varepsilon\kappa_{\varphi}\varphi(t)+\frac{(\lambda+L)}{\Gamma(\alpha)}\int_0^t (t-s)^{\alpha-1}|z(s)-y(s)|ds$$

and by Gronwall's lemma, we get that for any $t \in J$:

$|z(t)-y(t)| \leq \varepsilon\kappa_{\varphi}\varphi(t)+\frac{K_1(\lambda+L)}{\Gamma(\alpha)}\int_0^t (t-s)^{\alpha-1}\varepsilon\kappa_{\varphi}\varphi(s)ds = \varepsilon\kappa_{\varphi}\varphi(t)+\frac{\varepsilon K_1\kappa_{\varphi}(\lambda+L)}{\Gamma(\alpha)}\int_0^t (t-s)^{\alpha-1}\varphi(s)ds,$

where $K_1 = K_1(\alpha)$ is a constant, and by (H4), we have:

$$|z(t)-y(t)| \leq \varepsilon\kappa_{\varphi}\varphi(t)+\varepsilon K_1\kappa_{\varphi}^2(\lambda+L)\varphi(t) = \left[1+K_1\kappa_{\varphi}(\lambda+L)\right]\varepsilon\kappa_{\varphi}\varphi(t)$$

Then for any $\in J$:

$$|z(t)-y(t)| \leq \left[\left(1+K_1\kappa_{\varphi}(\lambda+L)\right)\kappa_{\varphi}\right]\varepsilon\varphi(t) = c\varepsilon\varphi(t)$$

which completes the proof of Theorem (3.4).

Remark 3.1. Our results for BVP (1.1)-(1.2) are appropriate for the following problems:

- Initial value problem: $a = 1, b = 0, c = 0$.
- Terminal value problem: $a = 0, b = 1, c$ arbitrary.
- Anti-periodic problem: $a = 1, b = 1, c = 0$.

However, they are not for the periodic problem, i.e. for $a = 1, b = -1, c = 0$.

4 Examples

Example 4.1. Consider

$$^cD^{\frac{3}{2}}y(t) = \frac{1}{10}y(t)+\frac{y(t)+1}{t^2+9}, t \in [0,1], y(0)+y(1) = 0. \quad (4.15)$$

$$y(0)+y(1) = 0. \quad (4.16)$$

Define $f(t,y) = \frac{y(t)+1}{t^2+9}, t \in [0,1], \alpha = \frac{3}{2}, \lambda = \frac{1}{10}$

Clearly, the function f is continuous.

For any $y, \bar{y} \in \mathbb{R}$ and $t \in [0,1]$

$$|f(t,y)-f(t,\bar{y})| \leq \frac{1}{9}|y-\bar{y}|$$

Hence condition (H1) is satisfied with $L = \frac{1}{9}$. Thus condition

$$\frac{(\lambda+L)T^{\alpha}\left(1+\frac{|b|}{|a+b|}\right)}{\Gamma(\alpha+1)} = \frac{\left(\frac{1}{10}+\frac{1}{9}\right)\left(1+\frac{1}{2}\right)}{\Gamma\left(\frac{3}{2}+1\right)} < 1$$

is satisfied with $a = b = T = 1, c = 0$, and $\alpha = \frac{3}{2}$. It follows that from Theorem (3.1) that the problem (4.15)-(4.16) has a unique solution on [0,1]. Moverover, Theorem (3.3) implies that the problem (4.15)-(4.16) is Ulam-Hyers stable.

References:

1. Abbas, S., & Benchohra, M. (2014). On the generalized Ulam-Hyers-Rassias stability for Darboux problem for partial fractional implicit differential equations. *Applied Mathematics E-Notes*, 14, 20–28.
2. Agarwal, R. P., Belmekki, M., & Benchohra, M. (2009). A survey on semilinear differential equations and inclusions involving Riemann-Liouville fractional derivative. *Advances in Differential Equations*, 2009, Article ID 981728.
3. Agarwal, R. P., Benchohra, M., & Hamani, S. (2010). A survey on existence results for boundary value problems of nonlinear fractional differential equations and inclusions. *Acta Applicandae Mathematicae*, 109, 973–1033.
4. Benchohra, M., & Bouriahi, S. (2015). Existence and stability results for nonlinear boundary value problem for implicit differential equations of fractional order. *Moroccan Journal of Pure and Applied Analysis*, 1, 22–37.
5. Benchohra, M., Hamani, S., & Ntouyas, S. K. (2009). Boundary value problems for differential equations with fractional order and nonlocal conditions. *Nonlinear Analysis: Theory, Methods & Applications*, 71(7–8), 2391–2396.
6. Byszewski, L. (1991). Theorem about existence and uniqueness of continuous solution of nonlocal problem for nonlinear hyperbolic equation. *Applicable Analysis*, 40, 173–180.
7. Byszewski, L. (1991). Theorems about the existence and uniqueness of solutions of a semilinear evolution nonlocal Cauchy problem. *Journal of Mathematical Analysis and Applications*, 162, 494–505.
8. Cho, Y. J., Rassias, T. M., & Saadati, R. (2013). *Stability of functional equations in random normed spaces*. Springer.
9. Hyers, D. H. (1941). On the stability of the linear functional equation. *Proceedings of the National Academy of Sciences of the United States of America*, 27, 222–224.
10. Ibrahim, R. W. (2012). Stability for univalent solutions of complex fractional differential equations. *Proceedings of the Pakistan Academy of Sciences*, 49(3), 227–232.

11. Jung, S. M. (1998). On the Hyers-Ulam stability of the functional equations that have the quadratic property. *Journal of Mathematical Analysis and Applications*, 222, 126–137.
12. Jung, S. M. (2006). Hyers-Ulam stability of linear differential equations of first order. *Applied Mathematics Letters*, 19, 854–858.
13. Jung, S. M., & Lee, K. S. (2007). Hyers-Ulam stability of first order linear partial differential equations with constant coefficients. *Mathematical Inequalities & Applications*, 10, 261–266.
14. Kilbas, A. A., Srivastava, H. M., & Trujillo, J. J. (2006). *Theory and applications of fractional differential equations* (North-Holland Mathematics Studies, Vol. 204). Elsevier.
15. Obloza, M. (1993). Hyers stability of the linear differential equation. *Rocznik Naukowo-Dydaktyczny. Prace Matematyczne*, 13, 259–270.
16. Ortigueira, M. D. (2011). *Fractional calculus for scientists and engineers* (Lecture Notes in Electrical Engineering, Vol. 84). Springer.
17. Podlubny, I. (1999). *Fractional differential equations*. Academic Press.
18. Rassias, T. M. (1978). On the stability of the linear mapping in Banach spaces. *Proceedings of the American Mathematical Society*, 72, 297–300.
19. Rassias, J. M. (2010). *Functional equations, difference inequalities and Ulam stability notions*. F.U.N., Inc.
20. Rassias, T. M., & Brzdek, J. (2012). *Functional equations in mathematical analysis*. Springer.
21. Rus, I. A. (2010). Ulam stabilities of ordinary differential equations in a Banach space. *Carpathian Journal of Mathematics*, 26, 103–107.
22. Tarasov, V. E. (2010). *Fractional dynamics: Applications of fractional calculus to dynamics of particles, fields and media*. Springer; Higher Education Press.
23. Ulam, S. M. (1940). *Problems in modern mathematics*. John Wiley & Sons.
24. Ulam, S. M. (1960). *A collection of mathematical problems*. Interscience.
25. Ye, H., Gao, J., & Ding, Y. (2007). A generalized Gronwall inequality and its application to a fractional differential equation. *Journal of Mathematical Analysis and Applications*, 328, 1075–1081.

26. Wang, J., Feckan, M., & Zhou, Y. (2012). Ulam's type stability of impulsive ordinary differential equations. *Journal of Mathematical Analysis and Applications*, 395, 258–264.
27. Wang, J., Lv, L., & Zhou, Y. (2011). Ulam stability and data dependence for fractional differential equations with Caputo derivative. *Electronic Journal of Qualitative Theory of Differential Equations*, 63, 1–10.
28. Wang, J., & Zhang, Y. (2014). Existence and stability of solutions to nonlinear impulsive differential equations in β-normed spaces. *Electronic Journal of Differential Equations*, 83, 1–10.

MATHEMATICAL MODEL FOR THE DYNAMICS OF GLUCOSE, INSULIN AND β-CELL MASS UNDER THE EFFECT OF TRAUMA, EXCITEMENT AND STRESS

Isa Ibrahim Mohammed

Department of General studies,

Gombe State College of Health Sciences and Technology Kaltungo, Gombe State, Nigeria

Corresponding author E-mail: kombani45@gmail.com

Abstract:

In this work, we presented a mathematical model for the dynamics of glucose, insulin and beta_cell mass under the influence of trauma, excitement and/or stress, the model is an improvement on the work by [1]. We defined and incorporated a parameter ρ to represent the effectiveness of epinephrine in suppressing insulin secretion and a parameter G_8 representing epinephrine induced glucose increase as the factors that affect glucose and insulin homeostasis. The model which consists of a system of three nonlinear ordinary differential equations was used to investigate the effect of epinephrine on glucose, insulin and beta_cell mass dynamics. The result of the study showed that; In the presence of epinephrine, the blood glucose increased and the blood insulin decreased due to suppression by the hormone, despite the fact that there is an increase in Beta_cell mass the system remained extremely hyperglycemic. Furthermore, the result of the numerical experiment carried out indicated that frequent epinephrine secretion into the blood induced prolong and extreme hyperglycemia. Frequent epinephrine secretion increases the risk of diabetes in humans. In view of the findings of this study, we recommend that there should be a massive and continuous health education, especially for communities living in the areas where the stated agents (trauma, excitement and stress) of epinephrine secretion are common.

Keywords: Mathematical Model, Epinephrine, Prolong hyperglycemia, Normoglycemia, Beta-cells, Diabetic with Complication, Equilibrium and Stability.

1. Introduction:

Diabetes mellitus is the disease of metabolism, which is characterised by very high sugar levels in the blood and urine. The body is unable to metabolise all its sugars due to insufficient supply of insulin. One of the most finely tuned mechanism of the human body is the regulation of sugar in the blood-stream. A delicate balance is normally maintained between the amounts of glucose and insulin in the bloodstream [2]. Diabetes mellitus can also be defined as a disease of the glucose regulatory system characterized by fasting and/or postprandial hyperglycaemia [3].

According to [1], there are two types of diabetes, namely:

1. Type 1 diabetes
2. Type 2 diabe

1.1 The type1 diabetes

Type 1 diabetes (also referred to as juvenile onset or insulin-dependent diabetes) is due to autoimmune attack on the insulin secreting $\beta - cells$ [1]. Type 1 diabetes affects people under the age of 40, and represents 10 to 15% of the diabetic population [4]. Patients with type1 diabetes are recommended to take insulin injection [1].

1.2 The type2 diabetes

Type 2 diabetes (also referred to as adult onset or non-insulin-dependent diabetes) is associated with a deficit in the mass of $\beta - cells$ due to extreme elevated blood glucose level which reduced insulin secretion and resistance to the action of insulin [1]. Type 2 diabetes represents 85-90% of the diabetic population [4].

1.3 Symptoms of diabetes

According to report by [11], the symptoms of diabetes are as follows:

1. Frequent urination and excessive thirst
2. Disproportionate thirst
3. Intense hunger
4. Weight gain
5. Unusual weight loss
6. Increase fatigue
7. Irritability
8. Blurred vision
9. Sexual dysfunction among men
10. Numberless or tingling, especially in a feet or hands etc.

1.4 Diabetes complications

Diabetes if not properly controlled it will lead to the following complications:

1. Kidney failure
2. Blindness
3. Amputation
4. Cardiovascular diseases [4].

2. Model formulation

In this section, we developed model glucose, insulin and beta cells dynamics in which we incorporated the effect of trauma, excitement and stress as a factor that affect glucose and insulin homeostasis.

2.1 Existing model equations

[1] Obtained the model equations describing the $\beta - cell\,mass$, insulin and glucose dynamics which we described in the figures bellow as in the absence of epinephrine as follows:

$$\begin{aligned}\frac{dG}{dt} &= R_0 - (E_{GO} + S_I I)G,\\ \frac{dI}{dt} &= \frac{\beta\sigma G^2}{\alpha + G^2} - KI,\\ \frac{d\beta}{dt} &= \left(-d + r_1 G - r_2 G^2\right)\beta\end{aligned} \tag{3.1}$$

2.2 Assumption of model

i. Only trauma, excitement and stress are factors that trigger epinephrine secretion from kidney
ii. Epinephrine induced glucose production from kidney is negligible and ignored.
iii. Epinephrine induced glucose production from the liver is considered.
iv. Blood insulin level will also be decreased by Epinephrine suppression on insulin secretion

Table 1: Definition of variables and parameters of the model

Variable/Parameter	Description
$G(t)$	Blood glucose concentration at time t
$I(t)$	Blood insulin concentration at time t
$\beta(t)$	Beta cell mass at time t
R_0	The net rate of glucose production at zero glucose level
E_{GO}	Total glucose effectiveness at zero insulin
S_I	Total insulin sensitivity
σ	Maximum rate of insulin secretion
α	Inflection point of sigmoidal function
K	Insulin clearance rate for muscles, liver and kidney
d_0	Beta cell natural death rate
r_1 and r_2	Constant beta cell glucose tolerance ranges
ρ	Epinephrine effectiveness in suppressing insulin secretion
G_e	Amount of glucose increase due to epinephrine secretion

We present the model diagram for the dynamics of β – Cell mass, insulin, glucose and epinephrine as follows:

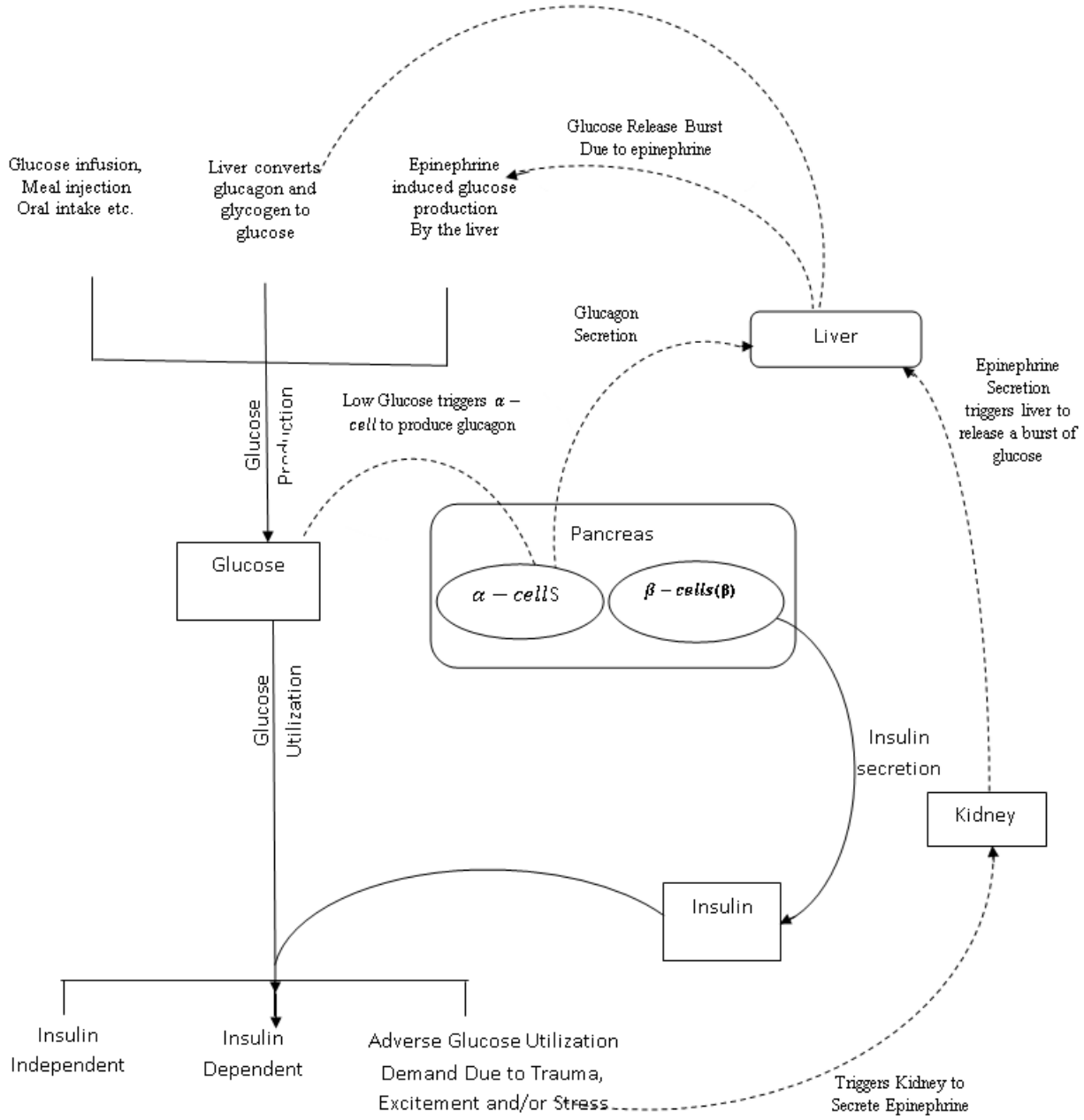

Key: *Dotted lines for stimulation* *Solid lines for action*

Fig. 1: flow diagram of the model
Model diagram for the dynamics of glucose, insulin, beta cell mass and epinephrine

In post-absorptive state, the glucose is released into the blood by the liver and kidneys, removed from the interstitial fluid by all the cells of the body, and distributed into many physiological compartments (e.g. arterial blood, venous blood, cerebral spinal fluid, interstitial fluid). These studies suggest that a single compartment model is appropriate

when glucose kinetics are relatively slow. Since we are primarily concerned with the evolution of fasting blood glucose levels over a time-scale of days to years, glucose dynamics are modelled with a single compartment mass balance equation [1].

$$\frac{dG}{dt} = production - utilization \qquad (3.2)$$

where; G is the concentration of glucose in the blood, and t is the time (measured in days).

Glucose Production

The rates of glucose production and utilization are normalized by the volume of glucose distribution to obtain the proper units [1]. Thus

$$production = P_0 - \left(E_{GOp} + S_{Ip} I\right)G \qquad (3.3)$$

where; P_0 is the rate of glucose production at zero glucose level, E_{GOP} is the glucose effectiveness at zero insulin for production, S_{IP} is insulin sensitivity for production, I is insulin concentration at a time t, and G is glucose concentration at a time t.

In an emergency situation (induced trauma, excitement and/or stress), the body releases an amount of epinephrine which quickly increases the concentration of glucose in the blood [2].

According to [5] during the infusion of epinephrine alone, plasma glucose concentrations quickly rose and within 1 hour reached a plateau value of $\sim 140 mg/\ dl$. Epinephrine is released by the adrenal medulla at a basal endogenous rate of approximately 0.18 (µg/min) and the epinephrine release modifier varies from 1 to 19.75. Meaning that, the epinephrine release rate will be 19.75 times the basal release rate with maximal exercise [12]

So let assume that the amount of the basal epinephrine release rate with maximal exercise be into the blood stream due to excitement, trauma and/or stress and let G_e be the amount of glucose production due to the effect of epinephrine. Then G_e increases the glucose concentration in the blood stream, we incorporate G_e into glucose production equation developed by [1].

Hence equation (3) becomes:

$$production = P_0 + G_e - \left(G_{GOp} + S_{Ip} I\right)G \qquad (3.4)$$

where; P_0 is the rate of glucose production at zero glucose level, G_e is the amount of glucose production from the breakdown of glycogen due to epinephrine secretion, E_{GOp} is the

glucose effectiveness at zero insulin for production and S_{Ip} is insulin sensitivity for production.

Glucose Utilization

The rates of glucose production and utilization depend on blood glucose and insulin levels. At constant insulin levels, glucose production decreases while uptake increases, both linearly with respect to glucose levels [1], we have;

$$Utilization = U_0 + (E_{GOU} + S_{Iu} I)G \qquad (3.5)$$

where; U_0 the rate of glucose utilization at zero glucose level, E_{GOu} is glucose effectiveness at zero insulin for utilization, S_{Iu} is insulin sensitivity for utilization, G represents glucose concentration and it represent blood insulin concentrations.

Epinephrine has effect on glucose utilization; however it is negligible and therefore ignored. Substituting equations (3.4) and (3.5) into equation (3.2),

$\frac{dG}{dt}$ = Production – utilization. We get the following

$$\frac{dG}{dt} = P_o + G_e - (E_{GOP} + s_{IP} I)G - U_o - (E_{GOU} + S_{IU} I)G$$

$$\frac{dG}{dt} = (P_0 - U_0) + G_e - [(E_{GOP} + E_{GOU}) + (S_{IP} I + S_{IU} I)]G$$

Hence, the equation of glucose dynamics under the influence of epinephrine hormones which is secreted in response to trauma, excitement and/or stress is given by

$$\frac{dG}{dt} = R_0 + G_e - (E_{GO} + S_I I)G \qquad (3.6)$$

where; $R_0 = P_0 - U_0$ in **Table 1** is the net rate of glucose production and at zero glucose level, G_e is the amount of glucose increase due to epinephrine hormones,

$E_{GO} = E_{GOP} - E_{GOU}$ in **Table 1 is** total glucose effectiveness at zero insulin for production and utilization, and $S_I = S_{IP} + S_{IU}$ in **Table 1** is the total insulin sensitivity for production and utilization.

3.2 Insulin dynamics

Insulin is secreted by pancreatic $\beta - cell$, cleared by the liver, kidneys, and insulin receptors, and distributed into several compartments (e.g. Portal vein, peripheral blood, and interstitial fluid) of the body. Our main concern is the long-time evolution of fasting insulin levels in peripheral blood. Since the dynamics of fasting insulin levels on this time-scale are slow, we use a single-compartment equation given by

$$\frac{dI}{dt} = Secretion - Clearance \qquad (3.7)$$

where Secretion and Clearance are rates normalized by insulin's volume of distribution [1].

Insulin Secretion

The rate of insulin secretion from pancreatic $\beta - cells$ is a sigmoidal function of glucose production [1]. Hence, we have

$$\frac{dI}{dt} = \frac{\beta\sigma G^2}{\alpha + G^2} \qquad (3.8)$$

where; β is the mass of pancreatic $\beta - cells$, all $\beta - cells$ are assumed to secrete insulin at the same maximal rate σ, α is a constant and $\frac{G^2}{\alpha + G^2}$ is a Hill function that describes the sigmoid nature of insulin secretion [1].

When epinephrine is secreted into the blood stream, the insulin secretion by pancreatic $\beta - cells$ will be suppressed by 41% [5]. This means insulin sensitivity to trigger glucose utilization by cells will be reduced. Let ρ be amount of insulin suppression by epinephrine, then we have a negative effect on insulin secretion thus:

Amount of Insulin secretion suppressed = - ρI $\qquad (3.9)$

Since ρ is the epinephrine effectiveness in suppressing insulin secretion. We incorporate (-ρI) to insulin secretion in equation (3.9) to obtain the total insulin secretion when epinephrine is secreted. Therefore, the rate of insulin secretion in the presence of epinephrine secretion is given by

$$\frac{dI}{dt} = \frac{\beta\sigma G^2}{\alpha + G^2} - \rho I \qquad (3.10)$$

Insulin Clearance

The rate of insulin clearance is proportional to blood insulin levels when the system is near steady state [1]. Clearance α I

Thus, $Clearance = KI \qquad (3.11)$

where; K is the insulin clearance constant by liver, kidney, muscle, and insulin receptors [1].

Substituting equations (3.10) and (3.11) into equation (3.7), we obtain the equation governing insulin secretion and clearance in the presence of epinephrine, as

$$\frac{dI}{dt} = \frac{\beta\sigma G^2}{\alpha + G^2} - \rho I - KI$$
$$\frac{dI}{dt} = \frac{\beta\sigma G^2}{\alpha + G^2} - (\rho + K)I \qquad (3.12)$$

where; β is the mass of pancreatic $\beta - cells$. σ is a rate of maximum secretion by the pancreatic $\beta - cells$ and $\frac{G^2}{\alpha + G^2}$ Hill function that describes the sigmoid ranging from 0 to 1, ρ is the parameter incorporated to insulin secretion which is epinephrine effectiveness in suppressing insulin secretion, and K is insulin clearance constant by liver, kidney, muscle, and insulin receptors, and I is insulin.

3.3 β – cell Mass

Dynamics

Despite a complex distribution of pancreatic $\beta - cells$ throughout the pancreas, $\beta - cell\,mass$ dynamics have been successfully quantified with a single compartment model [1].

$$\frac{d\beta}{dt} = Formation - Loss \qquad (3.13)$$

where; Formation and Loss represent the rates at which $\beta - cell$ mass is added to or removed from the population, respectively [1].

Replication of $\beta - cells$

New $\beta - cells$ can be formed by replication of existing $\beta - cells$. In vitro studies show that the percentage of $\beta - cells$ undergoing replication varies as a nonlinear function of glucose level in the medium. Replication rates for $\beta - cell\,mass$ increase with increasing glucose levels. However, at extreme hyperglycemia, $\beta - cells$ replication may be reduced. We modelled this behaviour with a simple second degree polynomial (patterned after logistic growth) [1].

$$\text{Re}\,plication = \left(r_{1r}G - r_{2r}G^2\right)\beta \qquad (3.14)$$

where; $r_{1r}\ and\ r_{2r}$ are constants in **Table 1**.

Loss of $\beta - cells$

Cells can be lost from the $\beta - cell\,mass$ by apoptosis (regulated cell death), necrosis (unregulated cell death). In vitro, $\beta - cells$ death has been shown to vary nonlinearly with glucose. Increasing the glucose level from 0 to approximately 11mM in a medium surrounding cultured $\beta - cells$ reduced the rate of $\beta - cells$ death. Above 11mM glucose,

the rate of $\beta - cells$ death either remained low or increased. We have modelled this behavour with a simple second degree polynomial,

$$Death = (d_0 - r_{1a}G + r_{2a}G^2)\beta \qquad (3.15)$$

where; d_0 is the death rate at zero glucose and r_{1a} and r_{2a} are constants.

Substituting equations (3.14) and (3.15) into equation (3.13), we obtain the equation for $\beta - cell\,mass$ dynamics as:

$$\frac{d\beta}{dt} = (-d_0 + r_1G - r_2G^2)\beta \qquad (3.16)$$

where; $r_1 = r_{1r} + r_{1a} and\ r_2 = r_{2r} + r_{2a}$ are constants in **Table 1** related to $\beta - cell$ dynamics

Therefore, from the assumptions, description and the schematic diagram of the modified model in Figure 1, we derived the following modified model equations and we described it as in the presence of epinephrine:

$$\begin{aligned}\frac{dG}{dt} &= R_0 + G_e - (E_{GO} + s_I I)G \\ \frac{dI}{dt} &= \frac{\beta\sigma G^2}{\alpha + G^2} - (\rho + K)I \\ \frac{d\beta}{dt} &= (-d_0 + r_1G - r_2G^2)\beta\end{aligned} \qquad (3.17)$$

4 Analytical Study

In this section, we carried out analytical and numerical studies on the modified model which is an extension of [1] model as indicated below:

4.1 Equilibrium points of the system

We studied the equilibrium solution of the system in equation (3.17) by splitting the glucose regulatory system into subsystems; slow **(**$\beta - cell\,mass$) subsystems and fast (***glucose/insulin***) subsystems.

From equation (3.17) we have

$$\frac{dG}{dt} = R_0 + G_e - (E_{GO} + S_I I)G$$

$$\frac{dI}{dt} = \frac{\beta\sigma G^2}{(\alpha + G^2)} - (\rho - K)I$$

$$\frac{d\beta}{dt} = (-d_0 + r_1G - r_2G^2)\beta$$

4.2 Equilibrium of the slow subsystems $\beta - cell$ ***mass***

Putting

$$\frac{d\beta}{dt} = 0$$

We have the following:

$$\left(-d_0 + r_1 G - r_2 G^2\right)\beta = 0$$

Either $\beta = 0$ or $\left(-d_0 + r_1 G - r_2 G^2\right) = 0$ (4.1)

We have

$$r_2 G^2 - r_1 G + d_0 = 0$$

Solving for G

$G_{1,2} = \frac{r_1 \pm \sqrt{r_2^{\,2} - 4 \times r_1 \times d_0}}{2r_2}$, Either $G_1 = \frac{r_1 + \sqrt{r_2^{\,2} - 4 \times r_1 \times d_0}}{2r_2}$ Or $G_2 = \frac{r_1 - \sqrt{r_2^{\,2} - 4 \times r_1 \times d_0}}{2r_2}$

4.3 Equilibrium of fast (Glucose/insulin) subsystems

Equating $\frac{dG}{dt} = \frac{dI}{dt} = 0$

We have

$$\frac{\beta \sigma G^2}{\left(\alpha + G^2\right)} - \left(\rho - K\right)I = 0 \quad (4.2)$$

From 4.1, $\beta = 0$ hence 4.2 gives

$$I = 0 \quad (4.3)$$

For glucose dynamics

At equilibrium point, we have

$$R_0 + G_e - \left(E_{GO} + S_I I\right)G = 0 \quad (4.4)$$

Using 4.3 in4.4, we have

$$R_0 + G_e - E_{GO} G = 0$$

$$E_{GO} G = R_o + G_e$$

$$G = \frac{R_0 + G_e}{E_{go}}$$

Therefore, the equilibrium point of the fast ***(Glucose/Insulin)*** subsystems is

Given by

$$G^*, I^* = \left(\frac{R_0 + G_e}{E_{GO}}, 0\right)$$

4.4 Stability Analysis

From equations (3.17) we should find the stability of the fast ***(glucose/insulin)*** subsystems

$$\frac{dG}{dt} = R_0 + G_e - \left(E_{GO} + S_I I\right)G$$

$$\frac{dI}{dt} = \frac{\beta\sigma G^2}{\alpha + G^2} - (\rho + K)I$$

Using Jacobian Matrix to find the stability

$$J = \begin{bmatrix} \frac{\partial F_1}{\partial G} & \frac{\partial F_1}{\partial I} \\ \frac{\partial F_2}{\partial G} & \frac{\partial F_2}{\partial I} \end{bmatrix} \qquad (4.5)$$

Let $F_1 = R_0 + G_e - (E_{GO} + S_I I)G$ and

$$F_2 = \frac{\beta\sigma G^2}{\alpha + G^2} - (\rho + K)I$$

Therefore, the Jacobian matrix in (4.5) becomes

$$J = \begin{bmatrix} -(E_{GO} + S_I I) & -S_{iG} \\ \frac{-2\alpha\beta\sigma G}{(\alpha + G^2)^2} & -(\rho + K) \end{bmatrix}$$

At equilibrium of the fast subsystems

$$J_0 = \begin{bmatrix} -E_{GO} & -S_i \frac{(R_0 + G_e)}{E_{GO}} \\ 0 & -(\rho + K) \end{bmatrix}$$

Using characteristics equation, We have

$$|J(E_o) - \lambda I| = 0$$

Putting the Jacobian into characteristics equation

$$\begin{vmatrix} -E_{GO} - \lambda & -S_i \frac{(R_0 + G_e)}{E_{GO}} \\ 0 & -(\rho + K) - \lambda \end{vmatrix} = 0$$

$$(-E_{GO} - \lambda)(-(\rho + K) - \lambda) = 0$$

$$-E_{GO} - \lambda = 0 \quad or \quad -(\rho + K) - \lambda = 0$$

$$\lambda_1 = -E_{GO} \qquad and \qquad \lambda_2 = -(\rho + K)$$

Therefore, the fast ***(Glucose and Insulin)*** subsystems is locally and asymptotically stable since all the values of $\lambda_i < 0$ for i = 1, 2 were negative.

For slow ($\beta - cell$ ***mass***) subsystem, we have the following

Either $\beta = 0$ or $-d_0 + r_1 G - r_2 G^2 = 0$

$$\lambda = -d_0 + r_1 G - r_2 G^2 \qquad (4.6)$$

The slow ***(β − cell mass)*** subsystems is locally and asymptotically stable since the Eigenvalue was negative, at $r_2 G^2 + d_0 > r_1 G$

Since the value ofh $r_2 = 0.0000024$ are in **Table 2**.we substituted the values in **Table 2** into (4.6) we have

$$-0.06 + 0.00084G - 0.0000024G^2 = 0$$

$$24G^2 - 8400G + 600000 = 0$$

Putting the above quadratic equation in (4.2), we have

$$G_{1,2} = \frac{8400 \pm \sqrt{8400^2 - 4 \times 24 \times 600000}}{2 \times 24}$$

Either

$$G_1 = \frac{12000}{48} = 250 \qquad \text{Or} \qquad G_2 = \frac{4800}{48} = 100$$

The one dimensional subsystem had three steady state solutions which were $\beta = 0$, G = 100 and G = 250. These three steady states were referred to as the pathological, physiological and unstable steady state Topp *et al., (*2000)

Analysing the system as a whole, consider (3.17) above

$$F_1 = R_0 + G_e - (E_{GO} + S_I I)G$$

$$F_2 = \frac{\beta \sigma G^2}{(\alpha + G^2)} - (\rho - K)I$$

$$F_3 = (-d_0 + r_1 G - r_2 G^2)\beta$$

Thus, the Jacobian Matrix J of the above system is given by

$$J = \begin{pmatrix} \frac{\partial F_1}{\partial G} & \frac{\partial F_1}{\partial I} & \frac{\partial F_1}{\partial \beta} \\ \frac{\partial F_2}{\partial G} & \frac{\partial F_2}{\partial I} & \frac{\partial F_2}{\partial \beta} \\ \frac{\partial F_3}{\partial G} & \frac{\partial F_3}{\partial I} & \frac{\partial F_3}{\partial \beta} \end{pmatrix} \qquad (4.4)$$

$$J = \begin{pmatrix} -(E_{GO} + S_I I) & -S_I G & 0 \\ \dfrac{-2\alpha\beta\sigma G}{(\alpha + G^2)^2} & -(\rho + K) & \dfrac{\sigma G^2}{\alpha + G^2} \\ (r_1 - 2r_2 G)\beta & 0 & (-d_0 + r_1 G - r_2 G^2) \end{pmatrix}$$

At equilibrium points, the whole system becomes

$$J(E_0) = \begin{pmatrix} -E_{GO} & -S_I \dfrac{(R_0 + G_e)}{E_{GO}} & 0 \\ 0 & -(\rho + K) & \dfrac{\sigma(R_0 + G_e)^2}{\alpha E_{GO} - (R_0 + G_e)^2} \\ 0 & 0 & -d_0 + r_1 \dfrac{(R_0 + G_e)}{E_{GO}} - r_2 \dfrac{(R_0 + G_e)^2}{E_{GO}} \end{pmatrix}$$

The characteristics equation is given by

$$\left|J(E_o) - \lambda I\right| = 0$$

$$E_{GO} - \lambda \begin{vmatrix} -(\rho + K) - \lambda & \dfrac{\sigma(R_0 + G_e)^2}{\alpha E_{GO} + (R_0 + G_e)^2} \\ 0 & -d_0 + r_1 \dfrac{(R_0 + G_e)}{E_{GO}} - r_2 \dfrac{(R_0 + G_e)}{E_{GO}} - \lambda \end{vmatrix}$$

Therefore,

$\lambda_1 = -E_{GO}$, $\lambda_2 = -(\rho + K)$ and

$$\lambda_3 = -\left(d_0 + r_2 \frac{(R_0 + G_e)}{E_{GO}} - r_1 \frac{(R_0 + G_e)}{E_{GO}} \right)$$

Since all the values of $\lambda_i < 0$ for i= 1, 2, 3 the whole system is locally and asymptotically stable.

Table 2: **Values of the parameters and variables of the model; some were obtained from existing model while the remaining values from other literatures**

Parameters	**Value**	**unit**	
$\overset{*}{G}$	600	mgd/dl	[1]
$\overset{*}{I}$	284.21	$\mu Um/dl$	[1]
$\overset{*}{\beta}$	0 G=100 or 250	$mgdl/dl$	[1]
β_1	300	$mgdl/day$	Assumed
β_2	600	$mgdl/day$	Assumed
β_3	900	$mgdl/day$	Assumed
R_0	864	mgd/dl	[1]
E_{GO}	1.44	d^{-1}	[1]
S_I	0.72	$ml\mu/dU$	[1]
σ	43.2	$\mu Um/dl$	[1]
α	20,000	mg^2dl/l^2	[1]
K	432	d^{-1}	[1]
d_0	0.06	d^{-1}	[1]
r_1	0.00084	mdl/dg	[1]
r_2	0.24×10^{-5}	$\mathrm{mgl^2/dg^2}$	[1]
G_e	140	mgd/dl	[5]
ρ	41%	$\mu Um/dl$	[6]

The results of the performance of the existing and modified models are shown in Figure MATLAB 2015a was being used to generate the simulations.

Existing model

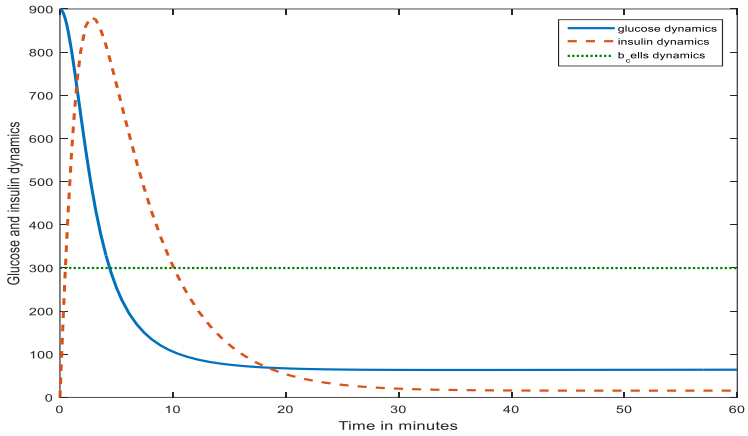

Fig. 2: *Glucose, Insulin and* $\beta - cell$ *mass dynamics in the absence of epinephrine.*

Modified model

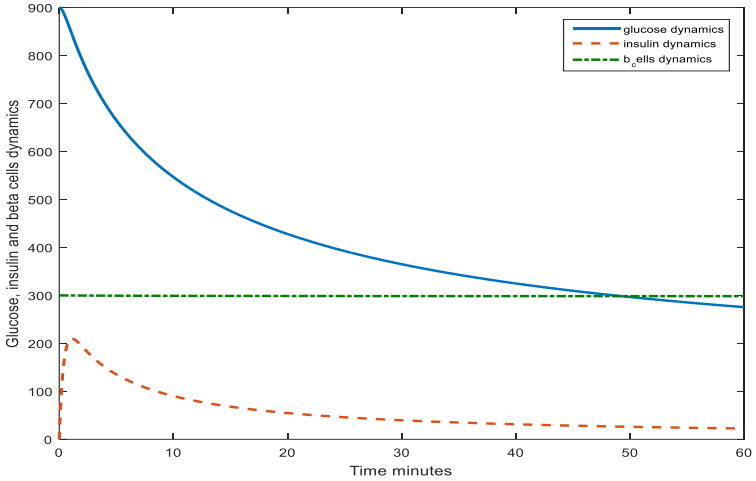

Figure 3: *Glucose, Insulin and* $\beta - cell$ *mass dynamics in the presence of epinephrine.*

Existing and Modified Models

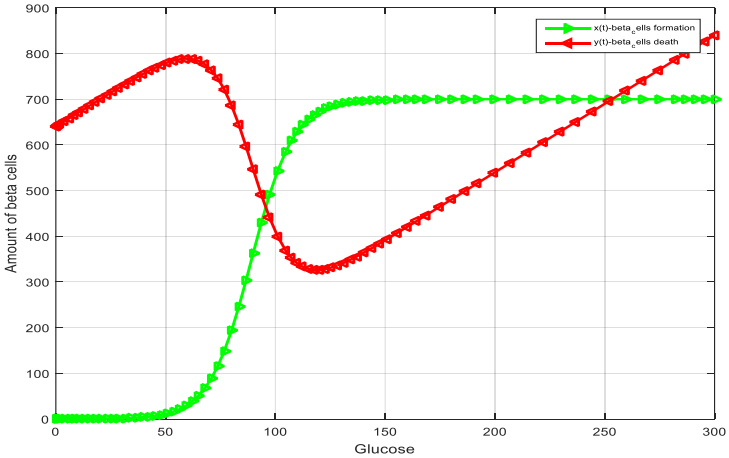

Fig. 4: Dynamics of $\beta - cell$ ***mass*** **formation and death in the absence and presence of epinephrine.**

Discussion:

Discussion of the results of the study is presented as follows:

Case 2: Glucose, Insulin and $\beta - cell\ mass$ dynamics in the absence of epinephrine.

Figure 3 shows the dynamics of glucose, insulin and $\beta - cell\ mass$ in the absence of trauma, excitement and stress. Blood glucose level decreases, blood insulin level increases while the $\beta - cell\ mass$ remain constant.

Case 3: Glucose, Insulin and $\beta - cell\ mass$ dynamics in the presence of epinephrine.

Figure 4 shows the dynamics of glucose, insulin and $\beta - cell\ mass$ in the presence of trauma, excitement and stress. Blood glucose level increases, blood insulin level decreases while $\beta - cell\ mass$ remain constant due to presence of epinephrine. This indicated that there is no effect of epinephrine on $\beta - cell\ mass$.

Case 4: Dynamics of $\beta - cell\ mass$ formation and death in the presence of epinephrine.

Figure 5 shows the effect of glucose on beta cells formation and death in the presence of trauma, excitement and stress.

The effect of epinephrine on three pathways to diabetic state are as followed:

Effect of epinephrine on Regulated Hyperglycemia; in this beta cells death is greater than formation. This will push glucose to high level in addition to the blood glucose burst from liver because of epinephrine secretion and low blood insulin due to suppression by epinephrine hormone.

Effect of epinephrine on Bifurcation; in this beta cells formation is greater than death which lead to high blood insulin and low blood glucose level but due to presence of epinephrine, the insulin secretion would be suppressed and blood glucose level will be increased. This will make blood glucose to remain at high level as a result of low insulin.

Effect of epinephrine on Dynamical Hyperglycemia; in this beta cells death is extremely greater than beta cells formation which lead to extreme elevated blood glucose level due extremely low insulin in addition to the burst in blood glucose due the epinephrine and low blood insulin level due to suppression by epinephrine hormone which will further increase blood glucose level and decrease blood insulin level.

Therefore, from the above discussion we understood that trauma, excitement and stress increased blood glucose level and decrease blood insulin level while in other side trauma, excitement and stress have no effect on beta cells formation and lost.

During the experiments three distinct amount of beta cell masses: 300, 600 and 900 were used. The result showed that in normal condition, beta_cell mass had significant effect in glucose utilization. However, in the presence of trauma, excitement and/or stress, the amount of beta cell mass had less effect in glucose utilization because of epinephrine suppression on insulin secretion. Beta cell mass increased blood insulin level but not enough to trigger more glucose utilization in such a way that will bring down the blood glucose level into homeostasis even with high number of beta cell mass 900. According to [10], the average mass of β-cell mass in a normal individual has been found to be 850 mg. This means in the presence of epinephrine the blood glucose level remains high despite the fact that there is increase in beta cell mass.

The model developed which was an extension of [1] model is similar to those of, [4], [9] and [10] for glucose, insulin, and $\beta - cell\ mass$ kinetics. However, it differs significantly by its peculiarity in the case of epinephrine hormone which is secreted by adrenal medulla of the kidney for taking care of emergency condition cause by trauma, excitement and/or stress which increase blood glucose level.

The results of equilibrium analysis showed that the fast subsystem and slow subsystem were independently locally and asymptotically stable since the Eigen values of both the systems were negatives. Analysing the system as a whole, the system was locally and asymptotically stable.

All the three pathways to diabetes state would be affected by epinephrine hormone because of its effect on increase in blood glucose level and decrease in blood insulin level. This showed that trauma, excitement and stress increase the risk of extreme and prolong hyperglycemia.

Summary, Conclusion and Recommendation:

In this work, we incorporated a parameter ρ by defining it as effectiveness of epinephrine in suppressing insulin secretion and a parameter G_e by defining it as epinephrine induced glucose increase as the factors that affect glucose and insulin homeostasis. The model which consists of a system of three nonlinear ordinary differential equations was used to investigate the effect of epinephrine on glucose, insulin and beta cell mass dynamics. The result of the study showed that; in the presence of epinephrine there is increase in blood glucose level and increase in Beta cell mass which increase blood insulin level but not enough to bring down blood glucose level into homeostasis. As a result of that, there is an

extreme hyperglycemia in all three distinct state. Furthermore, the result of the numerical experiment carried out indicated that frequent epinephrine secretion into the blood induced prolong and extreme hyperglycemia. An extreme hyperglycemia induced both beta cells death and insulin resistance which would lead to diabetes. In conclusion, frequent state of trauma, excitement and/or stress induced diabetes. In view of the findings of this study, we recommended that there should be a massive and continuous health education especially for communities living in the areas where the stated agents (trauma, excitement and stress) of epinephrine secretion are common, so that the people will understand the effect of these agents on their healthy living and this will minimize the occurrence of diabetic among the people. The government, non-governmental organization and public health workers should focus on public enlightenment programs aimed at enabling individuals in the society to understand how these three factors increase the risk of having diabetes in their lives.

Conclusion:

We modified [12] mathematical model for beta cell mass, insulin and glucose kinetics by incorporating the parameter 'G_e' and 'ρ' as the rate of glucose production due to epinephrine secretion and epinephrine effectiveness in suppressing insulin secretion to examine the effect of two parameters on glucose regulatory system. Analytical studies were carried out using Jacobian matrix. The equilibrium points were obtained and our results showed that the equilibrium point of the system is locally asymptotically stable since all the Eigen values were negative this showed that the disease will be controlled to avoid further spread. The result of the numerical experiment carried out indicated that frequent epinephrine secretion into the blood induced prolong and extreme hyperglycemia. An extreme hyperglycemia induced both beta cells death and insulin resistance which can lead to both type1 and type 2 diabetes.

References:

1. Topp, B., Promislaw K., de Vries G., Miura R., & Finegood D. (2000). A model of β-cell mass, insulin, and glucose kinetics: pathways to diabetes. *J. Theor. Biol., 206, 605-619.*
2. Kwacha, B., Ongati O., & Simwa R. (2011). Mathematical Model for Detecting Diabetes in the Blood. Applied Mathematical Sciences, 5(6): 279-286.
3. Ahlam, A. S. & Alaa, S. (2014). Developing a mathematical model to detect diabetes using multigene genetic programming. Advance journal in artificial intelligence, (3) 10.

4. Boutayeb, A., Chetouani, A., Achouyab, K. & Twizell, E. H. (2004). Mathematical model for the burden of diabetes and its complications. Biomed engineering online, 3:20. Doi: 10.1186/1475-925X-3-20.
5. David, C. & Ralph, A. (1980). Epinephrine induced insulin resistance in man. J. Clin. Invest. Inc. 65 717-721
6. Didier L. Kitt Falk, & Raymond R. (1998). Effect of epinephrine on muscle glycogenolysis and insulin stimulated muscle glycogen synthesis in human. The American Physiological society E130 0193-1849/98
7. Frank, N. & Mingxian, J. (2015) mathematical modelling and simulations of the pathophysiology of type 2 diabetes mellitus Biomathematics Engineering and Informatics 978-1- 5090-0022-7
8. Hussain, J & Zadeng, D. (2014). Mathematical model of glucose insulin interaction. Sci., 14(2), 2229-6026.
9. Ibrahim, I. A., Haruna, Y. & Garba, E. J. D. (2014). Mathematical model for the dynamics of glucose regulatory system under the combined effect of dieting and physical activity. International Journal of Pure and Applied Science and Technology, 20 (1), pp. 88-100.
10. Ryan, D., Danielle, J. L., Daniel, B. R., Thomas, B. V. & Stephen, A. W. (2001). Model of β-cell mass, insulin, glucose, and receptor dynamics with application to diabetes, cornel univ., dept. of biometric technical report BU-1579-M. Onlinelibrary.wiley.com>doi> full
11. Termitope, O. (2016). Current trends in preventing diabetes. Pharmnews, 38(11) pharmnews App on Google play store.
12. https://biogearsengine.com/document/ endocrine methodology.html

EXPLORING ANISOTROPIC BIANCHI TYPE IX COSMOLOGICAL SOLUTIONS IN BRANS-DICKE GRAVITY

Hasima Yasmin and Mukunda Dewri*
Department of Mathematical Sciences,
Bodoland University, Assam
*Corresponding author E-mail: dewri11@gmail.com

Abstract:
This study examines the Bianchi Type IX cosmic model in Brans-Dicke gravity, with a focus on anisotropy and dynamics of the scalar field. As the universe expands, its density decreases, and the equation of state parameter changes from negative to zero. Exact solutions demonstrate the significance of the Brans-Dicke parameter in cosmic evolution. The results provide new insights into isotropization, inflation, the early universe, and the impact of various gravity theories on astronomy.

Keywords: Bianchi Type IX, Anisotropic Cosmology, Brans-Dicke Gravity, Scalar Field, Cosmological Solutions

1. Introduction:

The study of Bianchi Type IX cosmic models has been a popular topic in theoretical physics because they provide valuable insights into how the universe behaves near singularities. In 2009, Heinzle and Uggla gave a solid proof of the Bianchi Type IX attractor theorem. This was a crucial first step toward understanding how these models behave as they become larger. Shortly after, de Andrade (2009) explored the limits of dynamo action in shear-free Bianchi Type IX cosmologies, broadening the scope of rotational constraints.

In subsequent years, research diversified into various aspects of Bianchi Type IX dynamics. Calogero and Heinzle (2010) analyzed oscillatory behavior in locally rotationally symmetric models with Vlasov matter, while Battisti *et al.* (2010) delved into quantum cosmology by examining inhomogeneous perturbations in Bianchi IX universes. Wilson-Ewing (2010) further extended these quantum investigations by studying Bianchi Type IX models within the framework of loop quantum cosmology.

Meanwhile, Tyagi *et al.* (2010) and Adhav *et al.* (2010) introduced general relativistic solutions involving string cosmological models and inflationary dynamics, respectively. Bali and Kumawat (2010) examined the effects of bulk viscosity in stiff fluid-tilted models, adding a new dimension to the understanding of dissipative processes. Misonoh *et al.*

(2011) later integrated these studies with Horava-Lifshitz gravity, exploring oscillatory solutions.

Further progress was made by Nourinezhad and Mehdipour (2012), who analyzed energy-momentum density descriptions, and Tyagi and Chhajed (2012), who incorporated electromagnetic fields into perfect fluid models. Pawar and Dagwal (2013) addressed two fluid cosmological models, while Czuchry and Piechocki (2013) focused on reducing the phase space of Bianchi IX cosmologies. Kim and Kawai (2013) examined chaotic dynamics within Gauss-Bonnet gravity, complemented by Lugo and Chauvet (2013), who revisited the Belinsky-Khalatnikov-Lifshitz (BKL) method.

In the mid-2010s, new perspectives emerged with the work of Patil *et al.* (2014) and Ghate and Sontakke (2014), who explored dust-filled universes and radiating cosmologies, respectively. Damour and Spindel (2014) ventured into supersymmetric quantum cosmology, while Fan *et al.* (2015) incorporated modular forms and spectral actions into their analyses. Manin and Marcolli (2016) expanded this work to include symbolic dynamics and modular curves.

During this period, Sofuoğlu (2016) introduced. $f(R,T)$ Gravity into rotating and expanding models, and Parikh *et al.* (2016) incorporated time-dependent cosmological constants. More recently, Saha (2018) investigated spinor fields in Bianchi IX spacetime, followed by Czuchry *et al.* (2019) and Canfora *et al.* (2019), who examined dynamics and topological charges in Einstein-Skyrme systems.

In the past few years, Chiovoloni *et al.* (2020) applied quantum mechanical approaches to the corner of Bianchi IX models, while Fahim and Ghezelbash (2021) introduced solutions within Einstein-Maxwell-dilaton theory. Sharma and Poonia (2021) investigated cosmic inflation with bulk viscosity, while Aditya *et al.* (2022) analyzed dark energy models within the Lyra geometry. Most recently, Giani *et al.* (2022) investigated the gravitational collapse of matter inhomogeneities, while Mishra and Sharma (2024) examined these models within the context of Brans-Dicke theory and deceleration parameters.

This extensive body of work demonstrates the various approaches and theories employed to elucidate the complexity of Bianchi Type IX cosmologies. It opens the door for more research in the future.

2. Metric and Field Equations

In this dissertation, we have considered the Bianchi type-IX universe as:

$$ds^2 = -dt^2 + A(t)^2[dx^2 - 2cosydxdz] + B(t)^2dy^2 + [B(t)^2sin^2y + A(t)^2cos^2y]dz^2 \tag{2.1}$$

where A and B represent cosmic scale factors that solely depend on cosmic time t.

The related field equations are expressed as

$$R_{kl} - \frac{1}{2}g_{kl}R = \frac{-8\pi}{\emptyset}T_{kl} - \frac{\emptyset_{;kl} - g_{kl}\emptyset^{,i}_{;i}}{\emptyset} - \frac{(\emptyset_{,k}\emptyset_{,l} - \frac{1}{2}g_{kl}\emptyset_{,i}\emptyset^{,i})\omega}{\emptyset^2} \tag{2.2}$$

and

$$\emptyset^{,i}_{;i} = \frac{8\pi T}{\emptyset(3+2\omega)} \tag{2.3}$$

where $R_{kl}, R, \emptyset, \omega, and\ T$ represent the Ricci tensor, Ricci scalar, Brans-Dicke scalar field, dimensionless coupling constant, and the trace of the energy-momentum tensor, respectively. The continuity equation is

$$T^{kl}_{;l} = 0 \tag{2.4}$$

Therefore, the adopted energy-momentum tensor of the fluid is

$$T^l_k = [T^0_0, T^1_1, T^2_2, T^3_3] \tag{2.5}$$

The energy-momentum tensor can be expressed using the following parameterization.

$$T^l_k = diag[-\rho, p_x, p_y, p_z] = diag[-1, w_x, w_y, w_z]\rho \tag{2.6}$$

Here ρ is the energy density and pressure components along three different directions are represented by p_x, p_y, and p_z .Also, the components w_x, w_y, and w_z are the directional components of the equation of state (EoS) parameter in three different directions.

$$T^l_k = diag[-1, w, w+\gamma, w+\gamma]\rho \tag{2.7}$$

Here, the symbol (w= $\frac{p}{\rho}$) is the deviation-free parameter of the fluid and represents the EoS parameter and γ is the skewness parameter.

The Brans-Dicke field Equations $(2.2) - (2.4)$ for the metric (2.1) can be expressed as

$$\frac{\ddot{A}}{A} + \frac{\ddot{B}}{B} + \frac{\dot{A}\dot{B}}{AB} + \left(\frac{\dot{A}}{A} + \frac{\dot{B}}{B}\right)\frac{\dot{\emptyset}}{\emptyset} + \frac{\omega}{2}\left(\frac{\dot{\emptyset}}{\emptyset}\right)^2 + \frac{\ddot{\emptyset}}{\emptyset} + \frac{A^2}{4B^4} = -\frac{8\pi}{\emptyset}(w+\gamma)\rho \tag{2.8}$$

$$2\frac{\ddot{B}}{B} + \left(\frac{\dot{B}}{B}\right)^2 + 2\frac{\dot{B}}{B}\frac{\dot{\emptyset}}{\emptyset} + \frac{\omega}{2}\left(\frac{\dot{\emptyset}}{\emptyset}\right)^2 + \frac{\ddot{\emptyset}}{\emptyset} + \frac{1}{B^2} - \frac{3A^2}{4B^4} = \frac{-8\pi}{\emptyset}w\rho \tag{2.9}$$

$$2\frac{\dot{A}\dot{B}}{AB}+\left(\frac{\dot{B}}{B}\right)^2+\left(\frac{\dot{A}}{A}+2\frac{\dot{B}}{B}\right)\frac{\dot{\emptyset}}{\emptyset}-\frac{\omega}{2}\left(\frac{\dot{\emptyset}}{\emptyset}\right)^2+\frac{1}{B^2}-\frac{A^2}{4B^4}=\frac{8\pi}{\emptyset}\rho \tag{2.10}$$

$$\ddot{\emptyset}+\dot{\emptyset}\left(\frac{\dot{A}}{A}+2\frac{\dot{B}}{B}\right)=-\frac{8\pi(3w+2\gamma-1)\rho}{\emptyset(3+2\omega)} \tag{2.11}$$

Here, the average scale factor $a(t)$ is given by:

$$a(t)=\log(\alpha t)^m \tag{2.12}$$

The spatial volume (V) is given by:

$$V(t)=AB^2=a^3(t) \tag{2.13}$$

The expansion scalar (θ) is defined as

$$\theta=3H=H_1+2H_2 \tag{2.14}$$

where

$$H=\frac{\dot{a}}{a} \tag{2.15}$$

is the Hubble Parameter.

Mean anisotropic parameter A_m quantifies the degree of anisotropic in the universe and is defined as :

$$A_m=\frac{1}{3}\left[\left(\frac{H_1}{H}-1\right)^2+2\left(\frac{H_2}{H}-1\right)^2\right] \tag{2.16}$$

We denote the Shear Scalar. σ^2 as

$$\sigma^2=\frac{1}{2}\sum_{i=1}^{3}{H_i}^2-\frac{1}{6}\theta^2 \tag{2.17}$$

where $H_1=\frac{\dot{A}}{A}$, $H_2=H_3=\frac{\dot{B}}{B}$ are the directional Hubble parameter

The deceleration parameter q is defined as follows:

$$q(t)=-\frac{\ddot{a}a}{\dot{a}^2} \tag{2.18}$$

3. Solutions of the Field Equations

Firstly, we consider the relation between the expansion scalar θ and the σ_1^1 of the shear scalar, which is given by $\sigma_1^1 \propto \theta$, leading to the expression

$$A = B^{\varepsilon_1} \tag{3.1}$$

where ε_1 is positive constant.

Secondly, we consider the well-accepted power-law relation between the scale factor $a(t)$ and the scalar field $\emptyset$ is given by

$$\emptyset = \emptyset_0[a(t)]^{\varepsilon_2} \tag{3.2}$$

Where ε_2 is an arbitrary constant. By equation (3.1) and (2.12) , we obtained

$$A = m^{\frac{3\varepsilon_1}{\varepsilon_1+2}}(\log(\alpha t))^{\frac{3\varepsilon_1}{\varepsilon_1+2}} \tag{3.3}$$

$$B = m^{\frac{\varepsilon_1}{\varepsilon_1+2}}(\log(\alpha t))^{\frac{\varepsilon_1}{\varepsilon_1+2}} \tag{3.4}$$

By applying equation (2.12) in (2.13), (2.15) and (2.18), the spatial volume (V),Hubble parameter (H) and the deceleration parameter $q(t)$ of the model are given by:

$$V = m^3(\log(\alpha t))^3 \tag{3.5}$$

$$H = \frac{1}{t\log(\alpha t)} \tag{3.6}$$

$$q(t) = \log(\alpha t) \tag{3.7}$$

By putting the value of H_1, H_2 and H in equation (2.16), Mean anisotropic parameter A_m is given by

$$A_m = \frac{2(\varepsilon_1 - 1)^2}{(\varepsilon_1 + 2)^2} \tag{3.8}$$

Solving equations (2.14), (2.15) and (2.17), the expansion scalar θ and shear scalar σ^2 as

$$\theta = \frac{3}{t\log(\alpha t)} \tag{3.9}$$

$$\sigma^2 = \frac{3(\varepsilon_1 - 1)^2}{(\varepsilon_1 + 2)^2 t^2\,(\log(\alpha t))^2} \tag{3.10}$$

Now, by solving the field equations (2.8), (2.9), (2.10) and putting the value of A, B and $\emptyset$, we obtain the values of energy density ρ, equation of state parameter w and skewness parameter γ

$$\rho = \frac{\emptyset}{8\pi}\left[\frac{1}{t^2(\log(\alpha t))^2}\left(\frac{18{\varepsilon_1}^2+9}{(\varepsilon_1+2)^2}+\frac{3\varepsilon_1\varepsilon_2+6\varepsilon_2}{(\varepsilon_1+2)}-\frac{{\varepsilon_2}^2\omega}{2}\right)\right] + \frac{\emptyset}{8\pi}\left[\frac{1}{m^{\frac{6}{\varepsilon_1+2}}(\log(\alpha t))^{\frac{6}{\varepsilon_1+2}}}\left(1-\frac{1}{4}\left(m^{\frac{6\varepsilon_1-6}{\varepsilon_1+2}}(\log(\alpha t))^{\frac{6\varepsilon_1-6}{\varepsilon_1+2}}\right)\right)\right] \quad (3.11)$$

$$w = \frac{-\frac{1}{t^2(\log(\alpha t))^2}\left[\frac{(6-6\varepsilon_1)+9}{(\varepsilon_1+2)^2}-\frac{6\log(\alpha t)-6\varepsilon_2}{(\varepsilon_1+2)}+\frac{{\varepsilon_2}^2 w}{2}+\varepsilon_2(\varepsilon_2-1-\log(\alpha t))\right]-\frac{1}{m^{\frac{6}{\varepsilon_1+2}}(\log(\alpha t))^{\frac{6}{\varepsilon_1+2}}}\left[1-\frac{3}{4}\left(m^{\frac{6\varepsilon_1-6}{\varepsilon_1+2}}(\log(\alpha t))^{\frac{6\varepsilon_1-6}{\varepsilon_1+2}}\right)\right]}{\left[\frac{1}{t^2(\log(\alpha t))^2}\left(\frac{18{\varepsilon_1}^2+9}{(\varepsilon_1+2)^2}+\frac{3\varepsilon_1\varepsilon_2+6\varepsilon_2}{(3\varepsilon_1+2)}-\frac{{\varepsilon_2}^2\omega}{2}\right)\right]+\left[\frac{1}{m^{\frac{6}{\varepsilon_1+2}}(\log(\alpha t))^{\frac{6}{\varepsilon_1+2}}}\left(1-\frac{1}{4}\left(m^{\frac{6\varepsilon_1-6}{\varepsilon_1+2}}(\log(\alpha t))^{\frac{6\varepsilon_1-6}{\varepsilon_1+2}}\right)\right)\right]} \quad (3.12)$$

$$\gamma = \frac{\frac{1}{t^2(\log(\alpha t))^2}\left[\frac{(12-6\varepsilon_1-6{\varepsilon_1}^2}{(\varepsilon_1+2)^2}-\frac{(3-3\varepsilon_1)\log(\alpha t)+3\varepsilon_1\varepsilon_2}{(\varepsilon_1+2)}\right]+\frac{1}{m^{\frac{6}{\varepsilon_1+2}}(\log(\alpha t))^{\frac{6}{\varepsilon_1+2}}}\left[1-\left(m^{\frac{6\varepsilon_1-6}{\varepsilon_1+2}}(\log(\alpha t))^{\frac{6\varepsilon_1-6}{\varepsilon_1+2}}\right)\right]}{\left[\frac{1}{t^2(\log(\alpha t))^2}\left(\frac{18{\varepsilon_1}^2+9}{(\varepsilon_1+2)^2}+\frac{3\varepsilon_1\varepsilon_2+6\varepsilon_2}{(3\varepsilon_1+2)}-\frac{{\varepsilon_2}^2\omega}{2}\right)\right]+\left[\frac{1}{m^{\frac{6}{\varepsilon_1+2}}(\log(\alpha t))^{\frac{6}{\varepsilon_1+2}}}\left(1-\frac{1}{4}\left(m^{\frac{6\varepsilon_1-6}{\varepsilon_1+2}}(\log(\alpha t))^{\frac{6\varepsilon_1-6}{\varepsilon_1+2}}\right)\right)\right]} \quad (3.13)$$

4. Graphical Representations

To show the graphical behavior, the values of $\varepsilon_1 = 0.001, \varepsilon_2 = 0.0012, m = 14, \alpha = 20.43$, $\emptyset_0 = 3.6$ and $\omega = 41000$ [Calcagni *et al.* (2012)] are considered.

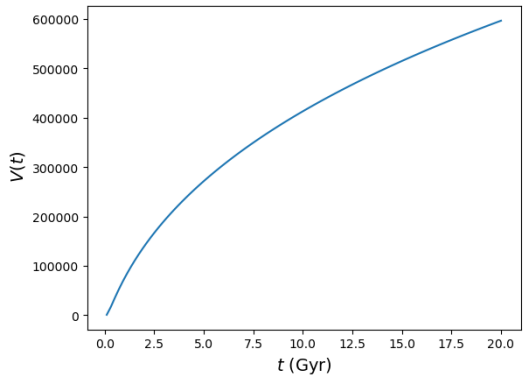

Figure 4. 1: Evolution of *V* vs. *t*

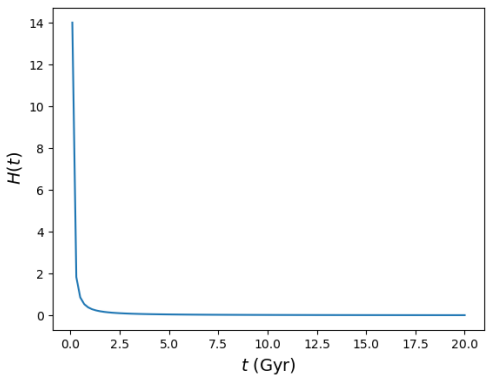

Figure 4. 2: Evolution of *H* vs. *t*

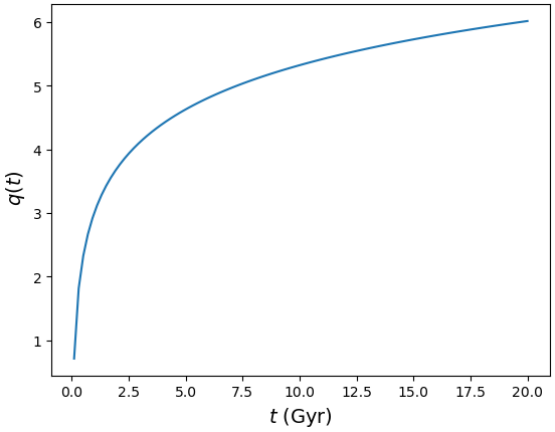

Figure 4. 3: Evolution of q vs. t

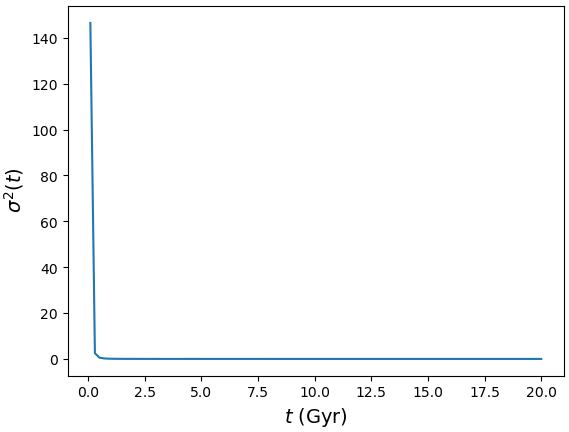

Figure 4. 4: Evolution of σ^2 vs. t

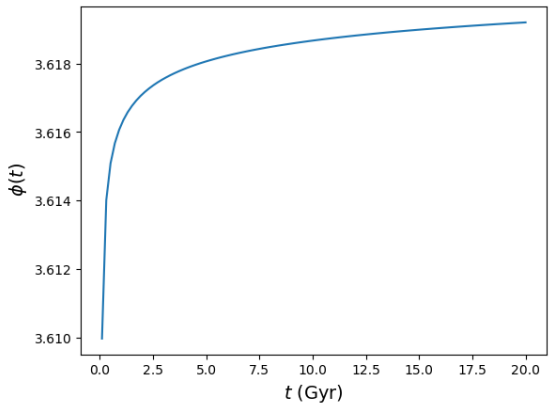

Figure 4. 5: Evolution of ϕ vs. t

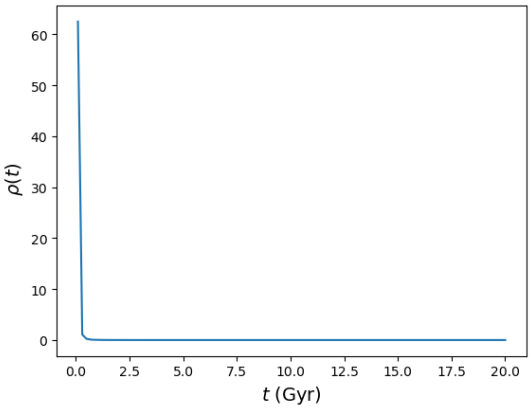

Figure 4. 6: Evolution of ρ vs. t

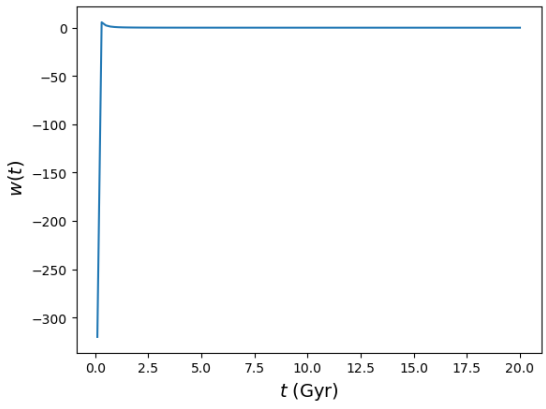

Figure 4. 7: Evolution of w vs. t

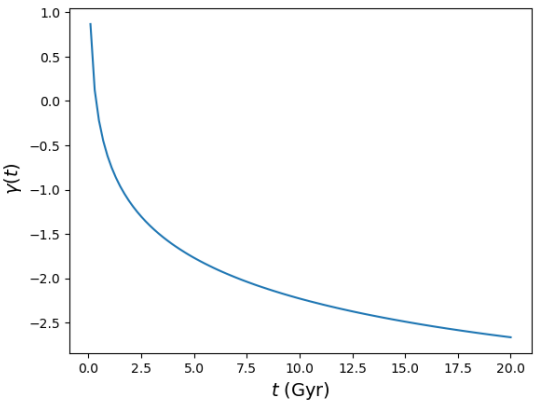

Figure 4. 8: Evolution of γ vs. t

Conclusion:

In this model of the universe, as illustrated in Figures 1–8, the universe's evolution is characterized by significant changes in various factors over time. The growing size (Figure 4.1) suggests an expanding universe, which aligns with current cosmological knowledge. A declining Hubble parameter (Figure 4.2) accompanies this expansion, indicating that the rate of expansion is slowing down.

The deceleration parameter (Figure 4.3) increases over time, suggesting that the mechanisms of cosmic acceleration are evolving. The decrease in the shear scalar (Figure 4.4) indicates a decrease in anisotropy, suggesting that the universe is becoming more uniform as it evolves.

The rise in the Brans-Dicke (BD) scalar field (Figure 4.5) backs up the idea of a dynamic gravitational coupling, which is a feature of scalar-tensor theories. At the same time, the falling density (Figure 4.6) is consistent with the expansion of the universe, which spreads matter and energy over a larger area.

The change in the equation of state parameter from a high negative value to zero (Figure 4.7) indicates that the system has transitioned from one dominated by dark energy-like particles (characterized by negative pressure) to one dominated by matter. Similarly, the change in the skewness measure from high positive to negative values (Figure 4.8) indicates that the distribution of matter and energy has shifted, suggesting a transition from less asymmetrical to more symmetrical states.

For a better understanding of how the world changes over time when scalar fields and evolving anisotropies act on it, this model makes sense. These changes in factors show that growth, the distribution of energy, and the geometry of the universe are all linked. We can gain a better understanding of how the structure and evolution of the universe on a large scale are controlled by this.

References:

1. Heinzle, J. M., and Uggla, C. (2009). A new proof of the Bianchi type IX attractor theorem. *Classical and quantum gravity*, 26(7), 075015.
2. de Andrade, L. G. (2009). Global rotation limits on dynamo action in shear-free Bianchi type-IX cosmology. arXiv preprint arXiv:0906.2044.
3. Calogero, S., and Heinzle, J. M. (2010). Oscillations toward the singularity of locally rotationally symmetric Bianchi type IX cosmological models with Vlasov matter. *SIAM Journal on Applied Dynamical Systems*, 9(4), 1244-1262.

4. Battisti, M. V., Marciano, A., and Rovelli, C. (2010). Triangulated loop quantum cosmology: Bianchi IX universe and inhomogeneous perturbations*. Physical Review D—Particles, Fields, Gravitation, and Cosmology,* 81(6), 064019.
5. Wilson-Ewing, E. (2010). Loop quantum cosmology of Bianchi type IX models. *Physical Review D—Particles, Fields, Gravitation, and Cosmology*, 82(4), 043508.
6. Tyagi, A., Sharma, K., and Jain, P. (2010). Bianchi Type-IX String Cosmological Models for Perfect Fluid Distribution in General Relativity. *Chinese Physics Letters*, 27(7), 079801.
7. Adhav, K. S., Ugale, M. R., and Raut, V. B. (2010). Axially symmetric Bianchi type-IX Inflationary Universe in general relativity*. International Journal of Theoretical Physics,* 49, 1753-1758.
8. Bali, R., and Kumawat, P. (2010). Some Bianchi type IX stiff fluid tilted cosmological models with bulk viscosity in general relativity. *Electronic Journal of Theoretical Physics,* 7(24), 383-394.
9. Misonoh, Y., Maeda, K. I., and Kobayashi, T. (2011). Oscillating Bianchi IX universe in Hoˇrava-Lifshitz gravity*. Physical Review D—Particles, Fields, Gravitation, and Cosmology,* 84(6), 064030.
10. Nourinezhad, Z., and Mehdipour, S. H. (2012). Some examples for different descriptions of energy-momentum density in the context of Bianchi IX cosmological model*. Indian Journal of Physics,* 86, 919-923.
11. Tyagi, A., and Chhajed, D. (2012). Homogeneous anisotropic Bianchi type-IX cosmological model for perfect fluid distribution with electromagnetic field. *American journal of Mathematics and statistics*, 2(3), 19-21.
12. Pawar, D. D., and Dagwal, V. J. (2013). Bianchi type IX two fluids cosmological models in general relativity. *Energy,* 2, 2.
13. Czuchry, E., and Piechocki, W. (2013). Bianchi IX model: Reducing phase space. *Physical Review D—Particles, Fields, Gravitation, and Cosmology,* 87(8), 084021.
14. Kim, E. J., and Kawai, S. (2013). Chaotic dynamics of the Bianchi IX universe in Gauss-Bonnet gravity. *Physical Review D—Particles, Fields, Gravitation, and Cosmology,* 87(8), 083517.
15. Lugo, L. M., and Chauvet, P. A. (2013). The BKL method in the Bianchi IX universe model has been revisited. *Applied Physics Research,* 5(6), 107.

16. Patil, V. R., Bolke, P. A., and Bayaskar, N. S. (2014). Bianchi Type-IX Dust-Filled Universe with Ideal Fluid Distribution in Creation Field. *International Journal of Theoretical Physics*, 53, 4244-4249.
17. Ghate, H. R., and Sontakke, A. S. (2014). Bianchi Type-IX Radiating Cosmological in Self-Creation Cosmology. *International Journal of Innovative Research in Science, Engineering and Technology*, 3, 13820-13825.
18. Damour, T., Spindel, P. (2014). Quantum supersymmetric Bianchi IX cosmology. *Physical Review D*, (9010), 103509.
19. Fan, W., Fathizadeh, F., and Marcolli, M. (2015). Spectral action for Bianchi type-IX cosmological models. *Journal of High Energy Physics,* 2015(10), 1-29.
20. Fan, W., Fathizadeh, F., and Marcolli, M. (2015). Modular forms in the spectral action of Bianchi IX gravitational instantons. arXiv preprint arXiv:1511.05321.
21. Manin, Y., and Marcolli, M. (2016). Symbolic dynamics, modular curves, and Bianchi IX cosmologies. *In Annales de la Facult´e des sciences de Toulouse: Math´ematiques* (Vol. 25, No. 2-3, pp. 517-542).
22. Parikh, S., Tyagi, A., and Tripathi, B. R. (2016). Time-dependent Λ in Bianchi Type IX Cosmological Model with Barotropic Perfect Fluid in C-field Theory. *Prespacetime Journal,* 7(12).
23. Sofuo˘glu, D. (2016). Rotating and expanding Bianchi type-IX model in f (R, T) theory of gravity. *Astrophysics and Space Science*, 361, 1-7.
24. Saha, B. (2018). Spinor field in Bianchi type-IX space-time. *Canadian Journal of Physics,* 96(10), 1074-1084.
25. Czuchry, E., Kwidzinski, N., and Piechocki, W. (2019). Comparing the dynamics of diagonal and general Bianchi IX space-time. *The European Physical Journal C,* 79, 1-12.
26. Canfora, F., Dimakis, N., Giacomini, A., and Paliathanasis, A. (2019). Bianchi IX cosmologies in the Einstein-Skyrme system in a sector with nontrivial topological charge. *Physical Review D*, 99(4), 044035.
27. Chiovoloni, R., Montani, G., and Cascioli, V. (2020). Quantum dynamics of the corner of the Bianchi IX model in the WKB approximation. *Physical Review D,* 102(8), 083519.
28. Fahim, B. H., and Ghezelbash, M. (2021). New class of exact solutions to Einstein–Maxwelldilaton theory on four-dimensional Bianchi type IX geometry. *The European Physical Journal C*, 81, 1-17.

29. Sharma, S., and Poonia, L. (2021). Cosmic inflation in Bianchi Type IX space with bulk viscosity. *Advances in Mathematics: Scientific Journal*, 10(1), 527-534.
30. Aditya, Y., Divya Prasanthi, U. Y., and Reddy, D. R. K. (2022). Bianchi type-IX model in the presence of anisotropic dark energy and massive scalar meson field in Lyra geometry*. International Journal of Modern Physics A,* 37(16), 2250107.
31. Giani, L., Piattella, O. F., and Kamenshchik, A. Y. (2022). Bianchi IX gravitational collapse of matter inhomogeneities. *Journal of Cosmology and Astroparticle Physics,* 2022(03), 028.
32. Mishra, R. K., and Sharma, R. (2024). Exploring the Bianchi-IX universe within Brans–Dicke theory and a deceleration parameter. *Modern Physics Letters A*, 2450169.
33. Calcagni, G. *et al.,* (2012) Quantum Gravity and Quantum Cosmology, Springer.

Innovations in Mathematics and Statistical Research

ISBN: 978-93-48620-58-3

About Editors

Dr. Sheetal R. Gomkar is an Assiociate Professor of Mathematics at Janata Mahavidyalaya, Chandrapur, with over nine years of teaching experience at the undergraduate level. She holds M.Sc., M.Phil., and Ph.D. degrees in Mathematics, specializing in Relativity. She has four years of research experience and has actively participated in various national and international conferences, seminars, and workshops. Dr. Gomkar has published nine research papers in reputed peer-reviewed journals, focusing on unified field theories and plane wave solutions in higher-dimensional space-time. She has contributed to curriculum development and served as a subject expert for Ph.D. coursework and placement committees under Gondwana University. Passionate about student engagement, she has conducted seminars, organized tours, and guided students in co-curricular activities. She was recognized as a "Master Trainer" for the "Empowerment of Girls" program by Gondwana University in 2015.

Mr. Dnyaneshwar Prakash Maule is currently serving in the Department of Mathematics at A.V. College of Arts, K.M. College of Commerce, and E.S.A. College of Science, Vasai Road, Palghar, Maharashtra. He holds an M.Sc. in Mathematics from the University of Mumbai and has qualified the NET examination in Mathematics. Presently, he is pursuing a Ph.D. in Mathematics from the University of Mumbai. With over six years of teaching experience at the undergraduate level, he has taught various subjects under the B.Sc. curriculum. Mr. Maule has also served as a university paper setter for one year and delivered invited lectures on NET/SET exam preparation for M.Sc. students at the Department of Mathematics, University of Mumbai.

Dr. P. V. Nirmaladevi is a distinguished Professor and Head of the Department of Mathematics at Kalpataru Institute of Technology, Tiptur, Karnataka, India. With a B.Sc. in Physics, Chemistry, and Mathematics from Bangalore University (1992), an M.Sc. in Mathematics (1995), an M.Phil. from Alagappa University (2007), and a Ph.D. in Fluid Mechanics from VTU (2020), she has a robust academic background. Her Ph.D. research focused on the dispersion of air pollutants through mathematical modeling. Dr. Nirmaladevi has 29 years of teaching experience, having served in various educational institutions. She has published several research papers in reputed journals and presented at national and international conferences. A life member of ISTE, she has also actively participated in numerous faculty development programs. Her dedication to education and research has significantly contributed to the field of mathematics.

Dr. Vicky Watkar is an Assistant Professor in the Department of Mathematics at Indira Mahavidyalaya, Kalamb, Dist. Yavatmal. He holds a Ph.D. in Mathematics with a specialization in Fuzzy Logic. His core research interests include Fuzzy Sets, Fuzzy Logic, and the algebraic semantics of logic. Dr. Watkar has published several research papers in reputed peer-reviewed international journals and has presented his work at various conferences. He is dedicated to fostering research and innovation in the field of mathematics. Currently, he is actively working on developing hybrid fuzzy-crisp models and exploring their real-life applications. His passion for teaching and research makes him a valuable contributor to the academic and research community.

Bhumi Publishing

ISBN 978-93-48620-58-3
9 789348 620583